ADDIS ABABA UNIVERSITY

ADDIS ABABA INSTITUTE OF TECHNOLOGY

SCHOOL OF CHEMICAL AND BIO ENGINEERING

Simulation and Modeling of Syngas Production via Glycerol Dry Reforming Using Aspen plus

Ali Hassen Ali

A thesis Submitted to School of Chemical and Bio Engineering, Addis Ababa Institute of Technology (AAiT), Addis Ababa University

Presented in partial fulfilment of the requirements for the degree of Master of Science in Chemical Engineering (Process Engineering)

Addis Ababa University

Addis Ababa, Ethiopia

November 2018

Addis Ababa University

Addis Ababa Institute of Technology (AAiT)

School of Chemical and Bio Engineering

This is to certify that the thesis prepared by **Ali Hassen Ali**, entitled "***Simulation and Modelling of Syngas Production via Glycerol Dry Reforming using Aspen Plus***" and submitted in partial fulfilment of the requirements for the degree Master of Science (Process Engineering) complies with the regulation of the university meets the accepted standards with respect to originality and quality.

Signed by the Examining committee

Dr.Eng.Hundessa Dessalegn	_____	_____
Advisor	Signature	Date
Dr. Shimelis K	_____	_____
Internal Examiner	Signature	Date
Eng.Gizachew S.	_____	_____
External Examiner	Signature	Date
_____	_____	_____
School or Centre chair person	Signature	Date

DECLARATION

I, the undersigned, declare that this thesis is my original work, has not been presented for degree in this or any other university/institution, and all source of materials used for the have been fully acknowledged.

Ali Hassen Ali _____ _____

Name Signature Date

Date of Submission: ----------

This thesis has been submitted for examination with my approval as a university advisor.

Dr.Eng.Hundessa Dessalegn _____ _____

Advisor Signature Date

ACKNOWLEDGMENTS

First and foremost, I give thanks to the Almighty Allah for giving me strength, patience and wisdom to finish this research. Then, I would especially like to express my deep gratitude to my advisor Dr.Eng.Hundessa Dessalegn Demsash for his boundless guidance, advice, support, and encouragement throughout my research work. His suggestion and ideas helped me to learn a lot throughout a course of my research. Also, would like to extend my gratitude to Dr.Eng Abubeker Yimam for his expert recommendation and helpful suggestions during this research proposal presentation.

I would like to thank, Haramaya University and Haramaya Institute of Technology for their financial support paying annual salary. Thanks to Addis Ababa Institute of Technology School of Chemical and Bio Engineering post graduate studies for facilitating and providing additional financial support.

I wish to acknowledge all AAiT post graduate computer lab employees for their help during installation of software and conduct my research using desktop computer.

I am very grateful to all my classmates for their motivation and support directly and indirectly during my study. I am thankful to all staffs and students of school of chemical and bio engineering of Addis Ababa Institute of Technology for their help and encouragement through the course of my study. I most acknowledge the motivation, support, encouragement and understanding of my dear family; especially, my dear father Mr.Hassen Ali Mohammed and my dear wife Hayat Tuha Mohammed.

ABSTRACT

The surfeit of crude glycerol as by product from biodiesel industry triggered alternative routes to valorise glycerol to value added fuels such as syngas, mixture of hydrogen and carbon monoxide. Dry reforming of glycerol uses carbon dioxide (CO_2) as reactant to produce syngas. The process of glycerol dry reforming has been simulated and the effect of thermodynamic properties on yield, selectivity and conversion were studied and optimized with the aid of ASPEN PLUS V8.8 in this paper. The process of simulating glycerol dry reforming was carried out using RGIBBS and RPLUG reactor types. The sensitivity analysis and the optimization of the process were accomplished using the sensitivity and optimization sections of the model analysis tools of the ASPEN PLUS. Furthermore, sensitivity analysis was carried out to observe the effect of several parameters. The kinetic data for glycerol dry reforming and water gas shift reactions were obtained from literature. The kinetic based simulation was performed using ASPEN PLUS RPLUG model blocks with rearranged Power law and Langmuir-Hinshelwood-Hougen –Watson (LHHW). The result obtained revealed that the simulation with RGIBBS and RPLUG gave different values of components. Furthermore, it was revealed from sensitivity analysis of the process that optimization was necessary to obtain the operating variable that would involved in the process. Optimization was able to give a satisfactory value of conversion of glycerol, carbon dioxide for reforming and carbon monoxide and water for water gas shift reaction. However, much has been reported about thermodynamic analysis of steam reforming of glycerol, little is known about thermodynamic analysis of glycerol dry reforming. In this regard, in the current work, with Aspen plus simulator glycerol dry reforming thermodynamic analysis is carried out. The effect of process such as: temperature, pressure, length of the reactor, catalyst particle density, and feed ratio to the reactor performance were investigated. Based on this the yield of syngas was 92% over the range of temperature 573 -1273K whereas, over the range of pressure 1-30 bar and feed ratio 1-5; the yield of syngas were 50% and 51.24% respectively

Key word: Sensitivity analysis, Aspen plus, Optimization, Syngas, Dry reforming

Table of Contents

Content	Page No.
DECLARATION	**ii**
ACKNOWLEDGMENTS	**iii**
ABSTRACT	**iv**
LIST OF TABLES	**viii**
LIST OF FIGURES	**ix**
NOTATION	**xii**
ACRONYMS	**xv**
1. Introduction	**1**
1.1 Background	1
1.2 Statement of the Problem	3
1.3 Objective of the Research	5
1.3.1 General Research Objective	5
1.3.2 Specific Objective	5
1.4 Significance of the Study	5
2. Literature Review	**6**
2.1 Syngas	6
2.2 Glycerol	7
2.2.1 Properties of Glycerol	8
2.2.2 Application of Glycerol	10
2.3 Conventional Process for Reforming to Produce Syngas	11
2.3.1 Steam Reforming Process	11
2.3.2 Auto thermal reforming process	12
2.3.3 Partial Oxidation Reforming Process	13
2.3.4 Dry Reforming Process	13
2.3.5 Water Gas Shift Reaction	14
2.4 Glycerol Dry Reforming	14

2.5 Factors Affecting the Reforming Process 15
2.5.1 Catalysts for Glycerol Reforming 15
2.5.2 Kinetics of Glycerol Reforming 16
2.5.2.1 Review of the Kinetics for Homogeneous Reaction 16
2.5.2.2 Kinetic Models for Heterogeneous Reactions 21
2.5.2.2.1 Basic Steps for Catalyzed Heterogeneous Reaction 21
2.5.2.2.2 Langmuir Isotherm 22
2.5.2.2.3 Dissociating Gases 24
2.5.2.2.4 Langmuir –Hinshelwood Kinetics (LHHW) 25
2.5.2.2.5 Non Competitive Adsorption 26
2.6 Thermodynamic Analysis 26
2.7 Process Simulation and Modeling using Apsen plus 28
2.7.1 Introduction to Aspen plus 29
2.7.2 Process Flow Description 30

3 Materials and Methods 32

3.1 Process Modelling and Simulation 32
3.1.1 Thermodynamic Investigation 33
3.1.2 Kinetic Modelling for Dry Glycerol Reforming 34
3.1.2.1 Power law Kinetic Modelling 34
3.1.2.2 Langmuir-Hinshelwood-Watson (LHHW) kinetic modelling 36
3.1.2.3 Steps of LHHW in Aspen plus for Dry Glycerol Reforming 37
3.1.2.4 Steps of LHHW in Aspen plus for WGS 41
3.1.3 Sensitivity Analysis for Dry Glycerol Reforming 44

4. Results and Discussion 46

4.1 Thermodynamics Analysis to Produce Syngas via Glycerol Dry Reforming 46
4.1.1 Effect of Temperature on RGIBBS Reformer 46
4.1.2 Effect of Pressure on RGIBBS Reformer 49
4.1.3 Effect of Feed ratio on RGIBBS Reformer 51
4.2 Thermodynamics Analysis of RGIBBS Water Gas Shift Reactions 53
4.2.1 Effect of Temperature on RGIBBS Water Gas Shift Reactions 53
4.2.2 Effect of Pressure on RGIBBS Water Gas Shift Reactions 55
4.3 Thermodynamics Analysis of Reforming RPLUG with Kinetic Models 57
4.3.1 Effect of Parameters on Reformer and Water Gas Shift Reaction with Power law Kinetic Model 57
4.3.1.1 Effect of Temperature on Reformer and Water Gas Shift Reaction with Power law Kinetic Model 58
4.3.1.2 Effect of Pressure on Reformer and Water Gas Shift Reaction with Power law Kinetic Model 59

4.3.1.3 Effect of Length of Reactor on Reformer and Water Gas Shift Reaction with Power law Kinetic Model 60
4.3.2 Effect of Parameters on Reformer and Water Gas Shift Reaction with LHHW Kinetic Model 67
4.3.2.1 Effect of Temperature on Reformer and Water Gas Shift Reaction with LHHW Kinetic Model 68
4.3.2.2 Effect of Pressure on Reformer and Water Gas Shift Reaction with LHHW Kinetic Model 68
4.3.2.3 Effect of Length of the reactor on Reformer and Water Gas Shift Reaction with LHHW Kinetic Model 69
4.3.2.4 Effect of Catalyst particle density on Reformer and Water Gas shift Reaction with LHHW Kinetic Model 70
4.3.3 Optimum Condition of the Parameters on Reforming and Water Gas Shift Reaction 77

5. Conclusion and Recommendation 78

5.1 Conclusion 78

5.2 Recommendation 79

References 81

Appendix A: Total Heat of Vaporization of Glycerol Mixture 85

Appendix B: Formulas to Check Optimum Condition 86

Appendix C: Optimum Parameters of Glycerol Dry Reforming 87

Appendix D: Aspen plus Process Flow diagram of DGR and WGS 89

Appendix E: Material and Energy Balance Data from Aspen plus Run 91

Appendix F: Steps of Sensitivity Analysis and Optimization for Aspen plus Reformer and Water Gas Shift Reaction 102

LIST OF TABLES

Table No.	Title Table	Page No.
Table 2.1 :	Physical and chemical properties of glycerol(Arif et al., 2016b)	9
Table 2.2:	Composition of Crude Glycerol from Milligan Bio fuels Inc. (MSDS)(Mahmoud & Ghani, 2014)	10
Table 2.3	Steps in a acatalytic reaction (Song, 2010)	22
Table 3.1:	kinetic parameters of the glycerol consumption rate from the power law modelling(Weng et al., 2015)	35
Table 3.2:	kinetic parameters of the carbon monoxide consumption rate from the power law modelling(Weng et al., 2015)	36
Table 3.3:	Rate parameters of glycerol dry (CO_2) reforming (Hundessa D. Demsash, Kondamudi, Upadhyayula, & Mohan, 2018)	39
Table 3.4:	The kinetic coefficient and equilibrium constants in equation [3.3]	40
Table 3.5:	Adsorption constants fitting in Aspen plus for dry glycerol reforming	40
Table 3.6:	Rate parameters of High temperature water gas shift (HWGS)(Ahmad, 2017)	42
Table 3.7:	Adsorption constants fitting in Aspen plus for HWGS	42
Table 3.8:	Rate parameters of Low Temperature water gas shift (LWGS)(Ayastuy, Gutiérrez-Ortiz, González-Marcos, Aranzabal, & González-Velasco, 2005)	43
Table 3.9:	Adsorption constants fitting in Aspen plus for LWGS	44
Table 3.10:	Possible reactions during the dry glycerol reforming (Hundessa Dessalegn Demsash & Mohan, 2016)	45

LIST OF FIGURES

Figure No. **Title of Figure** **Page No.**

Figure 2.1: Process flow diagram of glycerol dry reforming using Aspen plus 31
Figure 4.1: Product distributions of CO_2, $C_3H_8O_3$, CO, H2O, CH4, C2H4, C2H6 and H_2O versus temperature 47
Figure 4.2: (A) Conversion of CO_2, and $C_3H_8O_3$, and (B) Yield of CO, and H2 versus temperature 48
Figure 4.3: Syngas ratio and Selectivity of H_2 versus temperature 48
Figure 4.4: product distributions of CO_2, $C_3H_8O_3$, CO, H2O, CH4, C2H4, C2H6 and H_2O versus Pressure 50
Figure 4.5: Conversion of CO_2, and $C_3H_8O_3$, and Yield of CO, and H_2 versus Pressure 50
Figure 4.6: Syngas ratio and Selectivity of H_2 versus Pressure 51
Figure 4.7: product distributions of CO_2, CO, CH4, C2H4, C2H6 and H_2 versus Feed ratio 52
Figure 4.8: Conversion of CO_2, and $C_3H_8O_3$, Syngas ratio and Yield of CO, and H_2 versus Feed ratio 52
Figure 4.9: Water (H_2O) versus Feed ratio 53
Figure 4.10: (A) Product composition of H_2, CO_2 and CO and (B) conversion of H_2O versus Temperature 54
Figure 4.11: (A) Syngas ratio (B) Yield of H_2 and CO (C) Selectivity versus Temperature 55
Figure 4.12: (A) Product composition of H_2, CO_2 and CO and (B) conversion of H_2O versus Pressure 56
Figure 4. 13: (A) Syngas Ratio and (B) Selectivity of H_2 versus Pressure 57
Figure 4.14: (A) conversion of glycerol and CO_2 and (B) Selectivity of CO, CO_2, H_2, H_2O versus Temperature between 923 and 2800K 61
Figure 4.15 : Product composition of CO, H_2 CO_2, H_2O and $C_3H_8O_3$ versus Temperature of reformer 62
Figure 4.16: (A) Conversion of CO_2 and glycerol and (B) Selectivity of CO, H_2, CO_2, and H_2O versus Pressure 62
Figure 4.17: Product composition of CO, H_2 CO_2, H_2O and $C_3H_8O_3$ versus Pressure 63
Figure 4.18: (A) Conversion of CO_2 and glycerol and (B) Selectivity of CO, H_2, CO_2, and H_2O versus Length of reactor 63
Figure 4.19: Product composition of CO, H_2 CO_2, H_2O and $C_3H_8O_3$ versus Length of reactor 64

Figure 4.20: (A) Conversion of CO and H_2O and (B) Selectivity of CO, H_2, CO_2, and H_2O versus Temperature of WGS 64
Figure 4.21: Product composition of CO, H_2 CO_2, and H_2O versus Temperature of WGS 65
Figure 4.22: Syngas ratio (H_2 /CO), versus Temperature of WGS 65
Figure 4.23: (A) Conversion of CO and H_2O and (B) Product composition of CO, H_2, CO_2, and H_2O versus pressure of WGS 66
Figure 4.24: (A) Selectivity of CO_2, CO, H_2 and H_2O and (B) Syngas ratio versus Pressure of WGS 66
Figure 4.25: (A) Conversion of CO and H_2O and (B) Product composition of CO, H_2, CO_2, and H_2O versus length of WGS 67
Figure 4.26: (A) Selectivity of CO_2, CO, H_2 and H_2O and (B) Syngas ratio versus length of WGS 67
Figure 4.27: (A) conversion of glycerol and CO_2 and (B) Selectivity of CO_2, CO, H_2 and H_2O versus Temperature of reformer 71
Figure 4.28: (A) Selectivity of CO_2, CO, H_2 and H_2O and (B) conversion of glycerol and CO_2 versus Pressure of reformer 71
Figure 4.29: (A) conversion of glycerol and CO_2 and (B) Selectivity of CO_2, CO, H_2 and H_2O versus Length of reformer 72
Figure 4.30: (A) Selectivity of CO_2, CO, H_2 and H_2O and (B) conversion of glycerol and CO_2 versus Catalyst particle density of reformer 72
Figure 4.31: (A) conversion of water and CO and (B) Selectivity of CO_2, CO, H_2 and H_2O versus Temperature of WGS 73
Figure 4.32: (A) Syngas ratio and (B) product composition of CO_2, CO, H_2 and H_2O versus Temperature of WGS 73
Figure 4.33: (A) conversion of water and CO and (B) Selectivity of CO_2, CO, H_2 and H_2O versus Pressure of WGS 74
Figure 4.34: (A) product composition of CO_2, CO, H_2 and H_2O and (B) Syngas ratio versus Pressure of WGS 74
Figure 4.35: (A) conversion of water and CO and (B) Selectivity of CO_2, CO, H_2 and H_2O versus length of WGS 75
Figure 4.36: (A) product composition of CO_2, CO, H_2 and H_2O and (B) Syngas ratio versus Pressure of WGS 75
Figure 4.37: (A) conversion of water and CO and (B) Selectivity of CO_2, CO, H_2 and H_2O versus Catalyst particle density of WGS 76

Figure 4.38: (A) product composition of CO_2, CO, H_2 and H_2O and (B) Syngas ratio versus Catalyst particle density of WGS 76

NOTATION

Symbol	Definition	Units
a_{ik}	Number of atoms of the k th element present in each Molecule of species i	
CO_2	Carbon dioxide	----
CO	Carbon monoxide	----
C_2H_6	Ethane	----
C_2H_4	Ethylene	----
$C_3H_8O_3$	Glycerol	---
CH_4	Methane	----
CA	Concentration of A species	mol/cum
Ea	Activation energy	KJ/mol
Eads	Activation energy of adsorption	KJ/mol
Edes	Activation energy of desorption	KJ/mol
f_i^g	Fugacity of species of gases	BAR
FA	mole flow rate of A species	Kmol/sec
ΔG°	Standard Gibbs free energy change	KJ/mol
G^{tg}	Total Gibbs free energy of gases	KJ
H_2O	Water	
$\frac{H_2}{CO}$	Syngas ratio	---
Ko	Frequency factor	different units
K_{gly}	Equilibrium constant of glycerol	cum/Kmol
K_{CO2}	Equilibrium constant of carbon dioxide	cum/Kmol
K_{CO}	Equilibrium constant of carbon monoxide	cum/Kmol
K_{H2O}	Equilibrium constant of water	cum/Kmol
NaOH	Sodium hydroxide	----
P_{gly}	Partial pressure of glycerol	BAR

P_{CO2}	Partial pressure of carbon dioxide	BAR
P_{CO}	Partial pressure of carbon monoxide	BAR
P_{H2O}	Partial pressure of water	BAR
RGIBBS	Gibbs reactor	
RPLUG	Plug flow reactor	
r,ads	Rate of adsorption	
r,des	Rate of desorption	
R	Universal gas constant	KJ/Kmol K
r	reaction rate	Kmol/Kg cat. s
S	Catalyst surface reaction	-----
S_{H2}	Selectivity of hydrogen	%
T	Absolute temperature	Kelvin
Xgly	Conversion of glycerol	%
Y_{H2}	Yield of hydrogen	%
y_i	mole fraction of gas	%

Greek letters	Definition	Unit
θ_{Gly}	Glycerol surface coverage	
θ_{CO2}	Carbon dioxide surface coverage	
μ^{ig}	Chemical potential	
φi	Fugacity coefficient	
α	Reaction order with respect to glycerol	
β	Reaction order with respect to carbon dioxide	
γ	Reaction order with respect to carbon monoxide	
ϕ	Reaction order with respect to water	
Π	Product of partial pressure of component	
λ_{κ}	Lagrange multiplier	
Υ_i	Stoichiometric coefficient	
Λ	Heat of vaporization	KJ/kg

ACRONYMS

DGR	Dry glycerol reforming
DMC	Dimethyl carbonate
FAME	Fatty Acid Methyl esters
FFA	Free fatty acid
FTIR	Fourier transforms infrared spectroscopy
HTWGS	High temperature water gas shift
IPCC	Intergovernmental panel on climate change
LHHW	Langmuir Hinshelwood Hougen Watson
LTWGS	Low temperature water gas shift
MSDS	Material safety Data sheet
Wt%	Weight percent

1. Introduction

1.1 Background

The continued emission of greenhouse gas and release of crude glycerol (a bio-waste generated from biodiesel production), to the surrounding is caused climate change and global warming in the world. Furthermore, the growing science of the climate change research is increasingly demonstrating the need to produce more environmentally sustainable energy sources. According to(Mahmoud & Ghani, 2014) three confirmed facts were mentioned; they were the climate change on the earth is to become warmer; the percentage of carbon dioxide in the atmosphere has seen as a dramatically increase since the beginning of Industrial Revolution; carbon dioxide released from burning fossil fuel is a greenhouse gas that increase the heat capacity of the environmental air and thus, the energy reserved in the atmosphere. Then also (Mahmoud & Ghani, 2014) reported that the Intergornmental panel on climate change (IPCC,2014) report which was the net greenhouse gas emission of more than 49 billion tonnes of carbon dioxide equivalents in 2010 which was the maximum level in human history.

Therefore, in order to limited and eventually approaches to minimum the greenhouse gas emission, it is better to use renewable energy, such as biodiesel, syngas, solar, hydropower etc. Biodiesel which is biodegradable, non-toxic, near CO_2 neutral and environmentally beneficial fuel has become more attractive recently as alternative fuel to reduce dependency on fossil fuel imports. However, biodiesel industries are facing problem in how to utilize the large amounts of glycerol produced as a by-product. Adhikari, S., Fernando, S., & Haryanto, A. (2007)) have been reported that about 10wt. % of glycerol is produced during the production of biodiesel fuel through the catalytic transesterification process. Besides, it has been reported that 980 million litres of glycerol per year are produced compared to a demand of only 216 million litres. Glycerol production is expected to grow dramatically.

Production of syngas from glycerol had got an attractive attention during some years and has been considered as the most feasible options of energy resource to replace the fossil fuels as raw material. Syngas is mixture of hydrogen and carbon monoxide and it is used for different purpose in building block in chemical industry.

In the absence of climate change mitigation policies, energy related carbon dioxide emissions are expected to continue to increase with fossil fuel and industrial emissions reaching 50-70 Gt of carbon dioxide by 2050. Climate change can only be mitigated and a global temperature is stabilized when the total amount of carbon dioxide released is limited and eventually approaches to zero. (Hundessa Dessalegn Demsash & Mohan, 2016)

Approximately 3 megatons of crude glycerol is projected to be generated by the year 2020. The amount of glycerol used in commercial applications each year is less than 500 kilotons. Consequently, the biodiesel industries are managing the glut of glycerol as a waste because of its impurities and are also suffering from the impact of the increasing storage and management costs. The accumulation of crude glycerol not only delays the development of the biodiesel industry, but it also creates economic and environmental problems.(Sisinni, Carlo, Bocci, Micangeli, & Naso, 2013)

Furthermore , glycerol is one of the most enjoyable renewable sources associated with the environmental impacts from the usage of the fossil fuels in which it reduce the carbon dioxide emission which is more preferable in production of renewable energy.

To more advance efficient glycerol dry reforming process, it is necessary to model the process of production to set the most important parameters that favour maximum yield of syngas. From the process models; appropriate strategies can be formulated to maximize the desired products through the optimization of the reaction conditions, such as feed ratio, pressure and temperature of the reactor, space velocity (inlet flow), and internal diameter and length of the reactor.(Mahmoud & Ghani, 2014)

There are many research papers which based on the syngas production from glycerol in different conventional processes such as: steam reforming, auto thermal reforming, partial oxidation, aqueous phase reforming, and supercritical water reforming. However, most of researchers centre of interest was on the production of syngas from steam reforming, auto thermal reforming, partial oxidation, aqueous phase reforming, supercritical water reforming and over catalyst supported for synthesizing rather than attempt to study syngas production via dry glycerol reforming and its model process. Especially, Model process of glycerol dry reforming was not attempt to report until the preparation of this paper.

Many have been reported on the model analysis of glycerol steam reforming and glycerol auto thermal reforming. Little has been reported on thermodynamic analysis of glycerol dry reforming. (Weng et al., 2015)and co-workers carried out a thermodynamic analysis of glycerol dry reforming and reported optimized conditions for hydrogen production of temperature at 975 K, CO_2 to glycerol ratios of 0–5 and atmospheric pressure. (Arif, Vo, Azizan, & Abidin, 2016a) performed experimental hydrogen production via glycerol dry reforming at atmospheric pressure and temperature ranging from 973 to 1023 K employing CO_2 to glycerol ratio ranging from zero to five and reported 96% glycerol conversion at the CO_2 to glycerol ratio of 1.67. These two works considered only set of series reactions in which hydrogen, methane, carbon monoxide, carbon dioxide and water were as a products and/or by-products. In this study, the model analysis of glycerol dry reforming with comprehensive plausible reactions has been considered with Aspen plus ™ simulator. The model analysis has been simulated with RGIBBS and RPLUG reactor models. The detail of thermodynamic investigation and kinetic model analysis has been performed by RGIBBS and RPLUG reactor models respectively. Furthermore, formation of light hydrocarbon such as methane, ethane and ethylene has been considered in thermodynamic investigation in addition to report so far. The effects of operation parameters such as temperature, pressure, CO_2 to glycerol feed ratio on syngas production and product composition has been evaluated. The realistic situation of feedstock besides the comprehensive process model and simulation in this study are the key factors to implement this process at the industrial scale. This study will be offer comprehensive information in all aspects of syngas production via glycerol dry reforming.

1.2 Statement of the Problem

Nowadays, the critical of global warming and climate change of great concern for humanity which needs permanent and sustainable technical solution. The global warming and climate change; are related with the rising of global demand for fuels and industrial revolution. According to 2007 market analysis by ABG inc., the estimated production of crude glycerol from biodiesel industry is expected to exceed 5 billion pounds by 2020, which is really in huge volume. At the same time demand on free glycerol is not growing due to the saturation of the market, and this affects the

value of crude glycerol and consequently the efficiency of biodiesel production. As reported from(Wang et al., 2009) the overall reactions of glycerol dry reforming have been more environmentally friendly and probably it is more economic compared to other conventional process because of refining glycerol is very expensive. For the glycerol dry reforming, glycerol Steam reforming, partial oxidation and reforming, auto thermal reforming, the main reactants are: carbon dioxide, water, oxygen, water and oxygen respectively. However, carbon dioxide is one of the major causes for the global warming and climate change; in the other cases water and oxygen are environmentally friends for the process of reforming. Therefore, it is better to transform toxic wastes in valuable product rather than transform non-toxic wastes in to valuable product. Accordingly, Carbon dioxide can be alternatively used to replace steam water and oxygen with minimum costs in production of syngas. Besides, this paper has been focused on; utilization of carbon dioxide as raw material for the reforming of glycerol for the production of valuable syngas; instead of treating it as waste. As known the process of glycerol dry reforming for syngas production is new and not practiced at the level of industrial scale; As (Silva, Soria, & Madeira, 2015) reported that ,so many challenges have been faced by doing this process; such as sufficient conversion where high operating conditions have been needed and carbon formation problem. Consequently, different model analysis has been required to provide a fundamental study of syngas production from glycerol dry reforming.

The other issues were regarding the model analysis of the processes; many have been reported on the model analysis of glycerol steam reforming and glycerol auto thermal reforming. Little has been reported on thermodynamic analysis of glycerol dry reforming. (Weng et al., 2015) and co-workers carried out a thermodynamic analysis of glycerol dry reforming and reported optimized conditions for hydrogen production of temperature at 975 K, CO_2 to glycerol ratios of 0 -5 and atmospheric pressure. (Arif et al., 2016a) performed experimental hydrogen production via glycerol dry reforming at atmospheric pressure and temperature ranging from 973 to 1023 K employing CO_2 to glycerol ratio ranging from zero to five and reported 96% glycerol conversion at the CO_2 to glycerol ratio of 1.67. These two works considered only set of series reactions in which hydrogen, methane, carbon monoxide, carbon dioxide and water are products and/or by-products.

1.3 Objective of the Research

1.3.1 General Research Objective

The general objective of this work is modeling and simulation of the processs of syngas production via glycerol dry reforming over the main ranges of process parameters;

1.3.2 Specific Objective

- To investigate thermodynamic analysis with RGIBBS and Kinetic Reactor Models
- To estimate the main process parameters effects and its interactions in order to attain a maximum products yield, selectivity and conversion
- To find optimized condition of the model analysis for syngas production via glycerol dry reforming
- To couple the kinetics of syngas production via glycerol dry reforming at different models law analysis and see overall process change

1.4 Significance of the Study

This study will be offer comprehensive information in all aspects of syngas production via glycerol dry reforming, technically, socially and economically.

Technically the significance of this study is to analyse the effect of pressure, temperature and feed ratio to H_2/CO ratio; and apply concept of model analysis in to glycerol dry reforming to produce syngas. the other one is it will be reduces time that need for several experiments; and Aspen plus software will be employed to carry out model analysis of glycerol dry reforming; improve understanding of the process of dry glycerol reformig to produce syngas. Socially, the significance of this study is to reforming a toxic waste to create safe environment and produce renewable energy source. On the other hand the significance of this study is to enhance biodiesel production economy. Exploiting glycerol as feed-stock for the syngas will help to generate valuable product that reduce the refining cost in production biodiesel and it will also added some values towards this waste product and directly resolved the environmental problems.

2. Literature Review

This chapter provides a literature review for the current thesis on simulation and model analysis for syngas production process via glycerol dry reforming. It is divided into several sections in which the first section has been discussed on the syngas and its application. Second section discusses on glycerol, its properties, and application. Third section provides the conventional method to produce syngas, fourth section provides, dry reforming and the main factors affecting the reforming process. The fifth section discussed on kinetics of glycerol reforming. The final sections provide the model analysis, kinetics study of the glycerol dry reforming and introduction to Aspen plus for modelling of the process.

2.1 Syngas

(Binti & Yunus, 2015) and co-workers, try to define word syngas and reported interest of many researchers around the world in the use biomass as renewable energy. Word syngas is derived from "synthesis gas" or producer gas, which is a gas mixture comprises of carbon monoxide (CO), hydrogen (H_2), and very often some carbon dioxide (CO_2). The name of synthesis gas is actually comes from its use as intermediate for production of ammonia or methanol. Besides, synthesis gas is a vital building block for the petrochemical industry and it is also used to prepare various chemicals Synthesis gas is normally derived from a variety of different materials that contain carbon, such as natural gas or biomass.

Today, many researchers around the world were very interested in the use of biomass as a renewable energy. Source of biomass includes living organisms obtained from plant, trees or animal material. Examples of biomass are wood chips, corn, and left over food products such as; vegetable oils, animal fats that can produce biodiesel. The production of hydrogen or syngas is becoming one of popular process for biomass as a feedstock. The production of syngas can be performed by different processes such as; pyrolysis, gasification and reforming. Reforming includes steam reforming, auto-thermal reforming, aqueous phase reforming and dry reforming which are recently studied by researcher worldwide (Peres et al., 2011). Production of hydrogen which is also known as synthesis gas is a viable alternative to improve economic viability of biodiesel industry and to increase the use of crude glycerol.

Syngas can be produced by using biomass as a feedstock in order to reduce dependences of fossil fuels. Gradually, become less of the fossil fuels and petroleum reserves and the global warming issue related with this will drive to economic, social and political crisis; so it is extremely important to find alternative energy sources; so that it can sustain the world energy requirements. From the alternative energy source that can be mitigate the global warming is syngas is one .Now a day's Syngas is touted as the promising alternative energy due to its high efficiency, clean emission and it helps to reduce the dependency on this fossil fuel and also create safe environment, especially, while it produced from carbon dioxide and crude glycerol.

Crude glycerol was proven to be a viable alternative for producing hydrogen or syngas (al., Slinnet 2008). Gasification was the main employed technique. Thermo-gravimetric coupled with FTIR spectroscopy analysis proved that the thermal decomposition mechanism of crude glycerol mainly involved four phases and CO_2, H_2, CH_4, and CO were the main gas products (Dou et al., 2009). Gasification with in situ CO_2 removal was effective and had high energy efficiency. Supercritical water gasification of crude glycerol was performed under catalyzed and alkaline catalyzed conditions. The reaction temperature determined the decomposition degree. When NaOH was employed as catalyst nearly 90 vol. % of the product gas was H_2 and no char was produced (Onwudili et al., 2016). Additionally, co-gasification of crude glycerol and hardwood chips, in a downdraft gasified, was another promising option for utilizing crude glycerol. The loading amount of crude glycerol had significant influence on CO and CH_4 concentration, while having no effect on H_2 and CO_2 yield. Glycerol could be converted into syngas in each following processes: steam reforming, partial oxidation, auto thermal reforming, aqueous phase reforming, supercritical reforming, and dry reforming.

2.2 Glycerol

Glycerol, known as glycerine trihydric alcohols which are colorless, odorless and sweet-tasting.(Binti & Yunus, 2015) and co-worker, Lin (2012) stated that glycerol is classified as natural glycerol or synthetic glycerol. Natural glycerol can be derived from transesterification of biodiesel production and also through splitting of fats by saponification in the production of soap while synthetic glycerol can be derived from preparation of propylene oxide process.

Glycerol is naturally produced as by-product through the transesterification process of biodiesel. Transesterification is process in which the reaction of the vegetable oil (made up of mainly triglycerides) with an alcohol in the presence of alkali catalyst to produce a mixture of fatty acid ester (biodiesel) and glycerol. Glycerol is commercially used in various industries like, pharmaceutical and personal care applications, drug and cosmetics, food industry and syngas production. It was estimated that approximate 10% of crude glycerol will be produced from the transesterification process and it was expected to grow dramatically in the near future. Rising demand of biodiesel derived towards render production of glycerol. This surplus has caused the oversupply crisis that caused the development of biodiesel industry particularly in terms of economic viability and create safe environment.(Arif et al., 2016a)

2.2.1 Properties of Glycerol

(Arif, Vo, Azizan, & Abidin, 2016b) reported that the properties of Glycerol is commercial tri-OH alcohol and it is the simplest form of polyol compound and the chemical formula for glycerol is $C_3H_8O_3$. Other synonymous names for glycerol include glycerine, glycerine, propane -1,2,3-triol,1,2,3-propanetriol,1,2,3-trihydroxypropane,glyceritol and glycyl alcohol. In short glycerol is highly stable under normal storage conditions; compatible with many other chemical materials and physicochemical properties of glycerol at room temperature is shown below in table 2.1

Table 2.1: Physical and chemical properties of glycerol(Arif et al., 2016b)

Chemical formula	$C_3H_8O_3$
Melting point	18.17 °C
Heat of vaporization	88.174KJ/mole @55°C
Density	1.261 g/cm^3
Viscosity	1.5 Pa.s
Molecular mass	92 g/mol
Refractive index	1.474
Flash point	160 °C
Vapor pressure	0.3333 Pa @50°C
Boiling point	290°C
Heat of combustion	1662KJ/mole
Heat of fusion	18.3 KJ/mole
Thermal conductivity	0.29 W/m°K

(Mahmoud & Ghani, 2014), have been discussed the composition of crude glycerol for the commercial purpose. And from their report; unlike the purified one, the high amount of impurities in crude glycerol makes it unfavourable for commercial purposes. These impurities are usually methanol, ash, soap, water, free fatty acid (FFA) and FAME residues. Crude glycerol pertinent to Saskatchewan biodiesel production has been collected from Milligan Bio fuels Inc., the first Supplier of biodiesel in the province. Excluding the high percentage of potassium hydroxide present in Milligan's crude glycerol, the composition given in Table 2.2 was very similar to the composition reported by (Hu et al. 2012) in the United States.(Mahmoud & Ghani, 2014).

Crude glycerol generated from biodiesel operations should always be handled with caution. According to material safety data sheet (MSDS) of stripped glycerine by Milligan (2013), crude glycerine is a controlled product that contains toxic, flammable and corrosive materials. A short-term exposure to humans could result in skin damage, dizziness, serious problems in the nervous and respiratory systems, blindness and death. For a safe storage, crude glycerine should be stored in a proper container at a temperature below 38°C, and in a well ventilated area away from metals, acids and sunlight.(Mahmoud & Ghani, 2014)

Table 2.2: Composition of Crude Glycerol from Milligan Bio fuels Inc. (MSDS)(Mahmoud & Ghani, 2014)

Ingredients	Weights %
Potassium hydroxide	10 -30
Methanol	1 -5
Glycerine	40 -70
Fatty acids, Canola, methylester	7 -13
Organic material and soap	10 -30

2.2.2 Application of Glycerol

In fact various application of glycerol has been mentioned in the above of introduction parts of the paper and in some part of the literature review but, to make clear the idea; it is better if its application is written separately. So that, Glycerol is commonly used in various industries like as an ingredient or aid the process of cosmetics is produced. Different research papers shows that glycerol is being used in drugs and pharmaceuticals industry and in some case it is also used for the syngas production.

Syngas/hydrogen production is the first step toward a larger goal which is closer to renewable energy economy which is syngas. Many researchers reported as, it is emerging as future replacement energy for the traditional fossil fuels which is non-

renewable energy source that will capable of aiming our energy needs. Syngas/hydrogen may enable future energy systems and could be made to be a clean, more reliable, and more efficient; hence securing our future energy needs. Hydrogen /syngas production serves as an alternative energy source for fossil and biomass fuels. This can be achieved through the use of hydrogen energy derived from fossil and biomass sources with carbon captures. One of the major challenges of future hydrogen/syngas economy is the reduction in the production cost, storage issue and syngas transportation.

2.3 Conventional Process for Reforming to Produce Syngas

There is several ranking obviously researched conventional process for glycerol reforming over the last several years, which is, auto thermal reforming, partial oxidation reforming (gasification), steam reforming, dry reforming, supercritical water reforming, and aqueous phase reforming. But, from listed conventional process of glycerol reforming, dry reforming process is a relatively new research area which is compared to other conventional process of glycerol reforming. The detail of each of the conventional process of glycerol reforming is as follows.

2.3.1 Steam Reforming Process

Steam reforming of glycerol is a highly endothermic reaction that produces 7 moles of H_2 per 1 mole of glycerol decomposed according to the stoichiometric ratio. Over certain catalysts, glycerol can react with steam to produce hydrogen and carbon dioxide according to reaction(Mahmoud & Ghani, 2014)

$$C_3H_8O_3\,(g) + 3H_2O \rightarrow 7H_2\,(g) + 3CO_2\,(g)\ \ \Delta H = +123 KJ/mol \qquad [2.0]$$

Mahmoud & Ghani, 2014, reported that, generation of hydrogen from glycerol via steam reforming process using a commercial nickel based catalyst which was reported from Czernik et al. (2002) Even though the process had not been optimized by that time; their results were very promising with 77% hydrogen production yield. Additionally, Mahmoud & Ghani, 2014 reported that Adhikari et al. (2006) conducted a thermodynamic analysis on steam reforming of glycerol and found that operating conditions such as atmospheric pressure, temperature greater than 900 K and steam to glycerol ratio of 9:1 are the optimum in terms of hydrogen production

and coke and methane formation. Within that, Chen et al.(2012) presented an extensive work that include results of both thermodynamic analysis and pilot scale experiments. A fair agreement between thermodynamic results and experimental data was found for different operating parameters such as temperature, pressure, and steam to glycerol, inert gas to glycerol and residence time. The study was reported an optimum condition for hydrogen production at high temperature and low pressure. On the same procedure many catalysts have been reported based on their capabilities of promoting the process of hydrogen production via glycerol steam reforming.

2.3.2 Auto thermal reforming process

Many research papers shows that, auto thermal reforming is process which is combines from the effect of partial oxidation and steam reforming by feeding fuel, air and water into reactor in the presence of catalyst. The steam reforming process absorbs the heat generated by the partial oxidation process. The process can be shown as: (Arif et al., 2016b)

$$C_3H_8O_3\,(g) + aO2 + bH_2O \rightarrow cH_2\,(g) + dCO_2\,(g) + e\,CO + f\,CH_4 \quad \Delta H = 0 \qquad [2.1]$$

Where, a,b,c,d,e and f are coeffiecents

The main benefit of the auto thermal process is it does not require any energy for reaction to occur. Although the auto thermal steam reforming process had advantages over conventional steam reforming, the amount of the syngas produced from auto thermal reforming process is less in amount on thermodynamic basis.

As (Mahmoud & Ghani, 2014) reported what Swami and Abraham(2006) were examined, and accordingly, the performance of auto-thermal reforming of glycerol over nickel, palladium, copper and potassium catalyst in temperature range of 823-1123K. The results obtained from Auto-thermal reforming process revealed higher hydrogen production rates and lower coke formation over the surface of catalyst than that of steam reforming. As (Dauenhauer et al.2006); a high reforming temperature 1135K; S/C ratio of 4.5 and C/O ratio of 0.9 were reported as the optimum operating conditions to completely convert glycerol and reach 79% hydrogen selectivity. In addition, their study demonstrated that undesirable products formation such as CO and CH_4 has been suppressed to a selectivity of less than 2% under optimum

condition. (Luo et al.2007) studied in different cases the thermodynamics of glycerol auto-thermal reforming as a combination of oxidation and aqueous steam reforming in temperature range of 300-500K. Methanation reactions were promoted in the tested regions leading to a dramatic drop in the yield of hydrogen production. In addition, CO formation was mostly controlled by reaction temperature, while hydrogen production was mostly affected by oxygen to glycerol ratio with a gas product mainly composed of CO_2 and CH_4 under the tested conditions.

2.3.3 Partial Oxidation Reforming Process

(Mcglocklin, Roberts, & Curtis, 2006), Define the process and mention its operating conditions. Accordingly, partial oxidation is another reforming process that is being researched as an option for hydrogen production. During partial oxidation heavy hydrocarbons, such as diesel, coal and heavy fuel oils, are reacted with oxygen exothermically at temperature between 1143-1673 K to produce a gaseous mixture containing hydrogen and significant amounts of carbon monoxide are due to the limited amounts of oxygen, typically from air, available to react with hydrocarbons fuel; which is not stoichiometrically enough to completely oxidize the hydrocarbons to carbon dioxide and water. The partial oxidation reaction is primarily influenced by the oxygen to carbon ratio in the feed. The minimum value for the oxygen to carbon ratio is one; values lower than one generate too much heat and decrease hydrogen concentration. It is obvious that, the oxidation reaction results in the heat generation and high temperature so that the scope of this process in the presence of air is to balance the energy required for the process by oxidizing some of the substrate. If excess air is added, all the substrate will be oxidized and produce mainly carbon dioxide and water. The process can be shown as follow:

$$C_3H_8O_3 + O_2 \rightarrow 4H_2O + 3CO \qquad \Delta H < 0 \qquad [2.2]$$

2.3.4 Dry Reforming Process

Dry reforming also known as carbon dioxide reforming is a process of producing syngas which is mixture of hydrogen and carbon monoxide from reaction between carbon dioxide and hydrocarbon such as ethanol, glycerol, methane, etc. In recent years, the issue of greenhouse gases is come with rendering of the global warming to

make the replacement of steam, air and others as reactant with carbon dioxide.(Wang et al., 2009)

Two stages of producing syngas by reforming of natural gas have been developed and the process consists of a two stage reformer. They are, dry reformer, in this reformer process substrate react with carbon dioxide to produce syngas which is hydrogen and carbon monoxide, while the second one is water gas shift reaction reformer, carbon monoxide react with steam to produce additional hydrogen and carbon dioxide as the end products.(Arif et al., 2016a)

2.3.5 Water Gas Shift Reaction

Water gas shift process is employed to convert mostly CO into H_2. This process consists of two reactors in series with inter cooling.

A high temperature shift (HTS) reactor (573–873 K) as an initial stage followed by a low temperature (LTS) reactor (453–523 K). The HTS reactor feed is heated by the effluent of the LTS to control the operating temperature.

$$CO + H_2O \leftrightarrow H_2 + CO_2 \quad [2.3]$$

Additionally, the effluent of the HTS is cooled producing high pressure steam and then it is fed in the second reactor.(Preciado, Ortiz-martinez, Gonzalez-rivera, Sierra-ramirez, & Gordillo, 2012)

2.4 Glycerol Dry Reforming

This is process of producing syngas by utilizing carbon dioxide by replacing steam and air as a reactant. It is known that the rising demand of fuels and biodiesel may lead to supply of glycerol as alternatives to syngas production. Glycerol, which is generated as major by product of biodiesel is expected to much the commodity market once biodiesel technology becomes mature. Significantly, from thermodynamic perspective, glycerol can be effectively converted into hydrogen or even hydrogen-rich synthesis gas. Therefore, glycerol dry reforming (CO_2) process needs to involve in this case. Several reasons tend to choose dry reforming process instead of steam reforming process is production by using CO_2 can totally lead to new materials such as syngas, methane, dimethyl carbonate (DMC), and carbonic esters. Besides, CO_2 is a non-toxic feedstock that can replace toxic chemicals. It is a new route to existing

chemical intermediates and the product could be safer, more efficient and economical than current method which is steam reforming process.(Moon, Madhu, & Kale, 2013)
Many researchers mention some challenges that can be faced by doing this process including sufficient conversion where high temperature is needed and carbon formation problem when the catalyst resistive of carbon or regeneration is formed. (Moon et al., 2013) report that the synthesis gas in the equilibrium mixture increase with the temperature increases.

2.5 Factors Affecting the Reforming Process

- Temperature
- Pressure
- Feed Ratio
- Feed reactants to inert gas ratio
- Feed gas rate or space velocity
- Reactor length
- Catalyst loading (wt %)

2.5.1 Catalysts for Glycerol Reforming

Catalyst is a substance that speeds up the rate of a chemical reaction without being consumed itself. The accelerated rate of catalyzed reactions is due to the higher contact frequency between reactants involved in the rate-limiting step (slowest step), and this will consequently reduce the activation energy making the reaction easier to take place.(Mahmoud & Ghani, 2014)
In general, catalysts can be classified into two main categories; homogenous where the catalyst and reactants have the same phase and heterogeneous where the phases are different.
Several metal-based catalysts have been used to promote glycerol reforming and increase hydrogen productivity such as Ruthenium, Nickel, Rhodium, Cobalt, Platinum and Iridium. The efficiency of Nobel-metal catalysts such as Ru, Rh, Ir and Pt in glycerol reforming to produce syngas has been widely investigated(Mahmoud & Ghani, 2014).

2.5.2 Kinetics of Glycerol Reforming

(Mahmoud & Ghani, 2014) have been reported on kinetics of glycerol reforming; in order to investigate different effects of operating parameters on the rate of glycerol reforming and hydrogen production, many scholars have been studied the kinetics of the corresponding reforming reactions. A kinetics analysis on glycerol aqueous decomposition over bimetallic Pt-Re/C catalysts to produce synthesis gas has been carried out was reported by Mahmoud & Ghani, 2014. The study revealed the positive effect of integrating Re catalyst into Pt supported on carbon carrier through increasing the value of turnover frequency for synthesis gas production. Although the values of turnover frequencies for H_2, CO and CO_2 production were reported based on the outlet gas composition and number of active sites, the study did not generate a mathematical model to describe the rate of glycerol reforming and its dependency on the major operating conditions. (Harriott, 2003) suggested that, kinetics of the reaction can be classified in to two part based on the phase of reactant, product and catalyst. They are: kinetics of homogeneous reaction and heterogeneous reaction.

2.5.2.1 Review of the Kinetics for Homogeneous Reaction

As (Harriott, 2003) suggested it is important to state clearly the definition of reaction rate, conversion, yield and selectivity when analyzing kinetic data or designing a chemical reactor. For homogeneous reaction, the reaction rate is defined either as the amount of product formed or the amount of reactant consumed per unit volume of the gas or liquid phase per unit time. We generally use moles (g mol, kg mol or lb mol) rather than mass to define the rate, since this simplifies the material balance calculation

$$R\text{ate} = \frac{\text{Moles consumed or produced}}{\text{Reactor volume} * \text{time}}. \qquad [2.4]$$

For solid catalyzed reactions, the rate is based on the moles of reactant consumed or produced per unit mass of catalyzed per unit time.

$$R\text{ate} = \frac{\text{moles consumed or produced}}{\text{Mass of catalyst} * \text{time}} \qquad [2.5]$$

In the definitions given for homogeneous and heterogeneous reactions all the rates are defined to be positive, even though the amounts of reactants are decreasing. In some

texts, the rate is defined to be negative for materials that are consumed and positive for products formed, but (Harriott, 2003) suggested, it is generally unnecessary.

i. Conversion, Yield, and Selectivity

The conversion, X is defined as the fraction (or percentage) of the more important or limiting reactant that is consumed with two reactants A and B and nearly stoichiometric feed, conversion based on each reactant could be calculated and designated XA and XB. In most cases this is not necessary, and only one conversion is calculated based on A, the limiting reactant, and no subscript is needed for X.

$$\text{Conversion} = \frac{\text{mole of A reacted}}{\text{moles of A fed}} \qquad [2.6]$$

The yield, Y is the amount of desired product produced relative to the amount that would have been formed if there were no by-products and the main reaction went to completion.

$$\text{Yield} = \frac{\text{Moles of product formed}}{\text{maximum moles of product}} \qquad [2.7]$$

For a system where n moles of A are needed to produce 1 mole of product B, but A also gives some by-products the yield can be expressed in terms of mole flow rate FA, the feed rate of A, and the rate of product formation, FB both in moles/hr.

$$nA \rightarrow B \qquad [2.8]$$

$$Yield = \frac{mole\ flow\ rate\ of\ product}{mole\ flow\ rate\ of\ fed/n} = \frac{\frac{FB}{FA}}{n} \qquad [2.9]$$

The selectivity is the amount of desired product divided by the amount of reactant consumed. This ratio often changes as the reaction progresses, and the selectivity based on the final mixture composition should be called an average selectivity. For

$$nA \rightarrow B \qquad [2.10]$$

$$\text{Selectivity} = \frac{\text{B formed}}{\text{A used}} = \frac{\text{FB}}{\text{FAX/n}} = \frac{\text{Yield Y}}{\text{conversion X}} \qquad [2.11]$$

ii. Reaction Order and Activation Energy

Kinetic data are often presented as simple empirical correlations of the following type.

$$r = KCA^n \ or \ \ r = KPA^n \ PB^m. \qquad [2.12]$$

The reaction order is the exponent in the rate equation or the power to which the concentration or partial pressure must be raised to fit the data. When the exponents are integers or half- integers values such as 0.5,1,1.5,2, they may offer clues about the mechanism of the reaction. For example, if the gas-phase reaction of A with B appears to be first order to A and first order to B, this is cosistent with the collision theory. The number of collisions per unit volume per unit time depends on the product of the reactant concentrations and a certain fraction of the collisions will have enough energy to cause reaction. This leads to the following equation.

$$A + B \rightarrow C \ , \ r = KCACB \qquad [2.13]$$

If the rate data fit this expression, the reaction is described as first order to A and first order to B. Calling the reaction second order is ambiguous, since a total order of two could mean,

$$r = KCA^{1.5} \, KCB^{0.5} \ , r = KCA^0 \, KCB^2 \qquad [2.14]$$

Many unimolecular reaction (only one reactant) appear first order over a wide range of concentrations, though second order might seem more logical. Mole acquire the energy needed to break chemical bonds by collision with other molecules; and if only type A molecules are present, the rate of collision would vary as CA^2. The Lindemann theory of unimolecular reactions explains first order behaviour and shows that the order may change with concentration. For the reaction,

$$A \rightarrow B + C \qquad [2.15]$$

High energy molecules A^* are created by collision, but this process is reversible .

$$A + A \rightarrow \ A^* + A \qquad [2.16]$$

$$A + \ A^* \rightarrow A + A \qquad [2.17]$$

Some of the A^* molecules decompose to $B + C$ before energy is reduced by step 2

$$A^* \rightarrow B + C \qquad [2.18]$$

If steps 1 and 2 are very rapid relative to step 3, so that $r_1 \ \cong \ r_2$,an equilibrium concentration of A^* is established, and the reaction to produce B and C appears first order to A.

$K1CA^2 \cong K2CA^* CA$ then $CA^* = \frac{K1}{K2} CA$ [2.19]

$r = K3CA^* = \frac{K3K1}{K2}$ CA [2.20]

In the general case CA^* is assumed to reach a pseudo equilibrium value, where the rate of formation of $\boldsymbol{A}^*$ is equal to the sum of the rates of the steps removing A^* for ,

$\frac{dCA*}{dt} = 0$, $K1CA^2 = K2CA\, CA^* + K3CA^*$ [2.21]

$CA^* = \frac{K1CA^2}{K2CA+K3}$ [2.22]

At moderate or high pressures, $K2 \gg K3$ and CA^* is proportional to CA, giving first order kinetics. At very low pressures, the reaction rate might appear second order if,

$K2 \ll K3\,, then\ CA^* \cong \frac{K1}{K3} CA^2$ [2.23]

$r = K3CA^* = K1CA^2$ [2.24]

At intermediate pressures, a unimolecular reaction might appear to have a non-integer order, such as 1.3 or 1.75, but such values have no physical significance, and the order is likely to change when the concentration is varied over a wider range.

If the reaction order is zero for one reactant, it means that the rate is independent of the reactant concentration, at least for the range of concentration covered in the tests. It does not mean that the reaction can take place at zero reactant concentration. Zero order to A may indicate that the overall reaction require several steps, and the rate limiting steps does not involve A. However, at very low values of CA, some reaction order for A will change to a positive value. For two phase reaction system, such as$A + B(gas) \rightarrow C$, mass transfer of B could be the rate limiting steps, making the reaction appear zero order to A over a wide range of concentrations.

Negative reaction orders are sometimes observed for bimolecular reaction on solid catalysts. Increasing the partial pressure of one reactant A which is strongly absorbed, can lead to a surface mostly covered with adsorbed A, leaving little space for adsorption of reactant B. However, the negative order for A would change to zero order and then to a positive order as the partial pressure of A is reduced to very low values.

Why Is It Worthwhile To Determine The Reaction Order When Analyzing Kinetic Data?

Finding the reaction order usually does not verify a proposed mechanism, since different models may lead to that the same reaction order. The first benefit is that the reaction order is convenient way of referring to the effect of concentration alternate reactor designs or specifications.

A. Activation energy

(Song, 2010) has been tried to determine the activation energies, definition and working principle. Accordingly, to begin a chemical reaction, the reactant gas molecules require energy to distort or stretch their bonds in order to form new bonds. If implies that the molecule in reactant gases should overcome an energy barrier, which is named activation energy, Arrhenius equation has been proposed. The activation energy (E) can be found from a lot of $\ln k_A$ as function of $\frac{1}{T}$. in general, the larger activation energy implies the more temperature sensitive for the rate of reaction.

$$lnK_A = ln_A - \frac{E}{R}\left(\frac{1}{T}\right) \quad [2.25]$$

$$K(T) = k(T_o)e^{\frac{E}{R\left(\frac{1}{To}-\frac{1}{T}\right)}} \quad [2.26]$$

B. Effect of Temperature

For most reactions, the rate expression can be written as the product of a rate constant, which is temperature dependent, and a concentration term:

$$r = K(T)f(CA, CB, CC \dots) \quad [2.27]$$

The rate constant often follows the Arrhenius relationship.

$$K = k_{oe^{-E/RT}} \quad [2.28]$$

Where:

K_o = frequency factor (different units

$E = \text{Activation energy}, \frac{J}{mol} \text{ or } \frac{Cal}{mol}$

$R = \text{gas constant}, \frac{8.314J}{mol.K} \text{ or } \frac{1.987Cal}{mol.K}$

$T = \text{Absolute Temperature , K}$

The activation energy has been equated to the energy needed by colliding molecules for reaction to occur. For an endothermic reaction,**activation energy** is at least somewhat greater than the **heat reaction**.

2.5.2.2 Kinetic Models for Heterogeneous Reactions

As reported from (Harriott, 2003),When studying the kinetics of heterogeneous reactions or when designing a large catalytic reactor, there are more factors to consider than when dealing with homogeneous reactions. For a solid catalyzed reaction, the rate depends on the reactant concentrations, beacuse some driving force is neeeded for masss transfer to the surface. If the catalyst is porous, as is usually the case, there are further differences in the concentration between the pores. Model must be developed to predict the surface concentrations as functions of the partial pressures or concentration in the gas liquid, and the rate expression can be in terms of the fluid concentrations.

When the reaction is between a solid and a reactant in the gas or liquid,one must consider not only the foregoing factors but also the problem of changing particle size or shape as the solid is consumed. In this section we deal mainly with reactions on a solid catalyst. The equations are derived for gaseous reactants, but they apply to liquids as well when partial pressures are replaced with concentrations.

2.5.2.2.1 Basic Steps for Catalyzed Heterogeneous Reaction

(Song, 2010) has been reported that, heterogeneous catalytic reactions are the combination of various reactions. Reactant gases should pass through a boundary layer in order to reach on the surface of the catalyst. In general, the sequence of individual steps is shown in table 2.3. as mentioned, those steps are classified as diffusion steps(step 1,2,6 and 7), and reaction steps(step3,4,and 5). In overall, when the diffusion steps are conducted very fast compared with the reaction steps, the effects of the transport limitation could be negligible.

Table 2.3 steps in a acatalytic reaction (Song, 2010)

steps	
1	External diffusion of reactant A: mass transfer of the reactants from the bulk fluid to the external surface of the catalyst pellet
2	Internal diffusion of reactant A: diffusion of the reactants from the pore mouth through the catalyst pores to the immediate vicinity of the internal catalyst pellet
3	Adsorption of reactant A: adsorption of reactants A on to the catalyst surface
4	Reactio of A to B: reaction of the surface of the catalyst ($A \rightarrow B$)
5	Desorption of product B: desorption of the products B from the surface
6	Internal diffusion of product B:diffusion of the products from the interior of the pellet to the pore mouth at the external surface
7	External diffusion of product B: mass transfer of the products form the external pellet surface to the bulk fluid

2.5.2.2.2 Langmuir Isotherm

The Langmuir isotherm is widely used for reactants that reversibly chemi-sorb on the catalyst surface. The surface is assumed to be completely uniform, with all sites having equal reactivity. Adsorption occurs when molecules with sufficient energy strike vacant sites or uncovered parts of the surface. The process is described as a reaction between a molecule from the gas and an unoccupied site, S:

$$A + S \rightarrow A_S \qquad [2.29]$$

The frequency of collisions is proportional to the partial pressure, and the probability of adsorption is incorporated in the rate constant, k_1 which has an exponential dependence on temperature. The concentration of vacant sites is expressed as$(1-\theta)$, where θ is the fraction of occupied sites, and the total site concentration is included in the rate constant k_1. Molecules already adsorbed are assumed to have no effect on the rate of adsorption for nearby vacant sites:

$$r_{ads,A} = k_{1A} P_A (1-\theta). \qquad [2.30]$$

$$\boldsymbol{k_{1A}} = ae^{-Eads/RT} \quad [2.30a]$$

The rate of desorption of A is proportional to the amount of A on the surface, and the rate constant for desorption is also an exponential function of temperature.

$$\boldsymbol{r_{des,A}} = \boldsymbol{k_{2A}}\theta_A \quad [2.31]$$

$$k_{2A} = be^{-Edes/RT} \quad [2.31a]$$

The difference between E_{ads} and E_{des} is the heat of adsorption. If only A is adsorbed, then $\theta = \theta_A$, and at equilibrium the rates of adsorption and desorption are equal

$$k_{1A}P_A(1 - \theta_A) = k_{2A}\theta_A \quad [2.32]$$

$$\theta_A = \frac{k_{1A}\,P_A}{k_{2A}+k_{1A}P_A}. \quad [2.32a]$$

The ratio of adsorption to desorption rate constants is equilibrium constant with the units of reciprocal pressure.

$$K_A = \frac{k_{1\,A}}{k_{2\,A}} \quad [2.32b]$$

Dividing both terms of equation(2.32) by $k_{2\,A}$ and introducing K_A gives

$$\theta_A = \frac{K_A P_A}{1+K_A P_A} \quad [2.32c]$$

Equation (2.32c) is the langmuir isotherm for adsorption of a single species, and it shows that the amount adsorbed is nearly proportional to the pressure at low values of $K_A P_A$ and nearly independent of pressure when $K_A P_A$ is much larger than 1.0. large values of $K_A P_A$ correspond to nearly complete or monolayer coverage. The adsorption constant K_A is a measure of the strength of adsorption of A on that surface. When $P_A = \frac{1}{K_A}$,the surface is half covered with adsorbed A.

When two or more types of molecule can be adsorb on the same type of sites, they compete for places on the surface. For a binary mixture where both A and B adsorb as molecules the equations are:

$$A + S \rightarrow A_S \quad [2.33]$$

$$B + S \rightarrow B_S \quad [2.34]$$

$$r_{ads,A} = k_{1\,A}P_A(1 - \theta) = k_{1\,A}P_A(1 - \theta_A - \theta_B) \quad [2.35]$$

$$r_{des,A} = k_{2\,A}\theta_A \quad [2.36]$$

$$r_{ads,B} = k_{1\,B} P_B (1-\theta) = k_{1\,B} P_B (1-\theta_A-\theta_B) \quad [2.37]$$

$$r_{des,B} = k_{2\,B} \theta_B \quad [2.38]$$

By equating the rates of adsorption and desorption for both gases, the equilibrium coverages are obtained:

$$\theta_A = \frac{K_A P_A}{1+K_A P_A + K_B P_B} \ , \ \theta_B = \frac{K_B P_B}{1+K_A P_A + K_B P_B} \quad [2.39]$$

Extending the derivation to multicomponent mixtures gives extra terms in the denominator, such as $K_C P_C$ for a reaction product, or $K_P P_P$ for a trace impurities or poison that is chemisorbed.

$$\theta_A = \frac{K_A P_A}{1+K_A P_A + K_B P_B + K_C + K_P + \cdots} \quad [2.40]$$

2.5.2.2.3 Dissociating Gases

Diatomic gases often dissociate when adsorbing on metal catalysts. Using H_2 as an example, an isotherm can be derived assuming that two adjacent sites are needed for adsoption, and the probability for this varies with $(1-\theta)^2$:

$$H_2 + 2S \rightarrow 2H_s \quad [2.41]$$

$$r_{ads} = K_1 P_{H2} (1-\theta)^2 \quad [2.42]$$

Desorption requires reaction of two adjacent atoms to form a molecule that then desorbs. The atoms may move from site to site by surface diffusion, and the rate of collisions is proportional to the square of the surface concentration:

$$2H_S \rightarrow H_2 + 2S \quad [2.43]$$

$$r_{des} = k_2 \theta^2 \quad [2.44]$$

To get the equilibrium coverage, the rates of adsorption and desorption are set equal, and the square root of both sides is taken to solve for θ.

$$k_1 P_{H2} (1-\theta)^2 = k_2 \theta^2 \quad [2.45]$$

$$\frac{\theta}{1-\theta} = (k_1 P_{H2} / k_2)^{0.5} = K_{H2}^{0.5} P_{H2}^{0.5} \quad [2.46]$$

$$\theta = \frac{K_{H2}^{0.5} P_{H2}^{0.5}}{1+K_{H2}^{0.5} P_{H2}^{0.5}} \quad [2.47]$$

When H_2 is present a long with other gases that compete for the same sites, the isotherms are similar to equation (2.40), with $K_{H2}^{0.5} P_{H2}^{0.5}$ included.

$$\theta_H = \frac{K_H^{0.5} P_{H2}^{0.5}}{1+K_{H2}^{0.5} P_{H2}^{0.5}+K_A P_A+K_B P_B} \quad [2.48]$$

$$\theta_A = \frac{K_A P_A}{1+K_{H2}^{0.5} P_{H2}^{0.5}+K_A P_A+K_B P_B} \quad [2.49]$$

2.5.2.2.4 Langmuir –Hinshelwood Kinetics (LHHW)

The use of langmuir isotherms to interpret kinetic data was proposed by Hinshelwood and discussed at length by Houngen and Watson. Surface reaction rates are assumed to depend on the fraction of sites covered by different species. If the surface is at adsorption- desorption equilibrium, the equations for θ_A, θ_B, θ_H,etc.are used in the rate expressions, and the surface reaction is assumed to be the rate controlling step.

Consider first a unimolecular decomposition reaction where the products are not adsorbed or are very weakly adsorbed.

$A_S \rightarrow B + C + s$

$$r = k\theta_A = \frac{kK_A P_A}{1+K_A P_A} \quad [2.50]$$

The reaction would appear first order to A at low pressures, fractional order at intermediate pressures,and zero order at high pressure,where nearly all sites are covered with A. For an irreversible bimolecular reaction between molecules that are competitively adsorbed on the same type of sites,the reaction rate depends on the probability that the molecules are on adjacent sites. This probability is approximately proportional to the product of fractional coverages:

$A_S + B_S \rightarrow C_S + D_S$

$$r = k\theta_A\theta_B \quad [2.51]$$

Equation 2.51 can also be obtained by considering surface mitigation of adsorbed species. The reaction rate then depends on the rate of collisions which is proportional to the product of the surface concentrations. Adding the langmuir isotherms to equation [2.51] gives:

$$r = \frac{kK_A P_A K_B P_B}{(1+K_A P_A+K_B P_B+K_C P_C+K_D P_D)^2} \quad [2.52]$$

2.5.2.2.5 Non Competitive Adsorption

If a catalyst has two types of sites, a reaction might take place between reactant A adsorbed on one type of site and reactant B adsorbed on an adjacent but different type of site. The reaction rate would then depend on the fractional coverage of each type of site. In the simple case where only A adsorbs on type 1 sites and only B on type 2 site, the rate expression is given in below equation [2.53].

$A + S_1 \rightarrow AS_1$

$B + S_1 \rightarrow BS_1$

$AS_1 + BS_1 \rightarrow C$

$$r = \frac{kK_A P_A K'_B P_B}{(1+K_A P_A)(1+K'_B P_B)} \qquad [2.53]$$

The primed variable refer to type 2 sites. If the product is adsorbed on either type of site, term $K_C P_C$ or $K'_C P_C$ could added to the denominator terms. The main difference between equation [2.52] and [2.53] is that with non-competitive adsorption,the rate becomes independent of P_A and P_B at high partial pressures, whereas the rate eventually decreases with P_A or P_B if A and B are competitively adsorbed.

2.6 Thermodynamic Analysis

(Silvey, 2011) reported that,several thermodynamic studies have been performed to determine the optimum operating conditions for pure glycerol reforming. For the study of (Silvey, 2011),the thermodynamic equilibrium versus temperature was based off the minimization of Gibbs free energy. The calculations were performed in Aspen plus for a variety of different reactant feed conditions using a Gibbs free energy reactor.

As the report of(Nikoo & Amin, 2011), the accurate function to specify the equilibrium composition of a reaction system can be defined by Gibbs free energy minimization. The total Gibbs free energy of a single-phase only for a gas or a solid system at certified temperature and pressure in a fuction of equilibrium composition of compounds and can be respectively represented as equations below.

$$G^{tg}_{(T,P)} = \sum_{i=1}^{N} n_i \overline{G_i^g} = \sum_{i=1}^{N} n_i \mu_i^g = \sum_{i=1}^{N} n_i G_i^{\circ g} + RT \sum_{i=1}^{N} n_i \ln(\hat{f}_i^g / f_i^{\circ g}) \qquad [2.54]$$

$$G^{ts}_{(T,P)} = \sum_{i=1}^{N} n_i \overline{G_i^s} = \sum_{i=1}^{N} n_i \mu_i^s = \sum_{i=1}^{N} n_i G_i^{\circ s} + RT \sum_{i=1}^{N} n_i \ln(\hat{f}_i^s / f_i^{\circ s}) \qquad [2.55]$$

The superscript t,s and g were total,solid phase and gas phase respectively. Hence, the Gibbs free energy of a two-phase system can be written as equation [2.56]:

$$G^{t}_{(T,P)} = \sum_{i=1}^{N} n\,i G_i^{\circ g} + RT \sum_{i-1}^{N} n\,i \ln(\hat{f}\,i^{g}/f_i^{\circ g}) + \sum_{i=1}^{N} n\,i G_i^{\circ s} + RT \sum_{i=1}^{N} n\,i \ln(\hat{f}\,i^{s}/f_i^{\circ s}) \quad [2.56]$$

Since the standard state is defined as the pure ideal gas state at 1 atm $f_i^{\circ g} = P^{\circ} = 1$ and since $G_{i,e}^{\circ g} = 0$ for each element in its standard state;hence $G_i^{\circ g} = \Delta G_{fi}^{\circ g}$. Meanwhile, the solid phase is assumed as a pure solid carbon. (Nikoo & Amin, 2011), propose as the reference state for the solid phase is at atmospheric pressure and 25℃ ,the partial fugacity can be written as shown in equation below.

$$\hat{f}i^{s} = f_i^{\circ s} \quad [2.57]$$

Considering equation of chemical potential of carbon in an equilibrated gas to solid phase and appyling equation [2.55], along with the solid phase obtained is shown in equation [2.58].

$$\mu_c^g = \mu_c^s = \bar{G}c^g = \bar{G}c^s = G_c^{\circ s} = \Delta G_{fc}^{\circ s} \cong 0 \quad [2.58]$$

By substituting $\hat{f}i^{g} = y_i\,\varphi_i P$, $\hat{f}i^{g} = P^{\circ} = 1$ and $G_i^{\circ g} = \Delta G_{fi}^{\circ g}$ in equation [2.54]and using the lagrange multiplier method, the Gibbs free energy minimization of gaseous species can be expressed as equation [2.58].

$$\Delta G_{fi}^{\circ g} + RT \ln([\,y_i\,\varphi_i P]/P^{\circ}) + \sum_k a_{ik}\,\lambda_k = 0 \quad [2.59]$$

The equilibrium computations employing the RGIBBS reactor were accomplished with the Aspen plus,with the capability of simulating a maximum of nine phases of multicomponents at equilibrium in the reaction system. The pressure and temperature were varied in the range of 1-25 atm and 573-1473K respectively SOAVE-REDLICH-KWONG (SRK) model was used as the equation of state, since some polar components such as methanol and DME were considered as the products in the reaction system. Types of reactants, products and reaction phase have to be clarified to perform the equilibrium composition calculations.

The Gibbs free energy change of reaction for each reaction at different temperatures was calculated by equation [2.60]:

$$\Delta G_r^{\circ} = \sum_i \gamma_i\,\Delta G_{fi}^{\circ g} \quad [2.60]$$

Where γ_i is the stoichiometric coefficient of species i the equilibrium constant (k), obtained from equation [2.61], determined the feasible range of the spontaneous

occurance of the reactions.thermodynamic data such as Gibbs free energy of formation for all compounds were obtained else where.

$$\Delta G_r^\circ = -RT \ln k \qquad [2.61]$$

2.7 Process Simulation and Modeling using Apsen plus

Simulation model are tools that predict the performance and identify the limitations of processs by evaluating a proposed process flow sheet. Mathematical modeling is the primary basis for simulation models. Mathematical models are composed of material and energy balances, and are characterized by equations that relate process variables;such as: temperature, pressure, composition, and thermodynamic limitations of the system. These model solve for unknown process variables at steady state or dynamic conditions. A simulation model is represented by a process flow sheet with multiple units; where each unit signifies a certain process step. Each unit applies computer subroutines, which vary significantly in their degree of complexity due to their particular design specifications, to simulate the various process units. All raw material input stream are depicted by the arrow head pointing toward a process unit and the tail of the arrow is free. The temperature, pressure, component fraction of the flow rate must be defined for these input streams. The arrows between the units, where the arrow head and tail are connected to a unit, represent the flow information between the two individual units. This information is largely dependent upon the specific design constraints. Simulator include the most basic process equipment such as: heat exchangers, reactors, mixers,(Seider el al.,2004)

It is important to remember that a process model is nothing more than mathematical abstraction of real process. Processs modelling is both an art and a science. Creativity is required to make simplifying assumptions that result in appropriate model. The model should incoperate all of the important dynamic behaviour while being no more complex than is necessary. Thus, less important phenomena are omitted in order to keep the number of model equations variable, and parameters are reasonable levels. Process models can determine and closely approximate performance of different unit operation and unit processes. Additionally, energetic bottlenecks in the process and theoretical ceiling of a process can be determined quickly and accurately without need to carryout several additional experiments.Although, it must be emphasized that there is a definite place and value for experimental work, the advantages in determining

feasibility of processes make simulation software and models a powerful resource. Simulations are mathematical models that determine elemental material balances and energy balances. Based on these balances, the effect of parameters such as temperature, pressure and concentration during a given process can be ascertained either in steady state, equilibrium conditions or unsteady state scenarios.

Most simulation setups are first represented by a process flow sheet similar to a process flow diagram representing a flow of data from one block (which may be a unit operation or process or a piece of equipment) as opposed to a flow of actual chemical streams. Additionally, various unit operations and their design specifications can be specified such as heat exchangers, phase separators, distillation columns and so on. The most important outcome of running simulations is to not only obtain theoretical limitations, but to also test the effect of different process variables and their effect on the overall outcome of the process. This reduces the need for several time intensive experiments. Apart from optimizing the overall process, each individual unit operation can be looked at separately, eliminating and correcting bottlenecks in the process. Therefore, the use of process modelling and simulations represents a good starting point for a thorough analysis of a process and a process design. (Siddharth Rao Gumuluru, 2012).

2.7.1 Introduction to Aspen plus

Aspen Plus is advanced system process engineering software which is used to simplify calculations of unit process and unit operation. It is a versatile computing tool that allows users to simulate actual plant behaviour, using realistic operating conditions, accurate equipment models thermodynamic data together with a vast range of engineering relationships, such as mass and energy balances, phase and chemical equilibrium and reaction kinetics. Aspen Plus enables companies to reduce capital and operating costs and to maximize plant performance and profitability.

The program includes a library of standard unit operation blocks, such as pumps, heat exchangers, reactors, splitters, which represent processes taking place in an actual chemical plant. The simulation of a process plant is done by specifying configurations of unit operations and the flow of material, heat and work streams. Aspen Plus also

has an extensive components database containing physical properties of a large number of pure components.

Within the program there exist mathematical routines or convergence algorithms for solving different equations of material and energy balances as well as equilibrium equations. Aspen Plus uses a sequential modular approach to flow sheet convergence, where mass and energy balances for individual unit operation blocks are computed sequentially.

Aspen Plus is also able to handle recycle streams, using a feature called tear-streams. Stream and block variables have to be manipulated iteratively, to converge upon the mass and energy balance, until it obtains a solution. To be able to construct a process model in a flow sheet program the following three steps are necessary:

i. Flow sheet definition: all inlet streams to the system have to be defined as well as different unit operations and their interconnecting streams. The flow sheet also indicates all outlet or product streams.
ii. Chemical components: all chemical components in the system, from reactants to intermediates and products must be specified.
iii. Operating conditions: the operating conditions, such as temperature, pressure, heat duties etc., for every unit operation must be specified. All input streams have to be completely defined.

2.7.2 Process Flow Description

Glycerol dry reforming is potential method in production of CO rich syngas by consuming greenhouse gases ($CO2_)$ and glycerol. This is endothermic reaction which is supported by heat from the reformer furnace. This support is direct; through the heating of catalyst filled tube that from the reactor. This reformer model incorporates three separate equilibrium reactors. The synthesis gas from the reformer is rich in CO, the shift reaction can be used to increase the Hydrogen content and decrease the content of CO. The equilibrium for this reaction favours the product at low reaction temperatures, but high temperature is required to achieve a practical reaction rate.

This dilemma is normally addressed through the use of two stage shifting system. In the first stage high temperature is required typically (573 – 873 K) reactor inlet temperature. The temperature will increase in the reactor due to the exothermic nature of the shift reaction. At this temperature the shift is promoted by a low cost iron based

catalysts and reduce the CO concentration to a few percent. In the second stage of the shift a lower temperature is used (453 – 523 K) to increase equilibrium concentration of hydrogen. A more expensive, copper based catalyst is required.

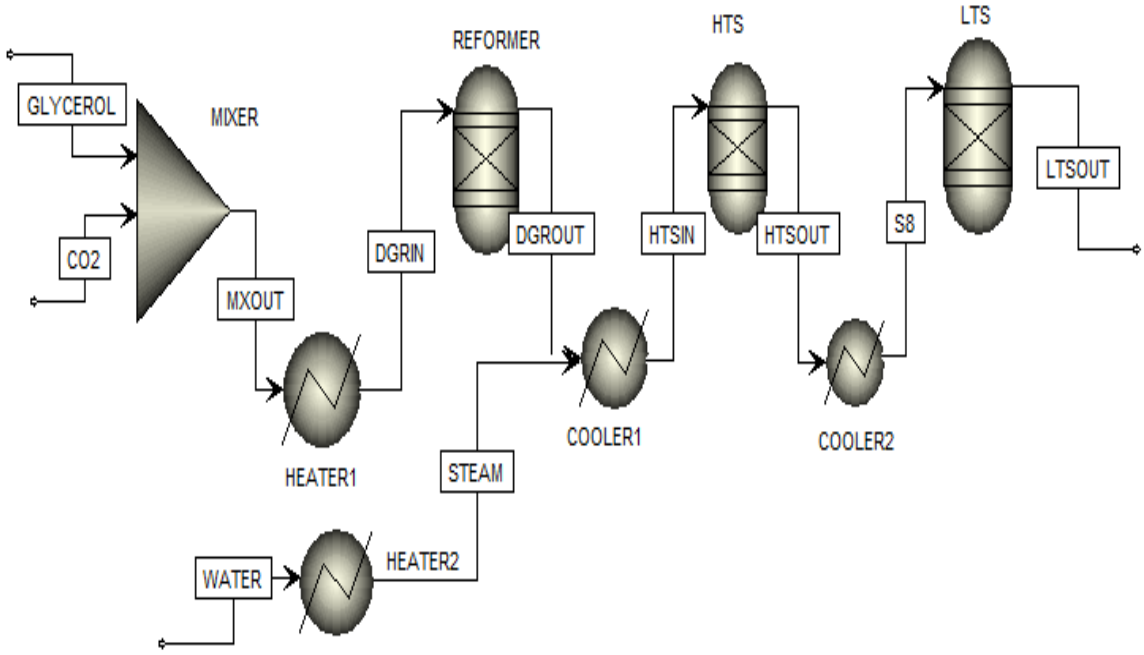

Figure 2.1: Process flow diagram of glycerol dry reforming using Aspen plus

3 Materials and Methods

3.1 Process Modelling and Simulation

The modelling process and simulation were classified in to two parts; the first part was RGIBBS modelling and simulation and the second part was RPLUG which was kinetic modelling. RGIBBS models single phase chemical equilibrium, or simultaneous phase and chemical equilibrium. RGIBBS minimizes Gibbs free energy, subject to atom balance constraints. This reaction does not require stoichiometric. It can determine phase equilibrium without chemical reaction, particularly for multiple liquid phases. The other is RPLUG rigorously models plug flow reactors. A cooling stream around the reactor is optional. RPLUG handled rate based kinetic reactions only. The detail of the two parts mentioned as follows. For the first detail which was the RGIBBS modelling and simulation; the syngas production process was modelled with Aspen plusV8.8. The components involved in this study for RGIBBS were glycerol($C_3H_8O_3$) and carbon dioxide (CO_2) as a feed meanwhile, ethylene (C_2H_4), ethane (C_2H_6), hydrogen (H_2), methane (CH_4), carbon monoxide (CO) were the reaction products. The thermodynamic method used in this is SRK and this method is suitable for non polar and polar compounds in combinations with light gases. The feed stream to the dry glycerol reformer (DGR) reactor was glycerol and carbon dioxide and methane for furnace used as a fuel. Both of the feed streams to the DGR were mixed in mixer1 before heated up to the temperature specified in the thermodynamic investigation. The output streams from the heater were then introduced to the DGR reactor were then fed to the water gas shift (WGS) reactor at temperature specified in the thermodynamic investigation. Both the DGR and WGS reactors were modelled using RGIBBS model block from Aspen plus model libraries. The heat required for the phase change was calculated and see in Appendix A.

For the second detail; which was the RPLUG modelling and simulation; the syngas production process was modelled with Aspen plusV8.8. The components involved in this study for RPLUG were glycerol ($C_3H_8O_3$) and carbon dioxide (CO_2) as a feed meanwhile, hydrogen (H_2), and carbon monoxide (CO) were the reaction products. The thermodynamic method used in this is SRK and this method is suitable for non polar and polar compounds in combinations with light gases.

The feed stream to the dry glycerol reformer (DGR) reactor was glycerol and carbon dioxide. Both of the feed streams to the DGR were mixed in mixer1 before heated up to the temperature specified in the thermodynamic investigation. The output streams from the heater were then introduced to the DGR reactor were then fed to the water gas shift (WGS) reactor at temperature specified in the thermodynamic investigation. Both the DGR and WGS reactors were modelled using RPLUG model block from Aspen plus model libraries. The diameter of DGR reactor was 0.5 meter and the length was 10 meter. Higher water gas shift (HWGS) reactor was modelled using RPLUG model block. The HWGS reactor diameter was 0.3 meter and the length was 5 meter. Lower water gas shift (LWGS) reactor was modelled using RPLUG model block. The LWGS diameter was 2.5 meter and the length was 1 meter. For the two reactor model process flow diagrams see Appendix D-1 and AppendixD-2.

3.1.1 Thermodynamic Investigation

As mentioned in the specific objective, one of the aims of the research was set up thermodynamics investigation for the glycerol dry reforming by using Aspen plus software. Thermodynamics investigations for dry reforming of glycerol for different parameters sensitivity will be calculated by using commercial Aspen Plus software along with its physical property models. This thermodynamic investigation was classified into two parts: the first is the procedure available in the subroutine of RGIBBS which utilizes the Gibbs free energy minimization method was used to determine the thermodynamic equilibrium composition of each phase present. The SRK, PENG-ROB, LK-PLOCK (lee-kesler plocker) was available as the equation of state to correct the ideal Gibbs free energy value. The thermodynamic analysis was performed at temperature range of 573 K to 1273 K, pressure between 1 and 30 bars and feed ratio of glycerol to carbon dioxide is 1 to 5 for glycerol reforming. For both water gas shift reaction the thermodynamic investigation was performed at temperature range of 453K to 873 K and pressure range of 1 bar to 20 bars and temperature range 453 to 523 K and pressure range 1 bar to 15 bar for HWGS and LWGS respectively. The second is the procedure of kinetics and the detail is as follow in kinetic modelling.

3.1.2 Kinetic Modelling for Dry Glycerol Reforming

Kinetics data for glycerol dry reforming was obtained from literature and simulation was performed in ASPEN PLUS using kinetics based reactor model block with rearranged power law kinetic model and Langmuir –Hinshelwood Hougen Watson (LHHW) kinetic models. For Aspen plus flow diagram of DGR and WGS see Appendix D1. To reduce the complexity in the modelling of the reaction kinetics, only those reactions which play significant role in the overall process were considered. The chemical reactions used in the reactor modelling were, reactions of glycerol dry reforming and water gas shift reaction. In order to investigate the different effects of operating parameters on the rate of glycerol reforming and syngas production; two main kinetic models were used in this study. The first was **power law** kinetic modelling and the second was **Langmuir –Hinshelwood – Hougen Watson** (LHHW) kinetic modelling. The detail of the two kinetics models is as follows:

3.1.2.1 Power law Kinetic Modelling

In this study the power law kinetic model was developed for two reactor models. They are the DGR and WGS. For the DGR the glycerol consumption rates were also obtained at temperature of 923K and 1123K. The collected data sets were subsequently fitted with the power law equation to obtain the kinetic parameters as shown in equation [3.0] below.

$$r = k_o e^{-\frac{Ea}{RT}} (P_{C3H8O3})^{\propto} (P_{CO2})^{\beta} \qquad [3.0]$$

Where:

r = Glycerol consumption rate ($\frac{\text{mol}}{\text{g.sec}}$

k_o = Exponential factor

Ea = Activation Energy ($\frac{\text{KJ}}{\text{mol}}$)

R = Ideal gas constant

T = Temperature (K)

P_{C3H8O3} = Glycerol partial pressure (BAR)

P_{CO2} = Carbon dioxide partial pressure (BAR)

α = reaction order with respect to Glycerol

β = reaction order with respect to carbon dioxide

The resulting kinetics parameters from the fitting exercise are listed in table 3.1 below as follows:

Table 3.1: kinetic parameters of the glycerol consumption rate from the power law modelling(Weng et al., 2015)

Parameter	Value
k_o	$2.6 * 10^{-4}$
Ea (KJ/mol)	35
α	0.72
β	0.14

For the WGS reactor the carbon monoxide consumption rates were also obtained at temperature of 923K and 1000K. The collected data sets were subsequently fitted with the power law equation to obtain the kinetic parameters as shown in equation [3.1] below.

$$r = k_o e^{-\frac{Ea}{RT}} (P_{CO})^{\gamma} (P_{H2O})^{\emptyset} \qquad [3.1]$$

Where:

$r =$ Glycerol consumption rate $(\frac{\text{mol}}{\text{g.sec}}$

$k_o =$ Exponential factor

Ea = Activation Energy $(\frac{\text{KJ}}{\text{mol}})$

R = Ideal gas constant

T = Temperature (K)

P_{CO} = carbon monoxide partial pressure (BAR)

P_{H2O} = Water partial pressure (BAR)

γ = reaction order with respect to carbon monoxide

$\emptyset$ = reaction order with respect to water

The resulting kinetics parameters from the fitting exercise are listed in table 3.1 below as follows:

Table 3.2: kinetic parameters of the carbon monoxide consumption rate from the power law modelling(Weng et al., 2015)

Parameter	Value
k_o	$7.4 * 10^{11}$
Ea (KJ/mol)	288.3
γ	0.5
$\emptyset$	1

3.1.2.2 Langmuir-Hinshelwood-Watson (LHHW) kinetic modelling

LHHW is usually occurring when we have adsorption surface, which is typical of catalyst and from the typical of catalyst reaction syngas production is one. In this study LHHW kinetic model was applied for three kinetic model blocks; they are: 1.dry glycerol reforming reactor (DGR), 2. High temperature water gas shift reactor (HWGS) and 3. Low temperature water gas shift reactor (LWGS). The details of the three kinetic models via LHHW are as follows: Syngas production via glycerol dry reforming involves reaction between glycerol and carbon dioxide to produce syngas in catalytic fixed bed reactor with a molar ratio $C_3H_8O_3$ and CO_2 based on the following formula:

$$C_3H_8O_3 + CO_2 \rightarrow 4CO + 3H_2 + H_2O \quad [3.2]$$

The rate expression for the dry glycerol reforming reaction, r_{DGR}based on Langmuir – Hinshelwood-Watson (LHHW) mechanism on nickel based catalyst is as follows:

$$r_{DGR} = \frac{kK_{Gly}K_{CO2}P_{Gly}P_{CO2}}{N} \quad [3.3]$$

Where N represents

$$N = (1 + K_{H2O}P_{H2O} + K_{CO2}P_{CO2} + K_{CO2}K_{H2O}P_{CO2}P_{H2O} + K_{Gly}P_{Gly} + K_{Gly}K_{H2O}P_{Gly}P_{H2O} + K_{Gly}K_{CO2}P_{Gly}P_{CO2} + K_{Gly}K_{CO2}K_{H2O}P_{Gly}P_{CO2}P_{H2O})$$

Where, k is the rate constant for DGR. Pi and Ki are the partial pressure and adsorption equilibrium constant of component i, it represents$C_3H_8O_3$, CO_2 and H_2O.

3.1.2.3 Steps of LHHW in Aspen plus for Dry Glycerol Reforming

The rate of reaction is made of kinetic factor multiplied for theta (θ) glycerol and carbon dioxide that are the following.

$$r_{DGR} = k\theta_{Gly}\theta_{CO2} \quad [3.3a]$$

$$\theta_{Gly} = \frac{K_{Gly}P_{Gly}}{(1+K_{Gly}P_{Gly}+K_{CO_2}P_{CO_2})} \quad [3.3b]$$

$$\theta_{CO2} = \frac{K_{CO_2}P_{CO_2}}{(1+K_{Gly}P_{Gly}+K_{CO_2}P_{CO_2})} \quad [3.3c]$$

For every constant there were the pre-exponential value and the activation energy in table (3.4). The problem is that in Aspen Plus we have to insert Langmuir kinetics as the combination of three terms: a kinetic factor, the driving force and adsorption constant expressions. For this reason we have to combine the theta θ factors to obtain this expression. There were needs also the value for constants that are the products of constants because Aspen Plus requires only one input. Another problem is that Aspen plus wants the K in the logarithmic form. So we have to insert A and B values for every constant, where A is the logarithmic of the pre-exponential factor. We were converting the value in the international system and apply the logarithmic. B instead is the ratio of the activation energy and the universal constant with the opposite sign. Then add the Langmuir kinetics in Aspen plus. Go to in reactions and click on new choosing Langmuir (LHHW). Add the reactants on the left with negative coefficients, and the products on the right. Choose the reaction type as kinetic and click on next. Under the kinetic tab, see that the stoichiometric of the reaction is correct and set vapour reacting phase and cat (wt) for the rate basis. Add the kinetic factor, the pre-exponential constant is in the SI, while can choose the unit for the activation energy. Under this tab the value for reference temperature is not known, so leave it empty. Set the driving force. The concentration basis is partial pressure, the term 1 is for the direct reaction and the exponents are only for the reactants, accordingly, 1 for glycerol and 1 for carbon dioxide. Set the driving force constant as one so insert A usual zero. There was no reverse reaction, so click on term 2 and set a large negative value for A. The last step is defining adsorption expression that is the denominator of the rate of reaction. For the glycerol dry reforming adsorption expression the exponent is 1. In concentration exponents first of all add the species and then after insert the exponent

for eight terms in equation [3.3]. All the term have adsorption constants which are added using A and B coefficients as mentioned in equation [3.12].

The rate expression above cannot be used directly in Aspen plus as the general equation for LHHW used the following equations.

$$r = \frac{(kinetic\ factor)(driving\ force)}{Adsorption\ term} \quad [3.4]$$

Where,

Kinetic factor can be expressed as if To is not specified:

$$kinetic\ factor = k_o T^n e^{-Ea/RT} \quad [3.5]$$

Or

If To is specified the kinetic factor expression is as follows:

$$kinetic\ factor = k_o (T/T_o)^n e^{-\frac{Ea}{RT}(\frac{1}{T} - \frac{1}{T_o})} \quad [3.6]$$

Where $k_o$the pre-exponential factor in the Arrhenius expression, Ea is is the activation energy and it is possible to express dependence from temperature through the exponent n, which is often to zero. Alternatively, it is possible to refer the temperature dependence of the kinetic constant in comparison to a reference temperature To, where ko is known.

The "driving force" factor expresses the available amount of the reactants in gases phase is as follows:

$$Driving\ force = \ Ki \prod_{i=1}^{N} P_i^{\propto} \quad [3.7]$$

The term referred as "adsorption" must be entered in the following form:

$$Adsorption = [\sum_{i=1}^{m} Ki \ \prod_{i=1}^{N} P_J^M]^m \quad [3.8]$$

Where Ki, represent the adsorption constants for each species.

In Aspen plus, the pre-exponential constants and adsorption constants used the following equation:

$$K = Ae^{(\frac{B}{T})} T^C e^{(DT)} \quad [3.9]$$

The equation does not fit equation [3.9] and need to be rearranged using natural logarithm ln and some rearrangements. Aspen plus wants the k in the natural logarithmic form; therefore the expression for equation above in terms of natural logarithm ln was:

$$\ln K = A + \frac{B}{T} + C \ln T + DT \quad [3.10]$$

The natural logarithmic form of rate constant expression is as follows:

$$\ln K = \ln k_o - \frac{E}{RT} \quad [3.11]$$

Equalization of the two equations [3.10] and [3.11] above is giving the equality of the value as follows below:

$$A = \ln k_o \;\; and \; B = \frac{-E}{R} \quad [3.12]$$

Where, A is the logarithmic of pre –exponential factor we have to convert first the value in the SI and apply the logarithmic. B instead is the ratio of the activation energy and the universal constant with the opposite sign.

Table 3.3: Rate parameters of glycerol dry (CO_2) reforming (Hundessa D. Demsash, Kondamudi, Upadhyayula, & Mohan, 2018)

Species	$K_{reaction}$	Ea(KJ/mol)
$C_3H_8O_3$	$1.1 * 10^5$	70.82
CO_2	$0.91 * 10^5$	73.18
CO	$0.71 * 10^5$	90.42
H_2	$2.4 * 10^5$	55.79
H_2O	$5.57 * 10^{-5}$	88.68

Assumptions for this model:

- System is steady state conditions
- Coke formation is neglected
- The reactor is operated at adiabatically condition
- Weak adsorption for $H_2 \; and \; CO$ therefore neglected the adsorption constants of the two.

Table 3.4: The kinetic coefficient and equilibrium constants for equation [3.3]

Reaction constant		Pre-exponential factor	Activation Energy(Ea) KJ/mol
H_2O	K_{H2O}	$5.57 * 10^{-5}$	88.68
CO_2	K_{CO2}	$0.91 * 10^{5}$	73.18
$C_3H_8O_3$	K_{Gly}	$1.1 * 10^{5}$	70.82
	$K_{CO2}\,K_{H2O}$	5.0687	161.86
	$K_{Gly}\,K_{H2O}$	6.127	159.5
	$K_{Gly}\,K_{CO2}$	$1.0 * 10^{10}$	144
	$K_{Gly}\,K_{CO2}K_{H2O}$	$5.57 * 10^{5}$	232.68

Glycerol dry reforming Adsorption constants in Aspen plus in equation [3.3] are shown in table 3.5

Table 3.5: Adsorption constants fitting in Aspen plus for dry glycerol reforming

Parameter	A($\ln Ki$)	$B(-E/R)$
K_{H2O}	-9.7955	-10660
K_{CO2}	11.4188	-8802
K_{Gly}	11.6082	-8518.16
$K_{CO2}\,K_{H2O}$	1.6230	-19468.36
$K_{Gly}\,K_{H2O}$	1.8127	-19184.5
$K_{Gly}\,K_{CO2}$	23.0858	-17320.18
$K_{Gly}\,K_{CO2}K_{H2O}$	13.2303	-27986.53

$kinetic\ factor\ of\ DGR = kK_{Gly}K_{CO2} = 2.776 * 10^{-7}\ \frac{mol}{kg\ .s\ bar^2}$ and

$Activation\ Energy = 273.3\ KJ/mol$

The second rate expression was; the rate expression for the High temperature water gas shift (HWGS) reaction, r_{HWGS}based on Langmuir –Hinshelwood-Watson (LHHW) mechanism on nickel based catalyst is as follows:

$CO + H_2O \rightarrow H_2 + CO_2$ [3.13]

$r_{HWGS} = \frac{kK_{CO}K_{H2O}P_{CO}P_{H2O}}{N}$ [3.14]

Where N represents

$$N = (1 + K_{CO}P_{CO} + K_{H2O}P_{H2O} + + K_{CO2}P_{CO2})^2$$

Where, k is the rate constant for HWGS. Pi and Ki are the partial pressure and adsorption equilibrium constant of component i, it represents, CO, CO_2 and H_2O.

The rate expression above cannot be used directly in Aspen plus as the general equation for LHHW used the [3.4] equations.

The driving force and adsorption constants were discussed in equations [3.7] and [3.8] respectively. In Aspen plus, the pre-exponential constants and adsorption constants were discussed in equation [3.9]. Additionally, the expression of equations of [3.10 - 3.12] are all used for kinetic model of WGS in LHHW kinetic.

3.1.2.4 Steps of LHHW in Aspen plus for WGS

The rate of reaction is made of kinetic factor multiplied for theta (θ) carbon monoxide and water that are the following.

$$r_{WGS} = k\theta_{CO}\theta_{H2O} \quad [3.14a]$$

$$\theta_{CO} = \frac{K_{CO}P_{CO}}{(1+K_{CO}P_{CO}+K_{CO2}P_{CO2}+K_{H2O}P_{H2O})} \quad [3.14b]$$

$$\theta_{H2O} = \frac{K_{H2O}P_{H2O}}{(1+K_{CO}P_{CO}+K_{CO2}P_{CO2}+K_{H2O}P_{H2O})} \quad [3.14c]$$

For every constant there were the pre-exponential value and the activation energy in table (3.6 and 3.8). The problem is that in Aspen Plus we have to insert Langmuir kinetics as the combination of three terms: a kinetic factor, the driving force and adsorption constant expressions. For this reason we have to combine the theta θ factors to obtain this expression. There were needs also the value for constants that are the products of constants because Aspen Plus requires only one input. Another problem is that Aspen plus wants the K in the logarithmic form. So we have to insert A and B values for every constant, where A is the logarithmic of the pre-exponential factor. We were converting the value in the international system and apply the logarithmic. B instead is the ratio of the activation energy and the universal constant with the opposite sign. Then insert the Langmuir kinetics in Aspen plus. Go to in reactions and click on new choosing Langmuir (LHHW). Add the reactants on the left with negative coefficients, and the products on the right. Choose the reaction type as kinetic and click on next. Under the kinetic tab, see that the stoichiometric of the reaction is correct and set vapour reacting phase and cat (wt) for the rate basis. Add the kinetic factor, the pre-exponential constant is in the SI, while can choose the unit for the activation energy. Under this tab the value for reference temperature is not

known, so leave it empty. Set the driving force. The concentration basis is partial pressure, the term 1 is for the direct reaction and the exponents are only for the reactants, accordingly, 1 for carbon monoxide and 1 for water. Set the driving force constant as one so insert A usual zero. There was no reverse reaction, so click on term 2 and set a large negative value for A. The last step is defining adsorption expression that is the denominator of the rate of reaction. For the WGS reaction adsorption expression the exponent is 2. In concentration exponents first of all add the species and then after insert the exponent for four terms in equation [3.14]. All the term have adsorption constants which are added using A and B coefficients as mentioned in equation [3.12].

Table 3.6: Rate parameters of High temperature water gas shift (HWGS)(Ahmad, 2017)4

Species		(Frequency factor (bar^{-1})	Ea(KJ/mol)
CO	K_{CO}	2.2393	-910
H_2O	K_{H2O}	0.4053	-1420
CO_2	K_{CO2}	0.052689	-14400
H_2	K_{H2}	0.004762	-24720

Assumptions in HWGS kinetic model study was

- System is steady state conditions
- The reactor is operated at adiabatically condition
- Weak adsorption for H_2 therefore neglected the adsorption constants of the H_2 .

High Temperature Water Gas Shift reaction, Adsorption constants in Aspen plus in equation [3.14] are shown in table 3.7

Table 3.7: Adsorption constants fitting in Aspen plus for HWGS5

Parameter	A($\ln Ki$)	$B(-E/R)$
K_{CO}	0.806	109.45
K_{H2O}	-0.9031	170.78
K_{CO2}	-5.347	2973

$kinetic\ factor\ of\ HWGS = ko = 0.8961 \frac{mol}{kg\ .s\ bar^2}$ And

$Activation\ Energy = 4.08\ KJ/mol$

The third rate expression was; the rate expression for the Low temperature water gas shift (LWGS) reaction, r_{LWGS}based on Langmuir –Hinshelwood-Watson (LHHW) mechanism on nickel based catalyst is as follows:

$$CO + H_2O \rightarrow H_2 + CO_2 \quad [3.14]$$

$$r_{LWGS} = \frac{kK_{CO}K_{H2O}P_{CO}P_{H2O}}{N} \quad [3.15]$$

Where N represents

$$N = (1 + K_{CO}P_{CO} + K_{H2O}P_{H2O} + +K_{CO2}P_{CO2})^2$$

Where, k is the rate constant for LWGS. Pi and Ki are the partial pressure and adsorption equilibrium constant of component i, it represents, CO, CO_2 and H_2O.

The rate expression above cannot be used directly in Aspen plus as the general equation for LHHW used the [3.4] equations.

The driving force and adsorption constants were discussed in equations [3.7] and [3.8] respectively. In Aspen plus, the pre-exponential constants and adsorption constants were discussed in equation [3.9]. Additionally, the expression of equations of [3.10 - 3.12] are all used for kinetic model of LWGS in LHHW kinetic.

Table 3.8: Rate parameters of Low Temperature water gas shift (LWGS)(Ayastuy, Gutiérrez-Ortiz, González-Marcos, Aranzabal, & González-Velasco, 2005)6

Species		(Frequency factor (bar^{-1})	Ea(KJ/mol)
CO	K_{CO}	$1.737 * 10^{-11}$	-11.35
H_2O	K_{H2O}	$4.668 * 10^{-12}$	-14.90
CO_2	K_{CO2}	$3.563 * 10^{-12}$	-16.38
H_2	K_{H2}	$4.441 * 10^{-12}$	-14.44

Assumptions in LWGS kinetic model study was

- System is steady state conditions
- No reverse reaction
- The reactor is operated at adiabatically condition
- Weak adsorption for H_2 therefore neglected the adsorption constants of the H_2 .

Low Temperature Water Gas Shift reaction, Adsorption constants in Aspen plus in equation [3.15] are shown in table 3.9

Table 3.9: Adsorption constants fitting in Aspen plus for LWGS

Parameter	A($\ln Ki$)	$B(-E/R)$
K_{CO}	-24.776	1.365
K_{H2O}	-26.090	1.792
K_{CO2}	-26.361	1.970

$kinetic\ factor\ of\ LWGS = ko = 2.5975 * 10^5 \frac{mol}{kg\ .s\ bar^2}$ And

$Activation\ Energy = 57.47\ KJ/mol$

3.1.3 Sensitivity Analysis for Dry Glycerol Reforming

Sensitivity analysis of the reactor performance was done by changing several operating conditions, namely catalyst weight, reactor temperature, pressure and feed ratio of carbon dioxide to glycerol into the reactor. During sensitivity analysis, the manipulated variables were varied while the other design parameters remain unchanged. Thermodynamic analysis was evaluated under this analysis and following activity was conducted. The procedure available in the subroutine of RGIBBS which utilizes the Gibbs free energy minimization method was used to determine the thermodynamic equilibrium composition of each phase present. The SRK, PENG-ROB, was available as the equation of state to correct the ideal Gibbs free energy value. The thermodynamic analysis was performed for temperature range of 300 ℃ to 1000 ℃ pressure between 1 and 30 atm and feed ratio of glycerol to carbon dioxide is 1 to 5.Thermodynamic analysis was studied in order to estimate the effect of the following.

a. Glycerol total conversion
b. Glycerol conversion to gaseous product
c. Syngas (hydrogen and carbon monoxide) selectivity and yield
d. Selectivity of gaseous product
e. Molar ratio of glycerol to carbon dioxide and hydrogen to carbon monoxide
f. Possible reactions during dry reforming of glycerol are shown in table3.13 below, R_1 represent overall glycerol dry reforming while reaction R_2 to R_{11} are

possible side reactions. Equations listed below were used for conversion, selectivity and yield calculation respectively.

Table 3.10: Possible reactions during the dry glycerol reforming (Hundessa Dessalegn Demsash & Mohan, 2016)

NO. of Reaction	Reactions	Remark
R_1	$C_3H_8O_3+CO_2 \rightarrow 3H_2+4CO+H_2O$	Overall dry reforming
R_2	$C_3H_8O_3 \leftrightarrow 4H_2+3CO$	Direct glycerol decomposition
R_3	$CO + 3H_2 \leftrightarrow CH_4 + H_2O$	Methanation
R_4	$C_3H_8O_3 \leftrightarrow C_2H_4+CO+2H_2O$	Decomposition of glycerol
R_5	$C_2H_4 + H_2 \leftrightarrow C_2H_6$	Hydrogenation ethylene
R_6	$CH_4 + H_2O \leftrightarrow CO+3H_2$	Methane steam reforming
R_7	$CH_4 + CO_2 \leftrightarrow 2H_2 + 2CO$	Methane dry reforming
R_8	$CO + H_2O \leftrightarrow H_2 + CO_2$	Water gas shift reaction
R_9	$C_2H_4 \leftrightarrow 2C + 2H_2$	Ethylene decomposition
R_{10}	$CH_4 \leftrightarrow C(s) + 2H_2$	Methane decomposition
R_{11}	$2CO \leftrightarrow C(s) + CO_2$	Boudouard reaction
R_{12}	$CO + H_2 \leftrightarrow C(s) + H_2O$	CO gasification
R13	$C(s)+2H_2O \leftrightarrow CO_2 + 2H_2$	Coke gasification

4. Results and Discussion

4.1 Thermodynamics Analysis to Produce Syngas via Glycerol Dry Reforming

It is well known that glycerol dry reforming is strongly endothermic and ideally it must be carried out at high temperature, low pressure and partially high carbon dioxide to glycerol ratio to achieve high conversion. The thermodynamics analysis can be achieved maximum high yield based on the reaction conditions favoured. In this work, thermodynamics analysis was done using Aspen plus ^{TM} simulator. The simulation was classified in to two reactor model parts: RGIBBS reactor model and RPLUG kinetic reactor model. The details of the two reactor models are as follows with parameters affecting the process in each section.. The sensitivity analysis of each reactor model was based on the parameters affecting the process performed. The procedure of RGIBBS and RPLUG reactor model was available in the subroutine RGIBBS and RKSMHV2 respectively and used to determine the thermodynamic equilibrium compositions of each species present. SRK was chosen as the equation of state to correct the ideal value. The operating parameters of the two reactor model was somewhat different each other. The effect of operating parameters of RGIBBS reactor model such as temperature, pressure and feed ratio carbon dioxide to glycerol on syngas production and the effect of operating parameters of RPLUG reactor model was also temperature, pressure, feed ratio, length of the reactor, diameter, and catalyst particle density. Under this process the product composition were evaluated with follows water gas shift reactor.

4.1.1 Effect of Temperature on RGIBBS Reformer

The effect of variation on product composition, conversion, yield and selectivity are shown in fig below. During this sensitivity analysis, other reforming parameters such as feed ratio and pressure were held constant. The effect of temperature under this study was classified into effect of temperature before optimization and after optimization. Based on these; all of the parameters have been discussed, before optimization and after optimization. Conversion of glycerol over range of temperature was found 100% hence there is no point to discuss effect of temperature on glycerol conversion. The amount of syngas produced from dry glycerol was appreciably increased with temperature 573K to 1273K in the product stream. The amount of CH_4

and CO_2, decreased with increasing temperature. Meanwhile, the amount of CO_2 decreased gradually with increased temperature; this is because of the conversion of CO_2 was increased with increased temperature. Particularly the amount of H_2O and H2 concentration is found to rise in the whole range of temperature investigated (573K to1273K). The amount of C_2H_4, $C_3H_8O_3$ and C_2H_6 were remains negligible with increased temperature. The yields of H_2 and CO are found to be in the range of 0.146% to 70.3% and 100% to 434.4% respectively. The highest yields of H_2 and CO were obtained at temperature of 1273K .However; the highest yield of CO was start at temperature of 573K. The selectivity and the syngas ratio (H_2/CO) have reverse approach based on the figure 4.3. The selectivity of H_2 was highly increased with increase of temperature in the stream. On the other hand syngas ratio was decreased with increase of temperature. This is because CO being highly increased with increase temperature than H_2.

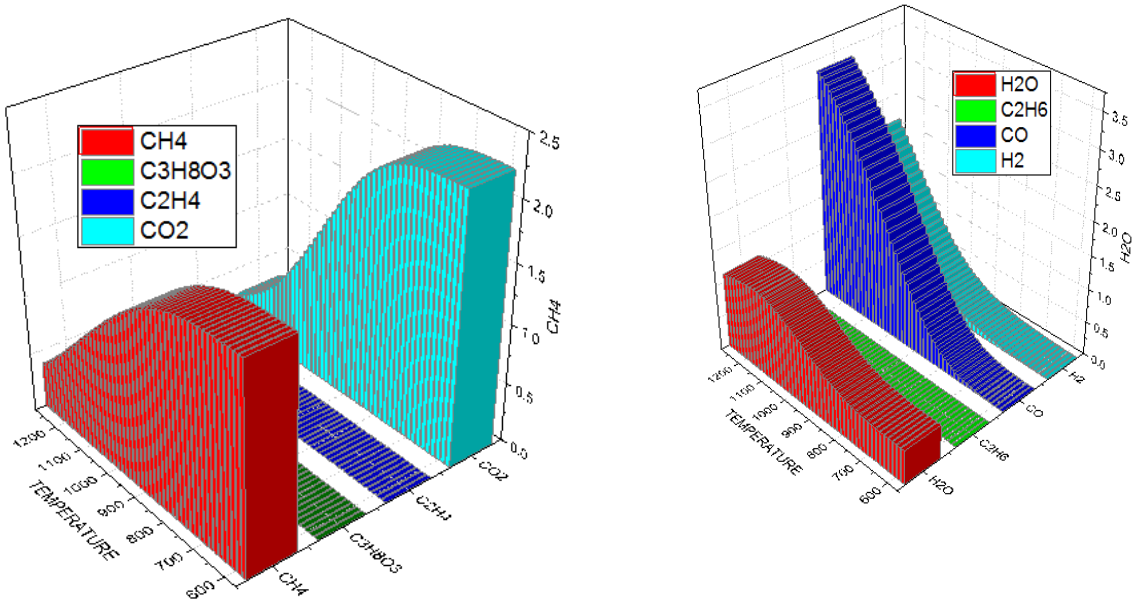

Figure 4.1: Product distributions of CO_2, $C_3H_8O_3$, CO, H2O, CH4, C2H4, C2H6 and H_2O versus temperature

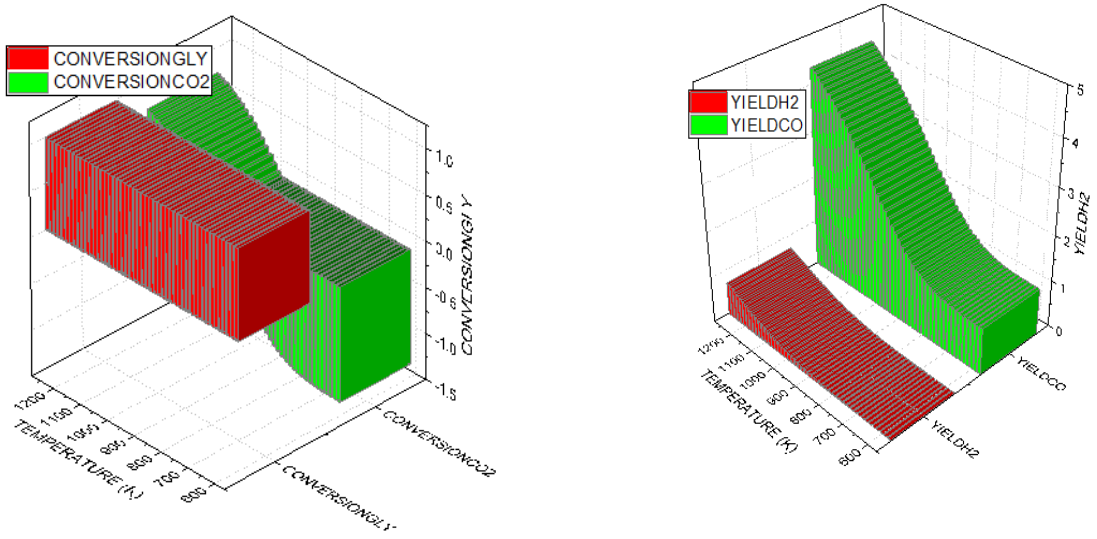

A B

Figure 4.2: (A) Conversion of CO_2, and $C_3H_8O_3$, and (B) Yield of CO, and H2 versus temperature

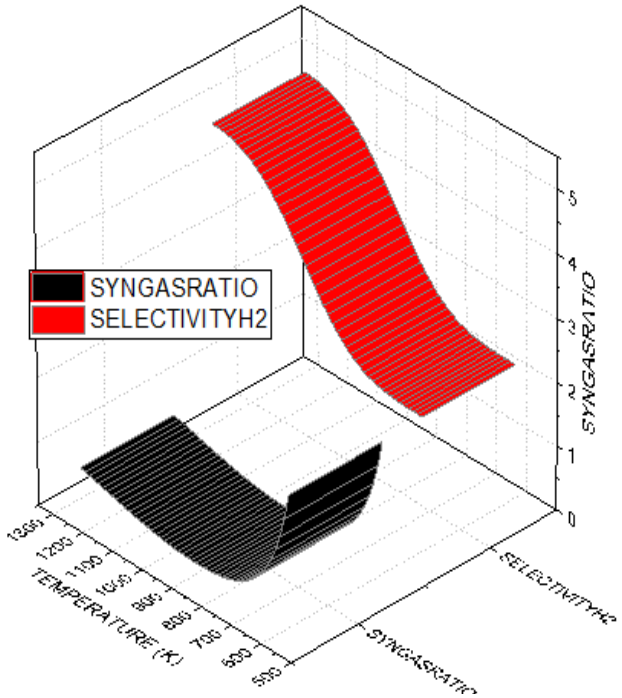

Figure 4.3: Syngas ratio and Selectivity of H_2 versus temperature

4.1.2 Effect of Pressure on RGIBBS Reformer

Since pressure significantly affects the thermodynamic equilibrium of dry glycerol reforming, the consequence of pressure variation was also examined at CO2 to glycerol molar feed ratio of 1:1 and temperature of 1273K. The effect of pressure under this study was classified into effect of pressure before optimization and after optimization. Based on these all of the parameters have been discussed, before optimization and after optimization. Conversion of glycerol over range of pressure was found 100% hence there is no point to discuss effect of pressure on glycerol conversion. The amount of syngas produced from dry glycerol was gradually decreased with increase of pressure from 1 bar to 30 bar in the product stream. Meanwhile, the amount of CO and H_2 was gradually decreased with increasing pressure. The amount of CO_2 increased gradually with increased pressure; this is because the conversion of CO_2 was decreases with increased pressure. Particularly the amount of H_2O concentration is found to rise in the whole range of pressure investigated (1 bar to30 bar). The amount of C3H8O3 and C_2H_6, were remains negligible with increased pressure. Apart from that the amount of C_2H_4 was gradually increased with an increased pressure. The yields of H_2 and CO are found to be in the range of 0.47% to 0.08% and 100% respectively. The highest yields of H_2 and CO were obtained at pressure of 1 bar. The overall yields of H2 and CO were decreased with an increased pressure. The selectivity and the syngas ratio (H_2/CO) have reverse approach based on the figure 4.6. The selectivity of H_2 was highly increased with increase of pressure in the stream. On the other hand syngas ratio was decreased with increase of pressure. This is because amount of CO being less decreased than H_2 with increased pressure.

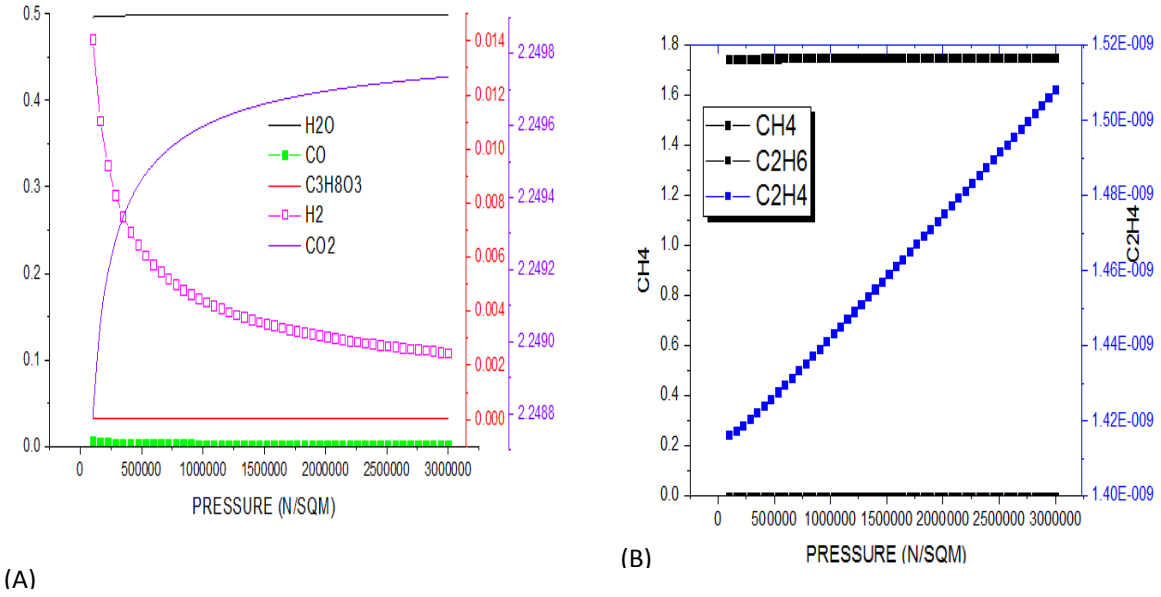

Figure 4.4:(A) product distributions of main product and (B) minor product versus Pressure

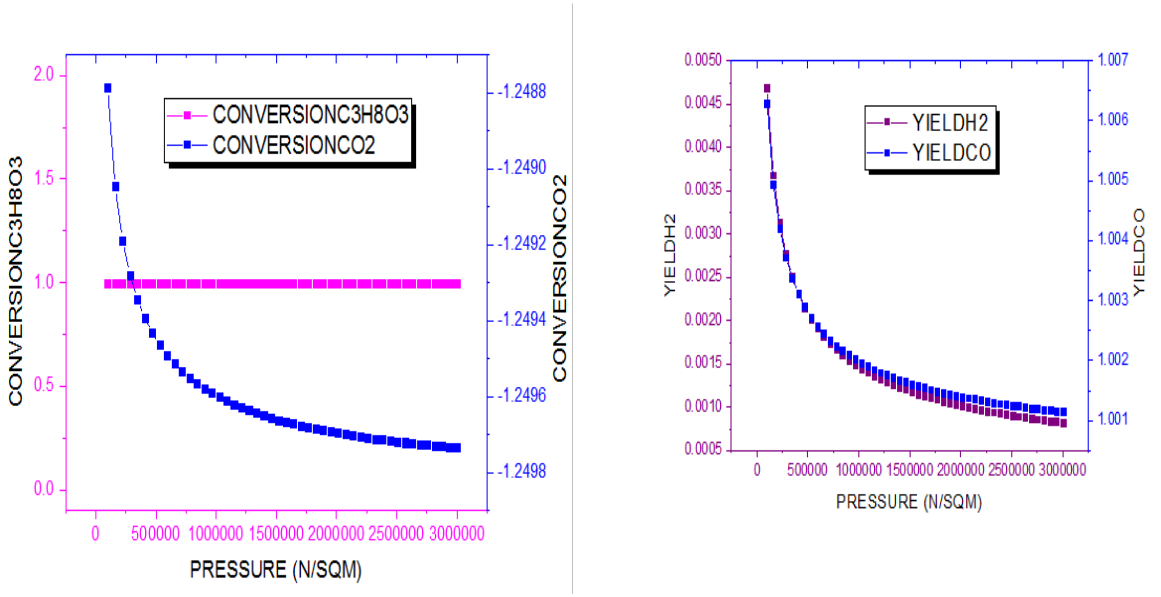

Figure 4.5: Conversion of CO_2, and $C_3H_8O_3$, and Yield of CO, and H_2 versus Pressure

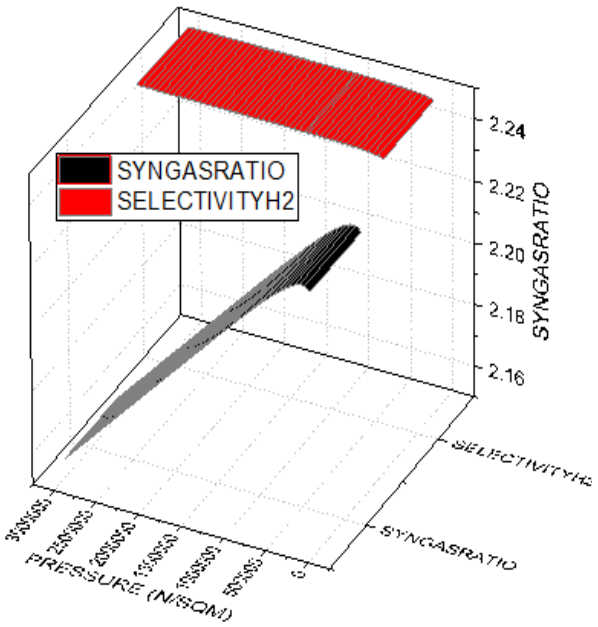

Figure 4.6: Syngas ratio and Selectivity of H_2 versus Pressure

4.1.3 Effect of Feed ratio on RGIBBS Reformer

The most important of glycerol dry reforming over the other reforming via glycerol is that carbon dioxide is used as reactant for production of syngas. In doing so it paves the way to remove CO_2 from the atmosphere and enables carbon biosphere cycle. At low molar feed ratio the syngas ratio (carbon monoxide/ hydrogen) produced was found to be increased with increased of feed ratio from (0.447-3.43). Particularly the concentration of H_2 was increased with increased feed ratio from 0.0052 to 0.0224 Kmol/sec. The yield of syngas is the summation of amount of hydrogen and carbon dioxide. Accordingly, the yield of syngas also increased with increased feed ratio and especially, the yield of the CO was highly increased with increased feed ratio 100%. In the higher side of CO_2 to glycerol molar feed ratio mole percent of C_2H_4 and C_2H_6 produced was almost negligible. As shown in the figure below the highest selectivity of H_2 was found at feed ratio of (92 % @0.4127). Conversion of $C_3H_8O_3$ was highly increased with increased of feed ratio and the 100% conversion has been recorded at feed ratio of 1:1.However, the conversion of carbon dioxide was less than zero. The amount of H_2O was increased with increase of feed ratio; this because of the conversion of glycerol is highly increased with increase of feed ratio.

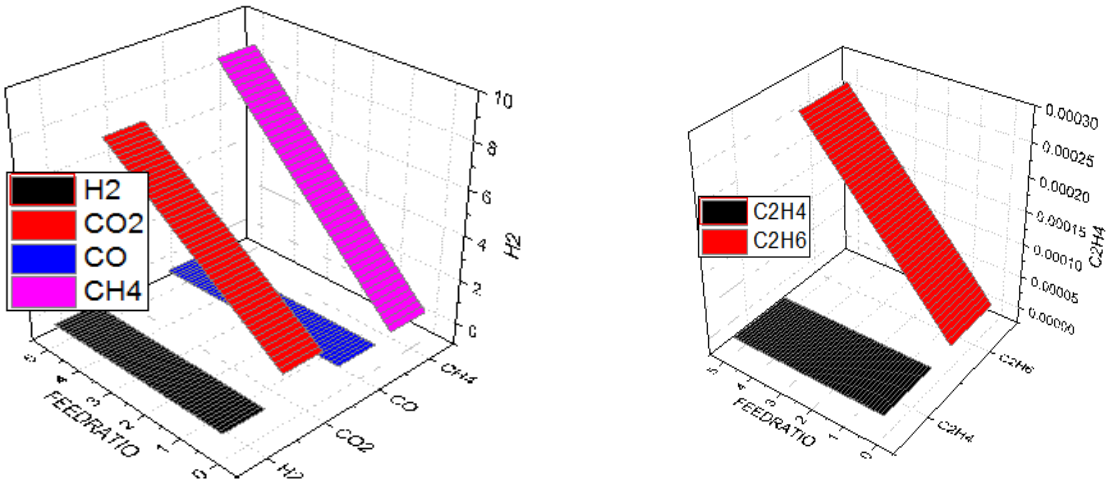

Figure 4.7: product distributions of CO_2, CO, CH4, C2H4, C2H6 and H_2 versus Feed ratio

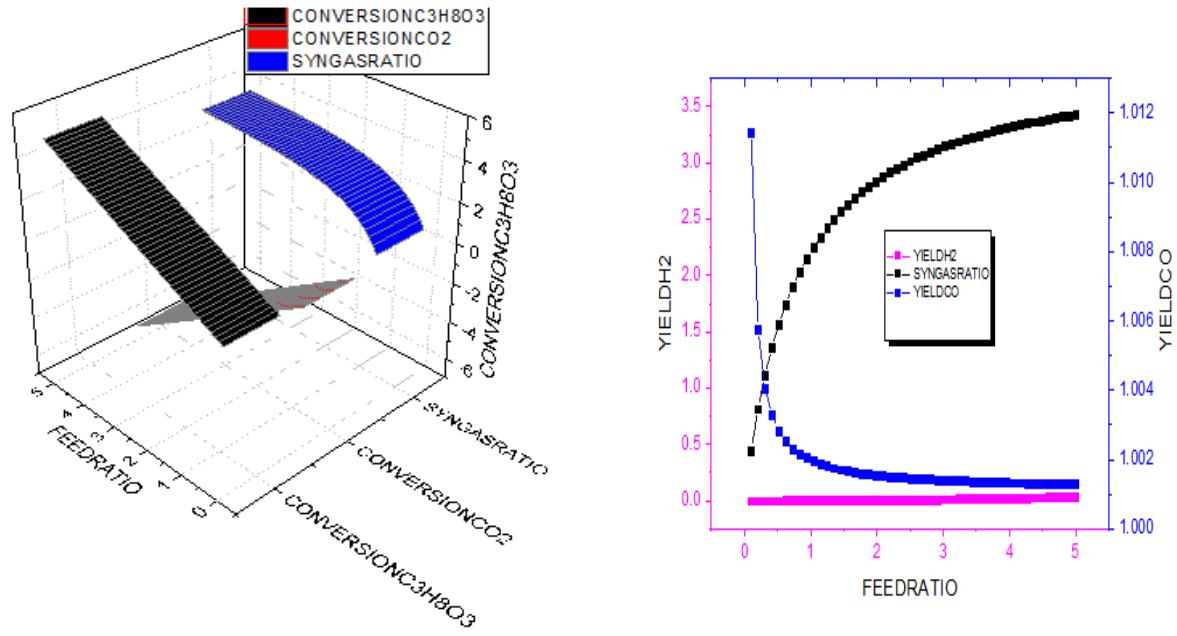

Figure 4.8: Conversion of CO_2, and $C_3H_8O_3$, Syngas ratio and Yield of CO, and H_2 versus Feed ratio

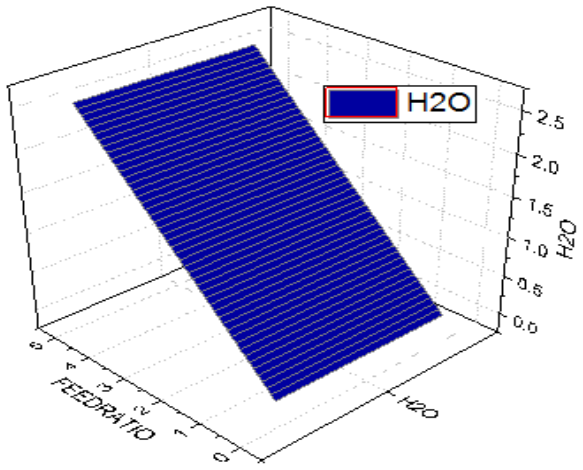

Figure 4.9: Water (H_2O) versus Feed ratio

4.2 Thermodynamics Analysis of RGIBBS Water Gas Shift Reactions

It is well known that water gas shift reaction is strongly exothermic and ideally it must be carried out at low temperature, high pressure. The thermodynamics analysis can be achieved maximum high yield based on the reaction conditions favoured. The effect of operating parameters such as temperature, pressure and feed ratio carbon monoxide to water and product composition were evaluated.

4.2.1 Effect of Temperature on RGIBBS Water Gas Shift Reactions

The effect of variation on product composition, conversion, yield and selectivity are shown in fig below. During this sensitivity analysis, other water gas shift reaction parameters such as feed ratio and pressure were held constant. The effect of temperature under this study was classified into effect of temperature before optimization and after optimization. Based on these all of the parameters have been discussed, before optimization and after optimization. Conversion of water over range of temperature was found 88% at temperature of 873K and this was indicated that the process parameter should be need optimized. The amount of syngas produced from water gas shift reaction was appreciably increased with temperature 473K to 873K in the product stream. This is because of the amount of CO was gradually decreased with increase of temperature and specifically related with the conversion of H_2O. This

means while the conversion of H_2O increased with increase of temperature; the amount of H_2 was increased. The amount of CO and CO_2, decreased with increasing temperature; this is because of the conversion of CO was increased with increased temperature. Particularly the yield of H_2 was found to rise in the whole range of temperature investigated (473K to 873K). However, selectivity of H_2 was decreased with increase of temperature. In this approach the selectivity of H_2 and the syngas ratio (H_2/CO) have reverse approach based on the figure 4.11C and figure 4.11A respectively.

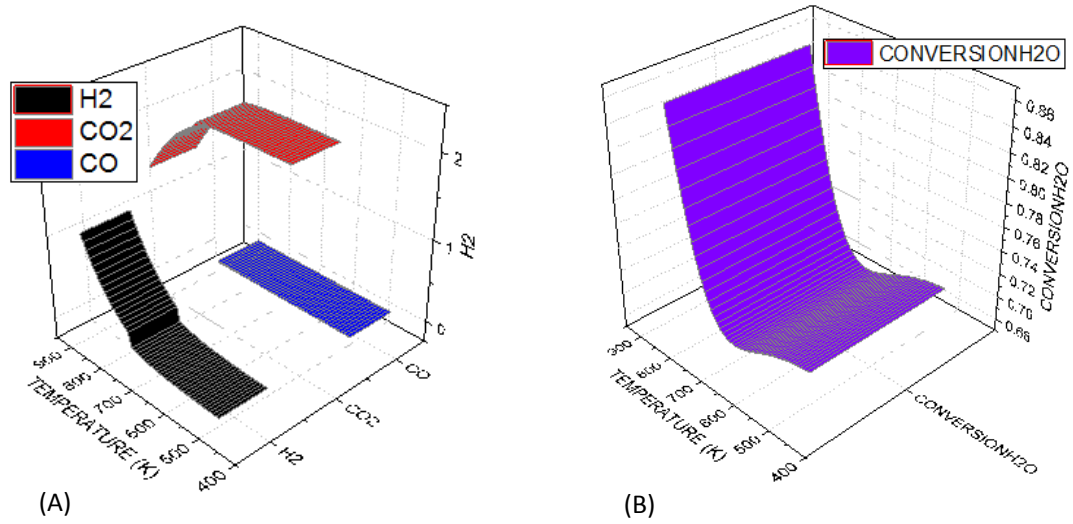

Figure 4.10: (A) Product composition of H_2, CO_2 and CO and (B) conversion of H_2O versus Temperature

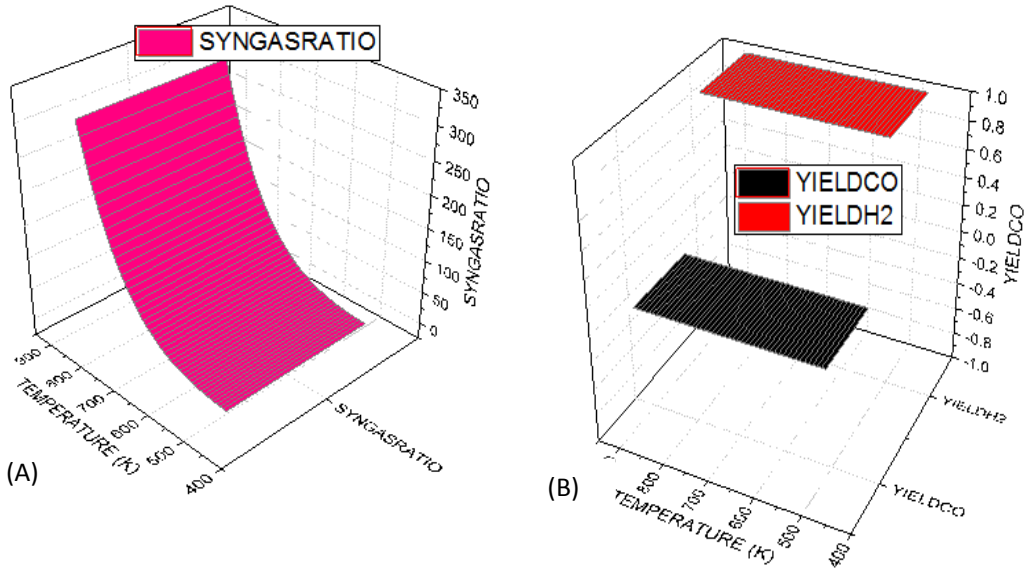

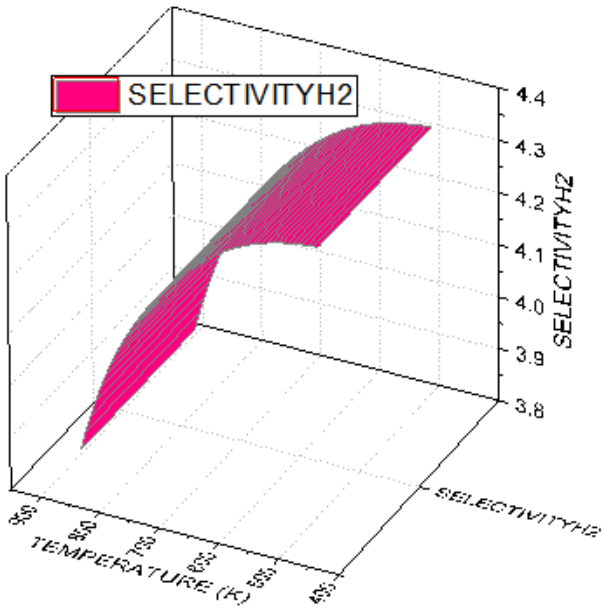

(C)

Figure 4.11: (A) Syngas ratio (B) Yield of H_2 and CO (C) Selectivity versus Temperature

4.2.2 Effect of Pressure on RGIBBS Water Gas Shift Reactions

Since pressure significantly affects the thermodynamic equilibrium of water gas shift reaction, the consequence of pressure variation was also examined at H_2O to CO molar feed ratio of 1:2.2 and temperature of 873K. As discussed in glycerol dry reforming, the effect of pressure under this study was also classified into effect of pressure before optimization and after optimization. Based on these all of the parameters have been discussed, before optimization and after optimization. Conversion of water over range of pressure was found 70%. The yield of CO produced from water gas shift reaction was remains negligible with increase of pressure from 1 bar to 20 bar in the product stream. Meanwhile, the yield of H_2 is 100% and exists at constant point with increasing pressure. The amount of CO_2 increased gradually with increased pressure. Particularly, the syngas ratio of water gas shift reaction was decreased with increased pressure. This is because of the amount of CO increase with increased pressure and meanwhile, the amount of H_2 concentration is found to rise in the whole range of pressure investigated (1 bar to 20 bar). Meanwhile, as the glycerol dry reforming; the selectivity and the syngas ratio

(H_2/CO) of water gas shift reaction also have reverse approach based on the figure 4.13A and figure 4.13B.

The selectivity of H_2 was highly increased with increase of pressure in the stream. On the other hand syngas ratio was decreased with increase of pressure. This is because CO being highly increased with increase pressure than H_2.

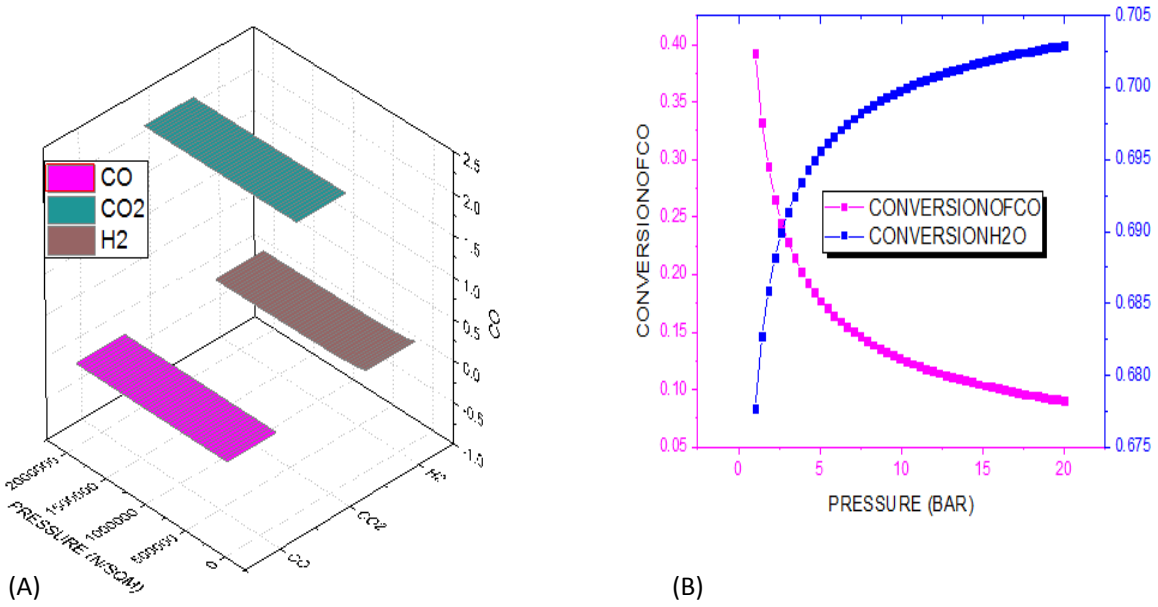

Figure 4.12: (A) Product composition of H_2, CO_2 and CO and (B) conversion of CO and H_2O versus Pressure

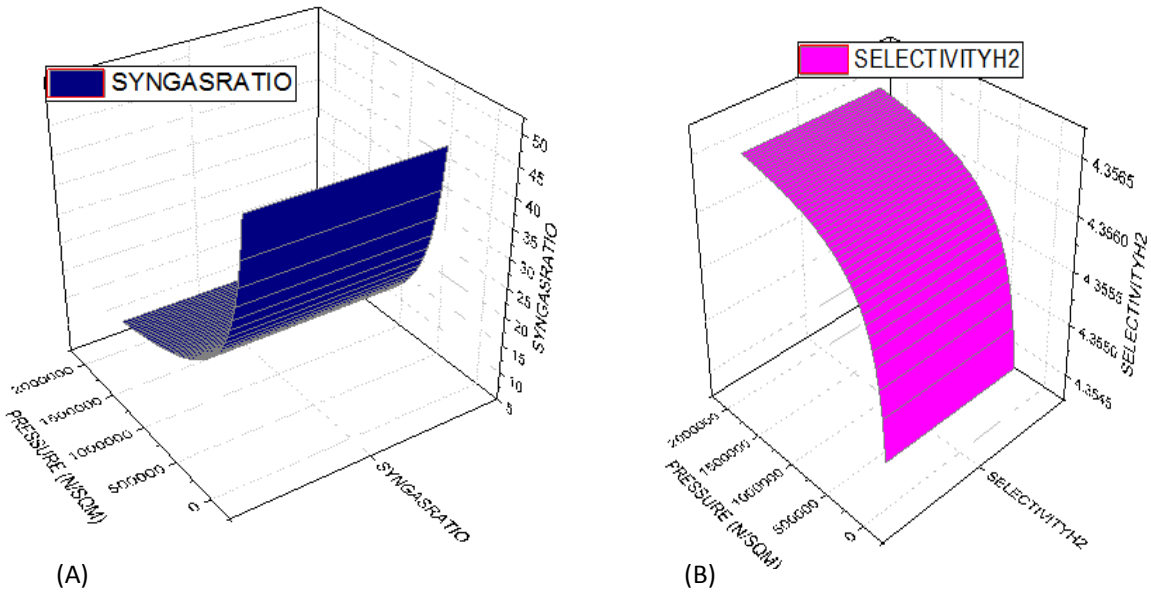

(A) (B)

Figure 4.13: (A) Syngas Ratio and (B) Selectivity of H_2 versus Pressure

4.3 Thermodynamics Analysis of Reforming RPLUG with Kinetic Models

As discussed in the section 4.1; glycerol dry reforming is strongly exothermic and ideally it must be carried out at high temperature, low pressure. The thermodynamics analysis can be achieved maximum high yield based on the reaction conditions favoured. Meanwhile, in this work, thermodynamics analysis was done using Aspen plus ^{TM} simulator. The same approach is considered as RGIBBS for RPLUG kinetic modelling. The procedure was available in the subroutine RKSMHV2 and used to determine the thermodynamic equilibrium compositions of each species present. SRK was chosen as the equation of state to correct the ideal RPLUG value. The effect of operating parameters such as temperature, pressure, feed ratio, catalyst particle density, length of reactor, diameter of the reactor and hence, product composition, selectivity, syngas ratio were evaluated based on this parameters.

4.3.1 Effect of Parameters on Reformer and Water Gas Shift Reaction with Power law Kinetic Model

Under this section for both reactor model (reformer and water gas shift reactor) effect of temperature, pressure, length of reactor were discussed to evaluate syngas ratio, selectivity, conversion, and product composition.

4.3.1.1 Effect of Temperature on Reformer and Water Gas Shift Reaction with Power law Kinetic Model

The effect of temperature variation for both reformer and water gas shift reaction on conversion, selectivity, product composition and syngas ratio are shown in fig 4.14A and 4.20A, and fig 4.14B and 4.20B and fig 4.15 and fig 4.21 and fig 4.22 respectively. As shown in fig 4.14A and 4.20A is the response of the conversion to the reactor temperature. For the reformer; conversion of glycerol and carbon dioxide are negligible and no further discussion. Meanwhile, for the water gas shift reaction the conversion of carbon monoxide and water started at temperature of 860.34K and highly increased from 120% at temperature 697.4K respectively. The effects of temperature on selectivity of the reformer and water gas shift reaction are follows: as shown in fig 4.14B and 4.20B selectivity of carbon dioxide and carbon monoxide is highly increased with increased of temperature from 923 up to 2800K. This is because of conversion of glycerol and CO_2 was negligible with increased of temperature. However, the selectivity of H_2 and H_2O is negligible with increased temperature. For the water gas shift reaction, it is found that as the temperature increased, the selectivity of H_2O and CO is gradually increased at constant point. Meanwhile, selectivity of $H_2$and CO_2 increased up to 3.7% and 5.2% respectively. From the fig4.15 product composition of reformer were glycerol, CO, CO_2, H_2, and H_2O. Among them amount of glycerol and carbon dioxide are higher than the left product composition, this is because of the conversion of the glycerol and carbon dioxide were negligible. Whereas from the fig 4.21 the product compositions of water gas shift reaction were H_2, H_2O, CO, and CO_2. Accordingly, the amount of H_2O increased drastically until 767.23K and after that amount of H_2O started to become decreased constant. Meanwhile, the amount of CO_2 become constant until 848.7K and started to become increased with increased temperature, however, the amount of CO and H_2O were decreased with increased temperature. This is because of the conversion of CO and H_2O were decreased with increased temperature. Syngas ratio of reformer was constant and 0.75 and whereas syngas ratio of water gas shift reaction was increased with increased of temperature.

4.3.1.2 Effect of Pressure on Reformer and Water Gas Shift Reaction with Power law Kinetic Model

The effect of pressure variation for both reformer and water gas shift reaction on conversion, selectivity, product composition and syngas ratio are shown in fig 4.16A and 4.23A, and fig 4.16B and 4.24A and fig 4.17 and fig 4.23B and fig 4.24B respectively. As shown in fig 4.16A and 4.23A is the response of the conversion to the reactor pressure. For the reformer; conversion of glycerol and carbon dioxide are negligible and no further discussion. Meanwhile, for the water gas shift reaction the conversion of carbon monoxide was drastically increased with increased of pressure until conversion of 1.7% and also the conversion of water to become increased with increased pressure. The effects of pressure on selectivity of the reformer and water gas shift reaction are follows: as shown in fig 4.16B and 4.24A respectively. Selectivity of carbon dioxide and carbon monoxide is highly increased with increased of pressure. This is because of conversion of glycerol and CO_2 was decreased with increased of pressure. However, the selectivity of H_2 and H_2O is negligible with increased pressure; this is also related with conversion of glycerol. For the water gas shift reaction, it is found that, as the pressure increased, the selectivity of H_2 and CO_2 was found on the ranges 2-4%. Whereas the selectivity of CO and H_2O was at the same percentage level this was 101.7%. From this trend the selectivity of CO_2 higher than H_2 and almost increased with increased of pressure. But, the selectivity of CO and H_2O started to become constant from the initial pressure to the final pressure.

From the fig4.17 product compositions of reformer were such as: glycerol, CO, CO_2, H_2, and H_2O. Among them amount of glycerol and carbon dioxide are higher than the left product composition, this is because of the conversion of the glycerol and carbon dioxide were decreased with increased pressure. However, amount of CO is increased with an increased of pressure. The other product compositions become negligible with increased pressure. Meanwhile, from the fig 4.23B the product compositions of water gas shift reaction were H_2, H_2O, CO, and CO_2. Accordingly, the amount of H_2O increased drastically until 34.68 Bar and after that amount of H_2O started to become constant with increased of pressure. Meanwhile, the amount of CO_2 increased and increased from 0.0001458 Kmol/sec to become reached 0.017 Kmol/sec. Particularly, the amount of CO was drastically decreased with increased pressure; this is because of the conversion of CO was drastically increased with

increased of pressure. Whereas, the expression of the amount of H_2 was became the same as with the expression of amount of CO_2. Syngas ratio of reformer was constant and 0.75 and whereas syngas ratio of water gas shift reaction was increased with increased of pressure.

4.3.1.3 Effect of Length of Reactor on Reformer and Water Gas Shift Reaction with Power law Kinetic Model

The effect of length of reactor variation for both reformer and water gas shift reaction on conversion, selectivity, product composition and syngas ratio are shown in fig 4.18A and 4.25A, and fig 4.18B and 4.26A and fig 4.19 and fig 4.25B and fig 4.26B respectively. As shown in fig 4.18A and 4.25A is the response of the conversion to the reactor length. For the reformer; conversion of glycerol and carbon dioxide are negligible and no further discussion. Meanwhile, for the water gas shift reaction the conversion of carbon monoxide was increased with increased of length of reactor until 387.6 meter. After that the conversion of carbon monoxide started to become constant, which is 100%. Meanwhile, the conversion of H_2O was increased with increased of length of the reactor. The effects of length of reactor on selectivity of the reformer and water gas shift reaction are follows: as shown in fig 4.18B and 4.26A, respectively. For the reformer selectivity of carbon dioxide and carbon monoxide was highly increased with increased of length of the reactor and reached 200% and 100% respectively. This is because of conversion of glycerol and CO_2 was negligible with increased length of the reactor. Meanwhile, the selectivity of H_2 and H_2O is negligible with increased length of the reactor; this is also related with conversion of glycerol. For the water gas shift reaction, it is found that, selectivity of H_2 and CO_2 increased with increased length of the reactor until 387 meter. After that the selectivity of H_2 and CO_2 started to became constant. Meanwhile, the selectivity of H_2O increased with increased length of the reactor. However, the selectivity of CO was increased with increased length of the reactor until 344.6 meter and after that the selectivity of CO started to become constant. From the fig4.19 product composition of reformer were such as: glycerol, CO, CO_2, H_2, and H_2O. Among them amount of glycerol and carbon dioxide are higher than the left product composition, this is because of the conversion of the glycerol and carbon dioxide were negligible with increased length of the reactor. The other product compositions become negligible with increased length of the reactor. However, mole flow rate of glycerol started to become

decreased after 7.8 meter. Meanwhile, from the fig 4.25B the product compositions of water gas shift reaction were H_2, H_2O, CO, and CO_2. Accordingly, the amount of CO_2 and H_2 increased with increased length of the reactor until 387 meter and after that amount of H_2 and CO_2 started to become constant with increased of length of the reactor. This is because of the conversion of H_2O and CO increased with increased of the length of the reactor. Particularly the conversion of CO started to become constant at the length of 387 meter. However, amount of H_2O and CO decreased with increased length of the reactor. Specifically, the amount of CO started to become zero flow rates after 387 meter length of the reactor. Syngas ratio of reformer was constant and 0.75 and whereas syngas ratio of water gas shift reaction was increased with increased of length of the reactor until 344.6 meter and after that the syngas ratio become zero. This is because of the amount of CO became zero after 344.6 meter length of the reactor.

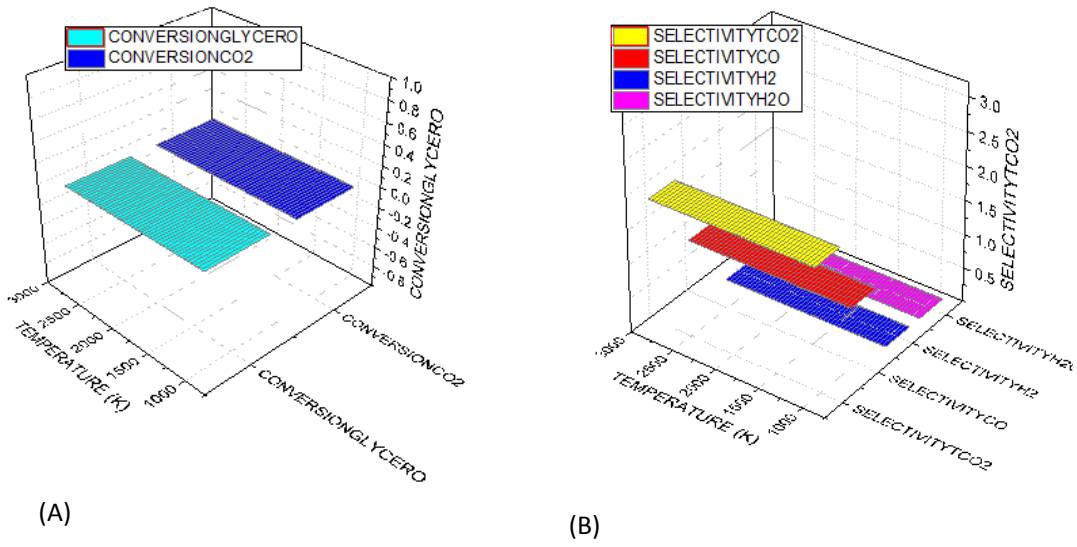

(A) (B)

Figure 4.14: (A) conversion of glycerol and CO_2 and (B) Selectivity of CO, CO_2, H_2, H_2O Versus Temperature between 923 and 2800K

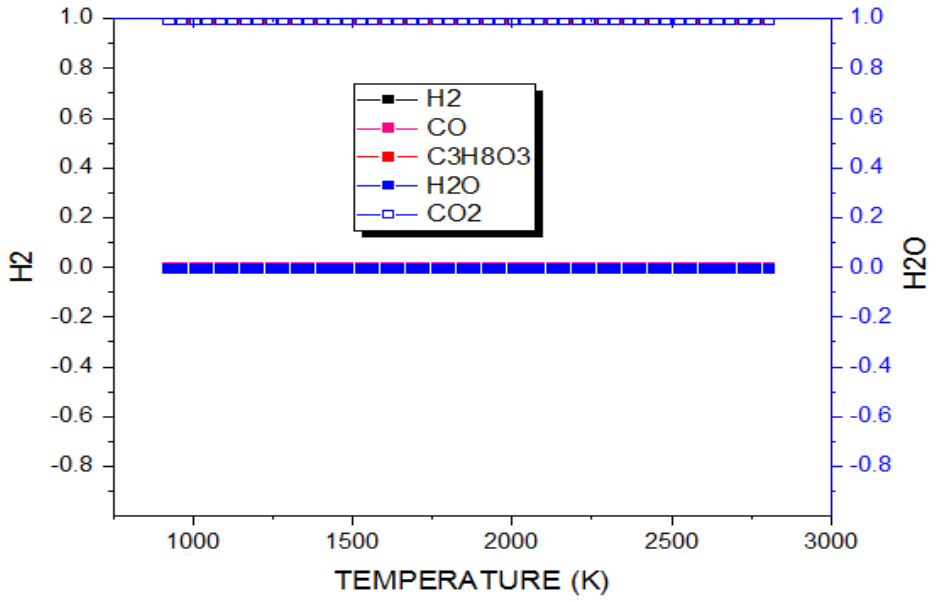

Figure 4.15 :Product composition of CO, H_2 CO_2, H_2O and $C_3H_8O_3$ versus Temperature of reformer

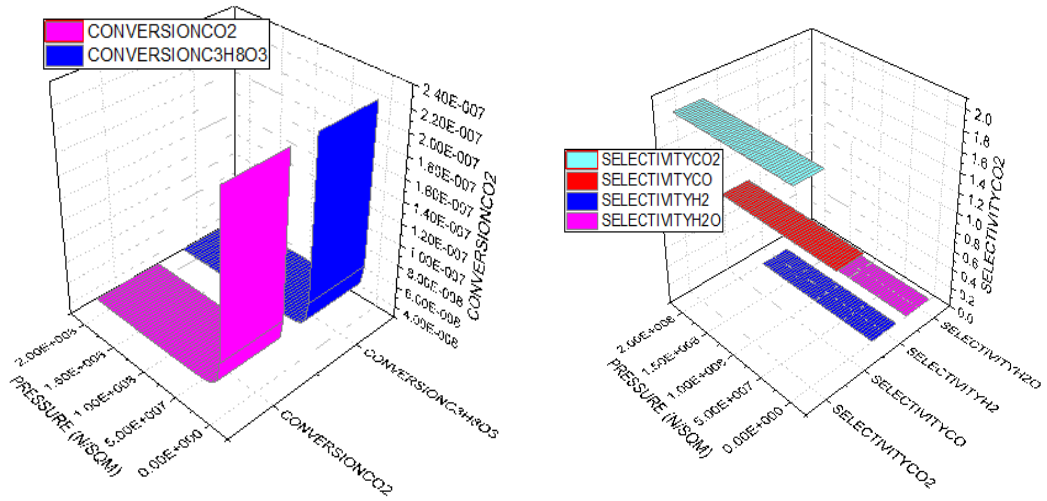

(A) (B)

Figure 4.16: (A) Conversion of CO_2 and glycerol and (B) Selectivity of CO, H_2, CO_2, and H_2O versus Pressure

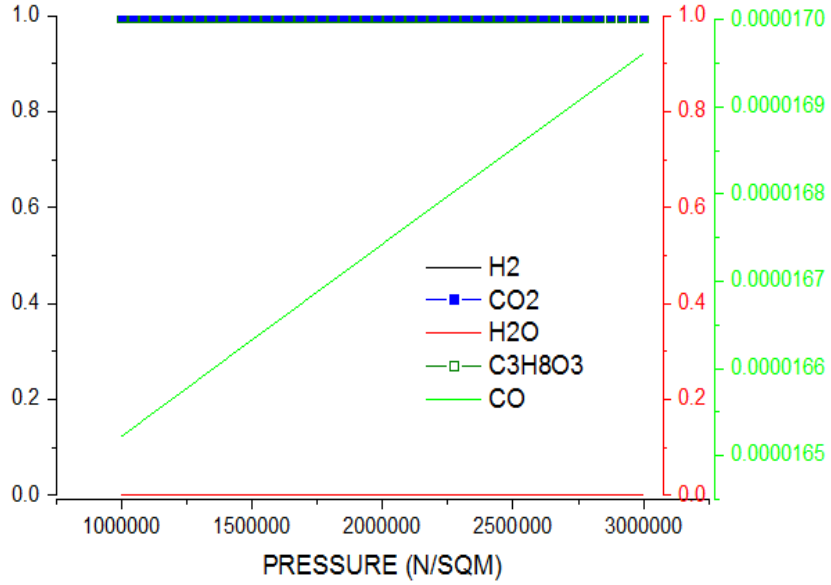

Figure 4.17: Product composition of CO, H_2 CO_2, H_2O and $C_3H_8O_3$ versus Pressure

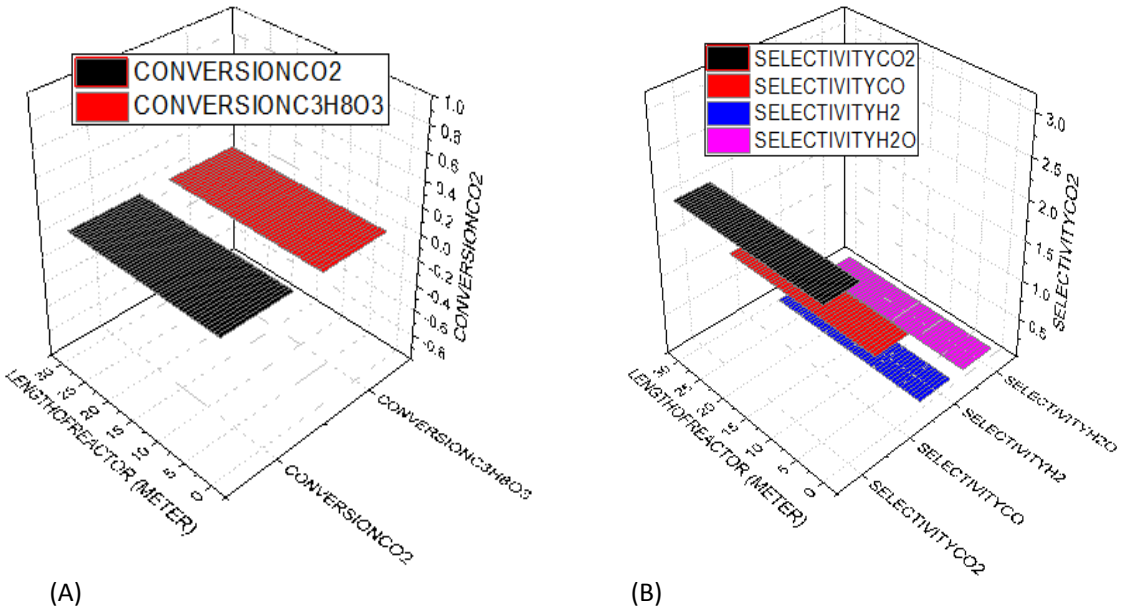

(A) (B)

Figure 4.18: (A) Conversion of CO_2 and glycerol and (B) Selectivity of CO, H_2, CO_2, and H_2O versus Length of reactor

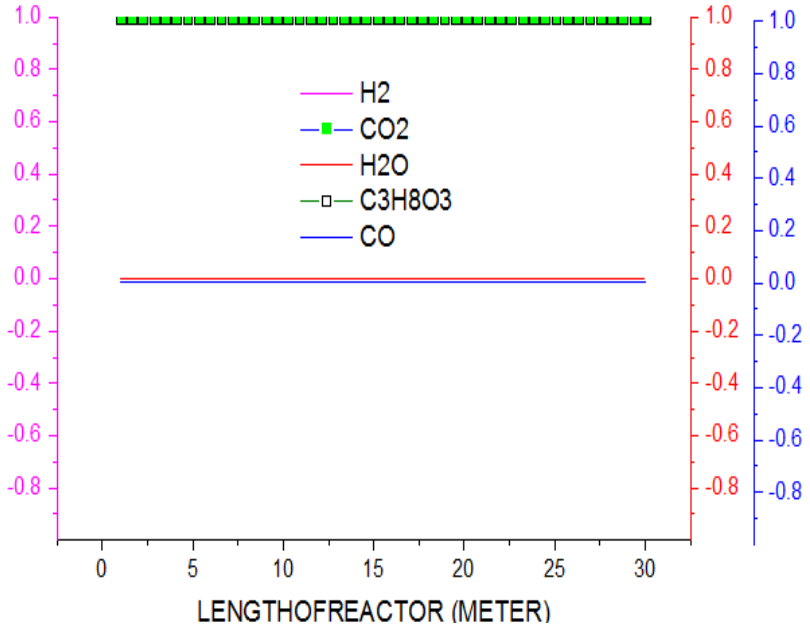

Figure 4.19: Product composition of CO, H_2 CO_2, H_2O and $C_3H_8O_3$ versus Length of reactor

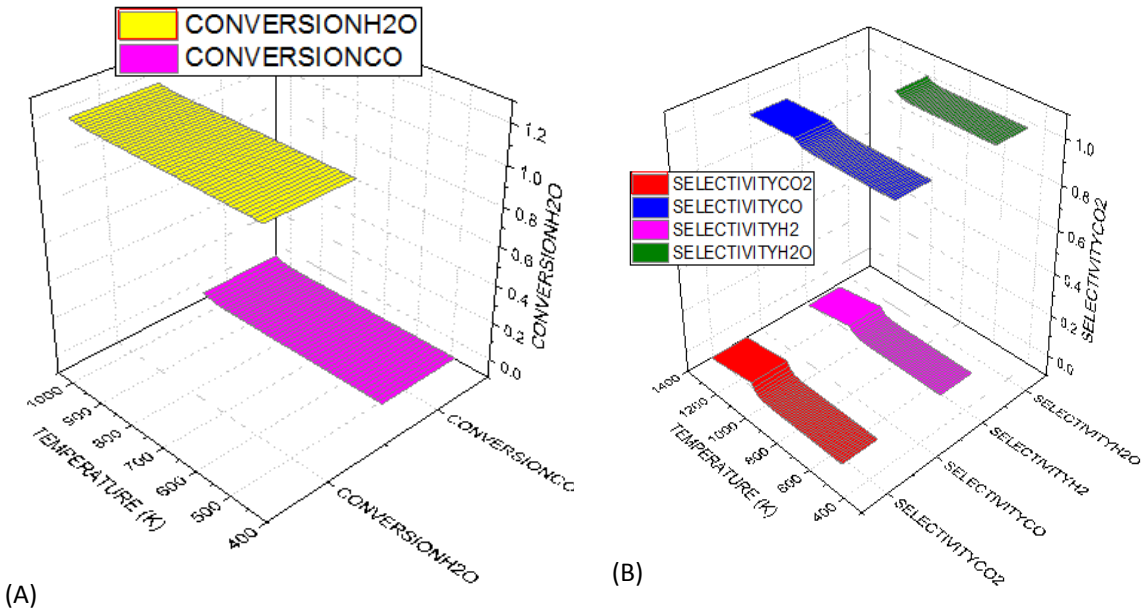

(A) (B)

Figure 4.20: (A) Conversion of CO and H_2O and (B) Selectivity of CO, H_2, CO_2, and H_2O versus Temperature of WGS

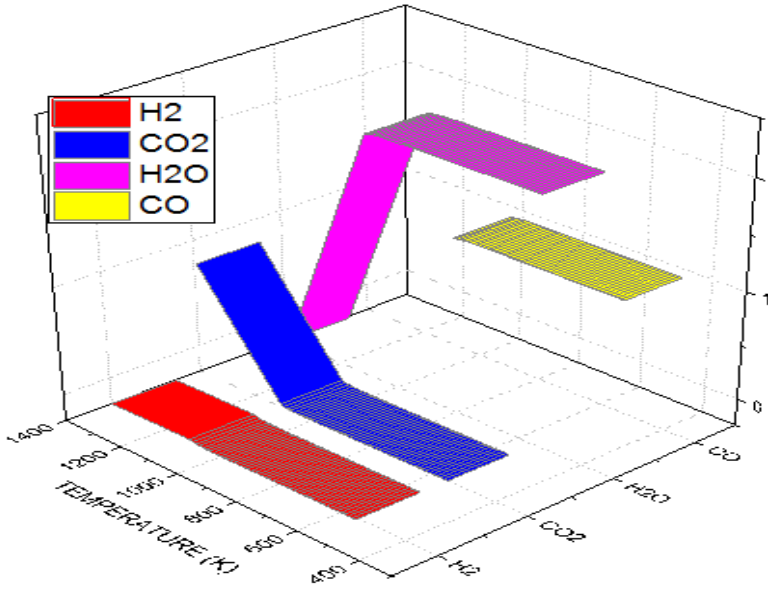

Figure 4.21: Product composition of CO, H_2 CO_2, and H_2O versus Temperature of WGS

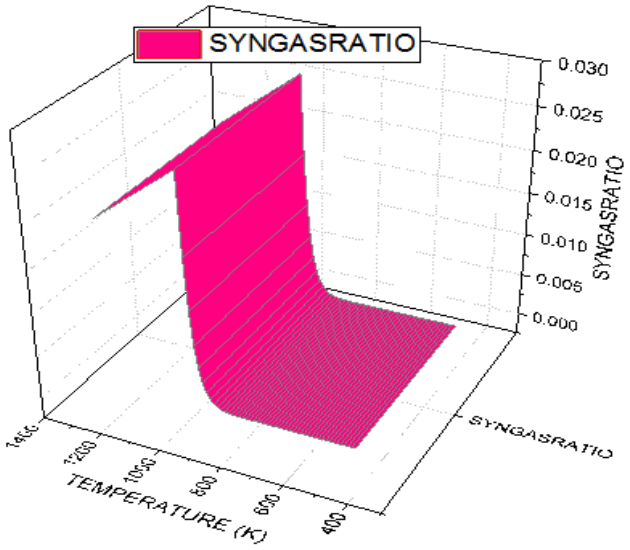

Figure 4.22: Syngas ratio (H_2 /CO), versus Temperature of WGS

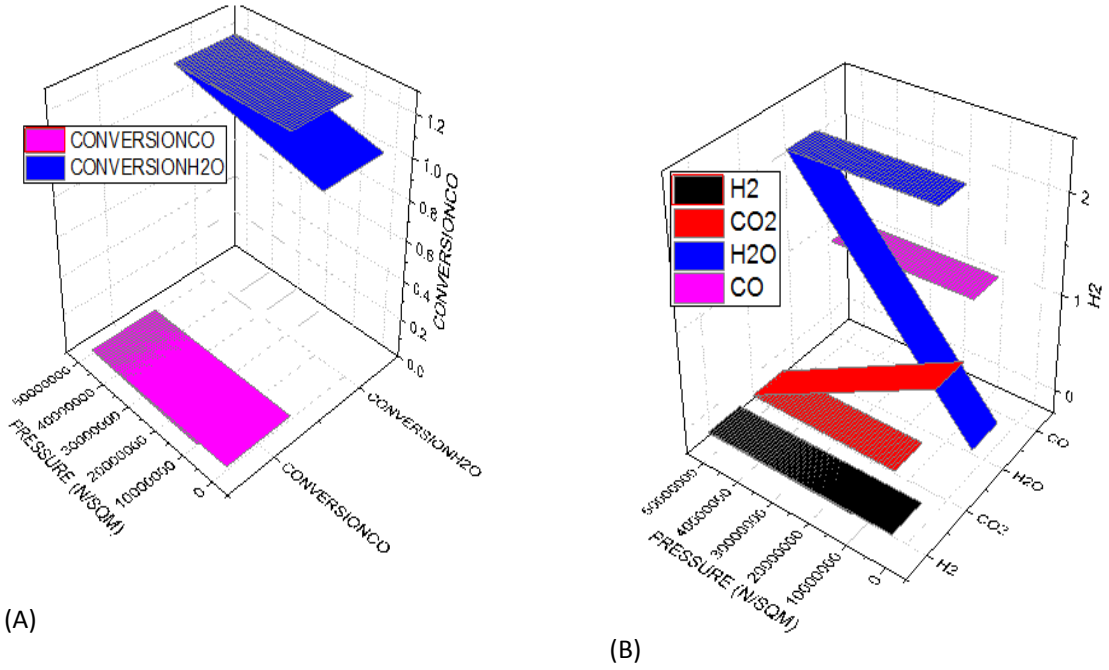

(A) (B)

Figure 4.23: (A) Conversion of CO and H_2O and (B) Product composition of CO, H_2, CO_2, and H_2O versus pressure of WGS

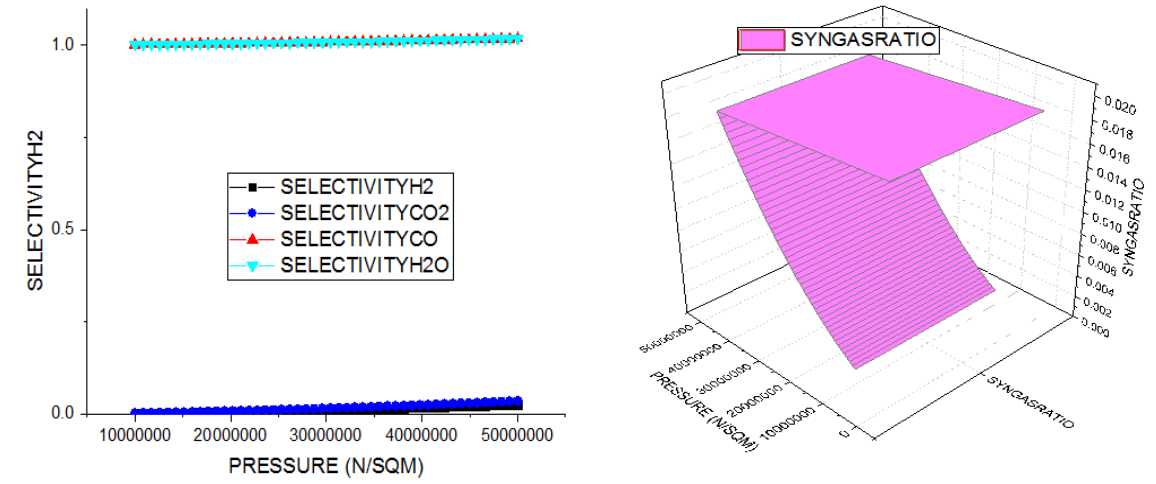

(A) (B)

Figure 4.24: (A) Selectivity of CO_2, CO, H_2 and H_2O and (B) Syngas ratio versus Pressure of WGS

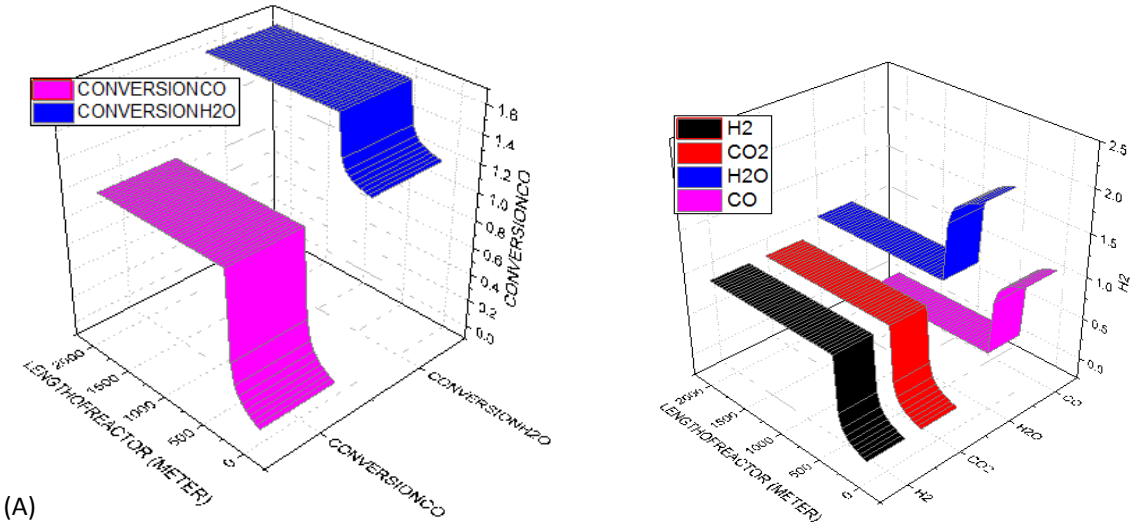

(A) (B)

Figure 4.25: (A) Conversion of CO and H_2O and (B) Product composition of CO, H_2, CO_2, and H_2O versus length of WGS

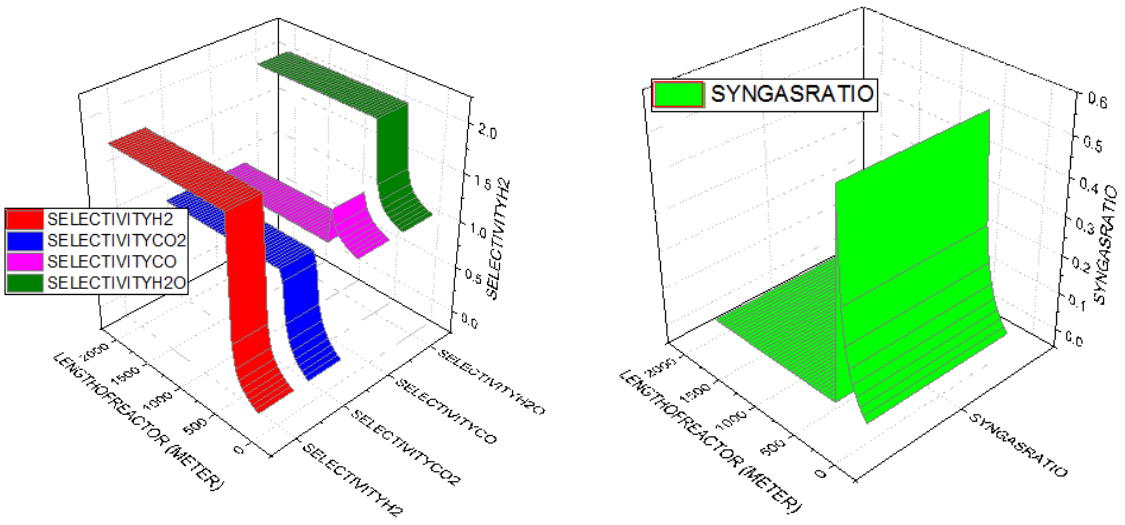

(A) (B)

Figure 4.26: (A) Selectivity of CO_2, CO, H_2 and H_2O and (B) Syngas ratio versus length of WGS

4.3.2 Effect of Parameters on Reformer and Water Gas Shift Reaction with LHHW Kinetic Model

Meanwhile, the power law model under this section also effect of parameters of both reactor models (reformer and water gas shift reactor) are discussed as follows:

consequently, effect of temperature, pressure, length of reactor, catalyst particle density were discussed to evaluate syngas ratio, selectivity, conversion, and product composition.

4.3.2.1 Effect of Temperature on Reformer and Water Gas Shift Reaction with LHHW Kinetic Model

The effect of temperature variation on reforming and water gas shift reaction are as follows: conversion of glycerol and carbon dioxide were increased with increased of temperature. However, as shown in fig 4.27A the values of conversion were minimal. For water gas shift reaction shown in fig4.31A the conversion of CO and H_2O were high and increased with increased temperature. For reformer from fig4.27B selectivity of H_2O was higher next to the selectivity of H_2. This means, selectivity of both components were drastically increased with increased of temperature. Meanwhile, as shown in fig4.31B the selectivity of CO and CO and CO_2 also drastically increased with increased of temperature. However, the selectivity of H_2O and H_2 were higher than the selectivity of CO and CO_2. Meanwhile, for water gas shift reaction the selectivity CO and H_2O were decreased with increased of temperature, whereas the selectivity of CO_2 and H_2 drastically decreased with increased temperature. From the fig4.32B, product compositions of water gas shift reaction were H2O, H_2, CO and CO_2. Among them, molar flow rates of H_2O and CO were decreased with increased of temperature. Whereas, molar flow rates of CO_2 and H_2 were increased with increased temperature. This is because of the conversion of CO and H_2O were increased with increased temperature. Syngas ratio of reformer was constant and 0.75, whereas syngas ratio of water gas shift reaction was increased with increased temperature. This is related with the amount of CO i.e. it was decreased with increased temperature.

4.3.2.2 Effect of Pressure on Reformer and Water Gas Shift Reaction with LHHW Kinetic Model

The effect of pressure variation on reforming and water gas shift reaction are as follows: conversion of glycerol and carbon dioxide were decreased with increased of pressure. However, as shown in fig 4.28B the values of conversion were minimal. For water gas shift reaction shown in fig4.33A the conversion of CO and H_2O were lower and gradually decreased with increased pressure. For the reformer fig4.28A illustrated

that, selectivity CO and CO_2 was constant starting from the initial to the final pressure point i.e. the selectivity of both components 200% and 100% respectively. Meanwhile, the selectivity of H_2 and H_2O were also constant to 400% and 200% respectively. As illustrated in fig 4.33B the selectivity of water gas shift reaction indicated that; the selectivity of H_2O and CO increased with an increased pressure. Meanwhile, the selectivity of H_2 and CO_2 increased with an increased pressure. The next effect of pressure is discussed versus product composition. As shown in fig 4.34A, amount of H_2O and CO drastically increased with an increased of pressure. However, the amount CO_2 and H_2 gradually decreased with an increased of pressure. Particularly, as the pressure increased, there was a drop in amount of CO_2 molar flow rates. This is because the equilibrium constant decreased with an increased of pressure, thus lower down the conversion of carbon monoxide at higher pressure. Syngas ratio of reformer was constant and 0.75, whereas syngas ratio of water gas shift reaction was decreased with increased pressure. This is related with the amount of CO i.e. it was increased with increased pressure.

4.3.2.3 Effect of Length of the reactor on Reformer and Water Gas Shift Reaction with LHHW Kinetic Model

The effect of pressure variation on reforming and water gas shift reaction are as follows: conversion of glycerol and carbon dioxide were gradually increased with an increased of length of the reactor. However, as shown in fig 4.29A the values of conversion were minimal. For water gas shift reaction shown in fig4.35A the conversion of CO and H_2O were constant with 89.5% conversion with an increased length of the reactor. For the reformer fig4.29B illustrated that, selectivity of CO and CO_2 was constant starting from the initial to the final length of the reactor point i.e. the selectivity of both components 200% and 100% respectively. Meanwhile, the selectivity of H_2 and H_2O were also constant to 400% and 200% respectively. As illustrated in fig 4.35B the selectivity of water gas shift reaction indicated that; the selectivity of H_2O and CO became constant with 22.3% with an increased length of the reactor. Meanwhile, the selectivity of H_2 and CO_2 became also constant with 110% with an increased length of the reactor. The next effect of length of reactor is discussed versus product composition. As shown in fig 4.36A, amount of H_2O and CO became constant with an increased length of the reactor. Meanwhile, the amount CO_2 and H_2 became constant with an increased of length of the reactor.

Syngas ratio of reformer and water gas shift were constant with an increased length of the reactor. This is because of the amount of CO and H_2 were constant with an increased length of the reactor.

4.3.2.4 Effect of Catalyst particle density on Reformer and Water Gas shift Reaction with LHHW Kinetic Model

The effect of catalyst particle density variation on reforming and water gas shift reaction are as follows: conversion of glycerol and carbon dioxide were gradually increased with an increased of catalyst particle density. However, as shown in fig 4.23B the values of conversion were minimal. For water gas shift reaction shown in fig4.37A the conversion of CO and H_2O were increased with an increased catalyst particle density. Particularly conversion of H_2O was increased until 86.33% conversion with an increased catalyst particle density. For the reformer fig4.30A illustrated that, selectivity of CO and CO_2 was constant starting from the initial to the final catalyst particle density point i.e. the selectivity of both components 200% and 100% respectively. Meanwhile, the selectivity of H_2 and H_2O were also constant to 400% and 200% respectively. The other one is as illustrated in fig 4.37B the selectivity of water gas shift reaction indicated that; the selectivity of H_2O and CO became constant with 22.3% with an increased catalyst particle density. Meanwhile, the selectivity of H_2 and CO_2 became also constant with 110% with an increased catalyst particle density. The next effect of catalyst particle density is discussed versus product composition. As shown in fig 4.36A and fig 4.38A the effect of catalyst particle density and effect of length of the reactor were shows the same effect on the product composition. Consequently, the effect of catalyst particle density on syngas ratio was the same as the effect of length of the reactor.

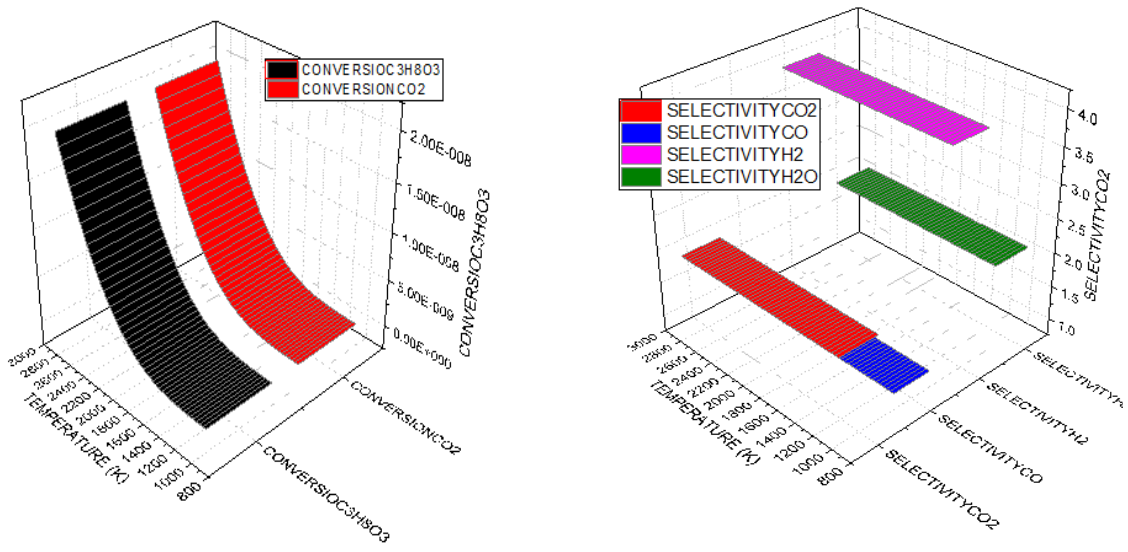

(A) (B)

Figure 4.27: (A) conversion of glycerol and CO_2 and (B) Selectivity of CO_2, CO, H_2 and H_2O versus Temperature of reformer

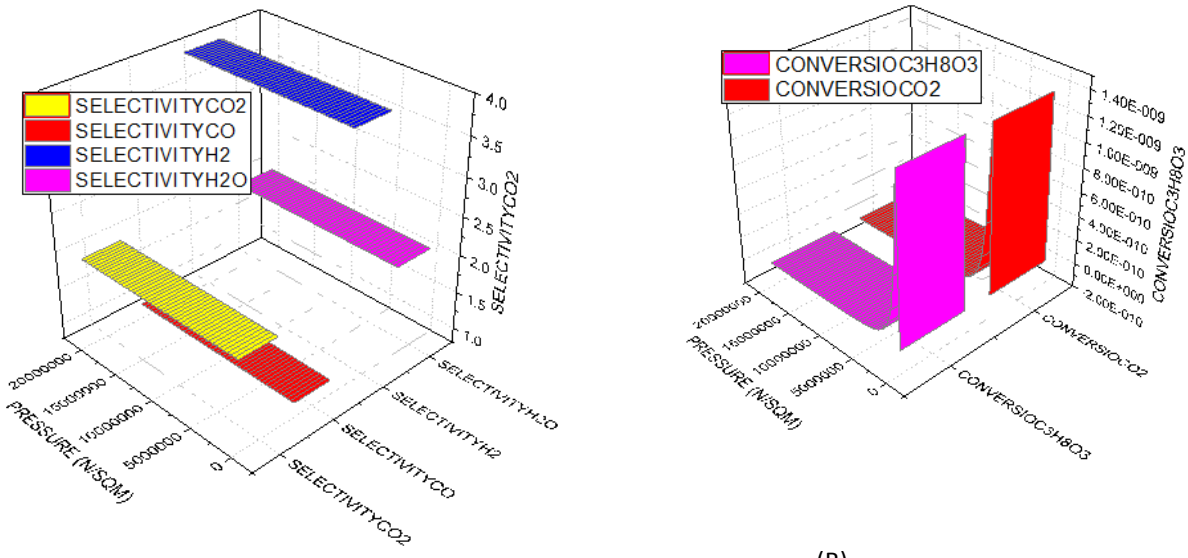

(A) (B)

Figure 4.28: (A) Selectivity of CO_2, CO, H_2 and H_2O and (B) conversion of glycerol and CO_2 versus Pressure of reformer

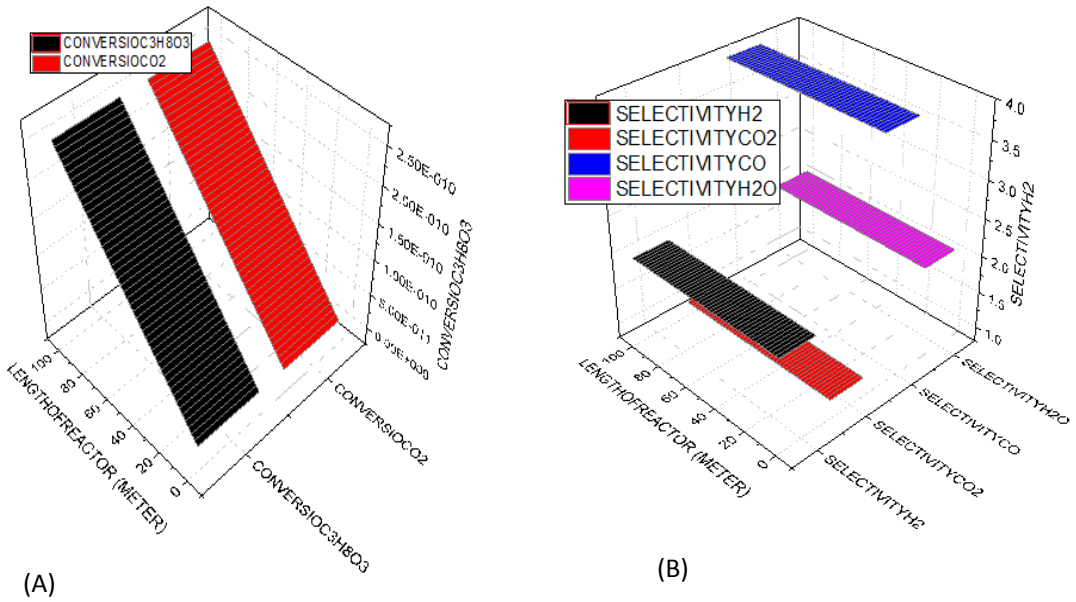

(A) (B)

Figure 4.29: (A) conversion of glycerol and CO_2 and (B) Selectivity of CO_2, CO, H_2 and H_2O versus Length of reformer

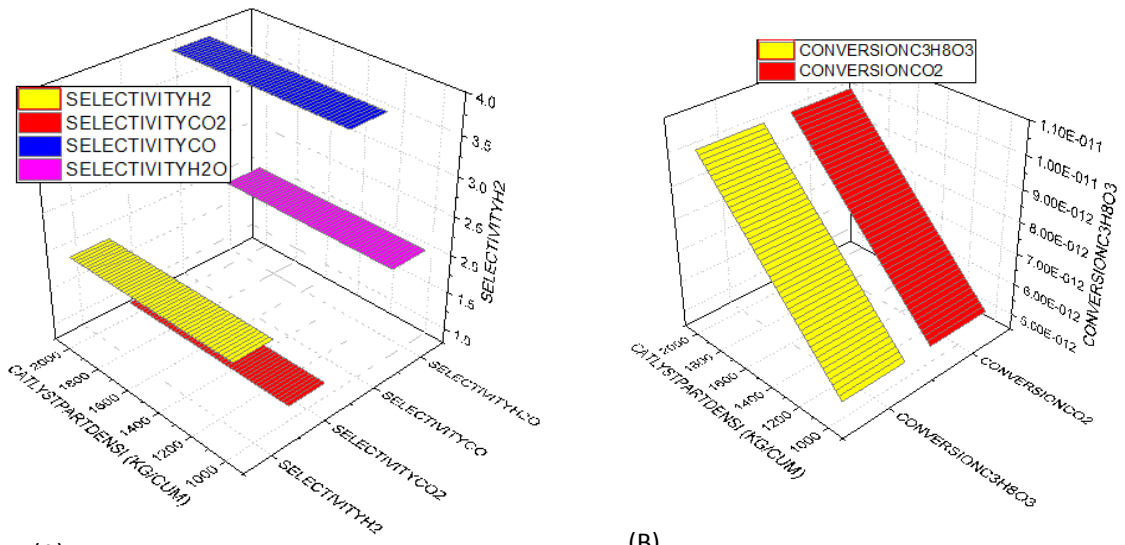

(A) (B)

Figure 4.30: (A) Selectivity of CO_2, CO, H_2 and H_2O and (B) conversion of glycerol and CO_2 versus Catalyst particle density of reformer

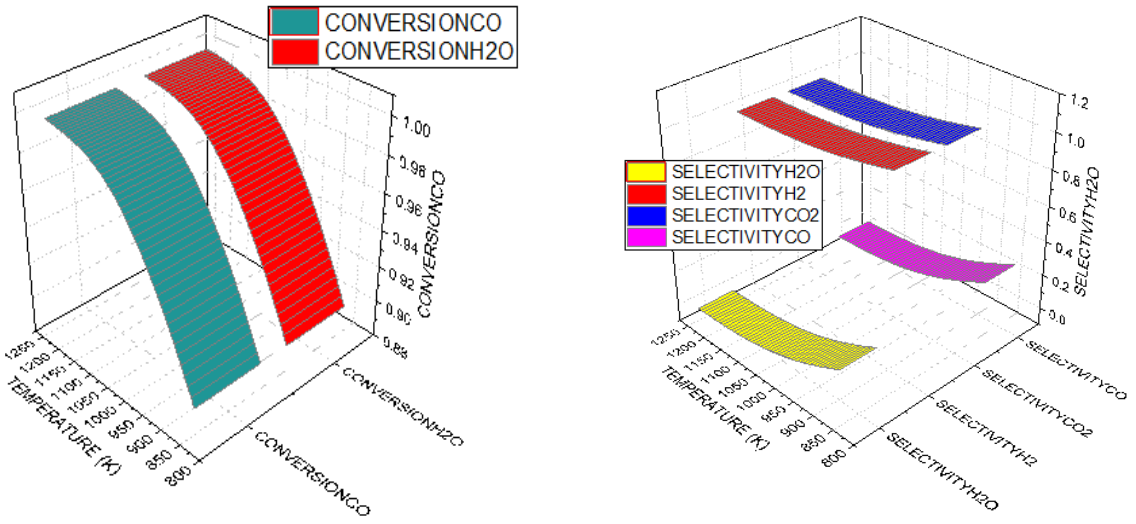

(A) (B)

Figure 4.31: (A) conversion of water and CO and (B) Selectivity of CO_2, CO, H_2 and H_2O versus Temperature of WGS

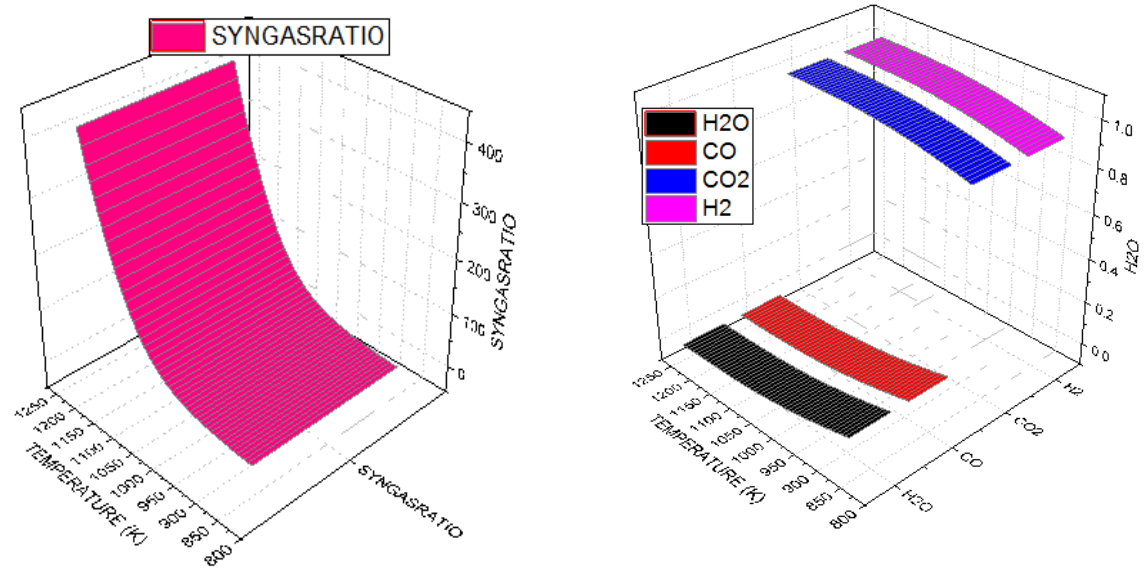

(A) (B)

Figure 4.32: (A) Syngas ratio and (B) product composition of CO_2, CO, H_2 and H_2O versus Temperature of WGS

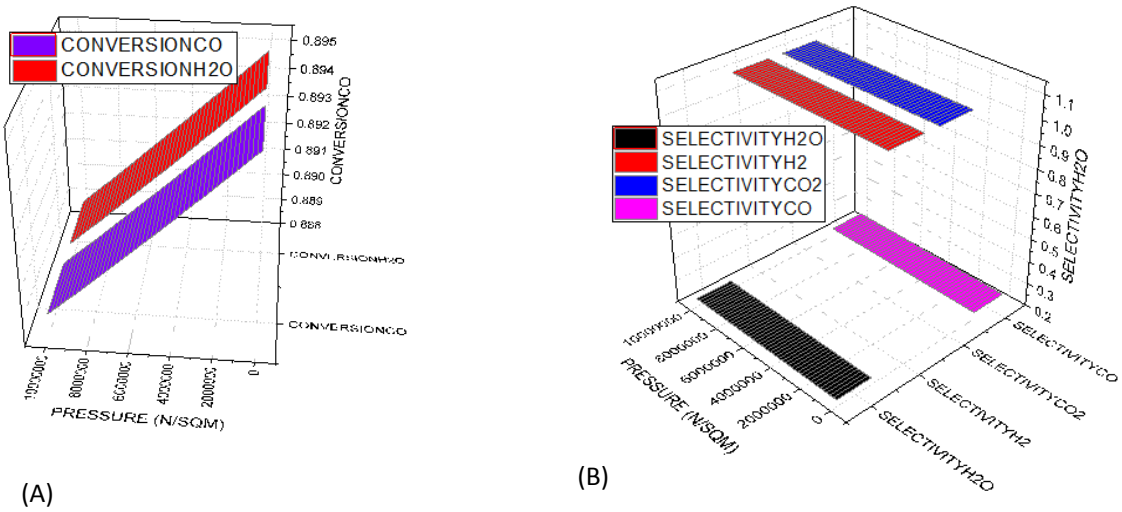

(A) (B)

Figure 4.33: (A) conversion of water and CO and (B) Selectivity of CO_2, CO, H_2 and H_2O versus Pressure of WGS

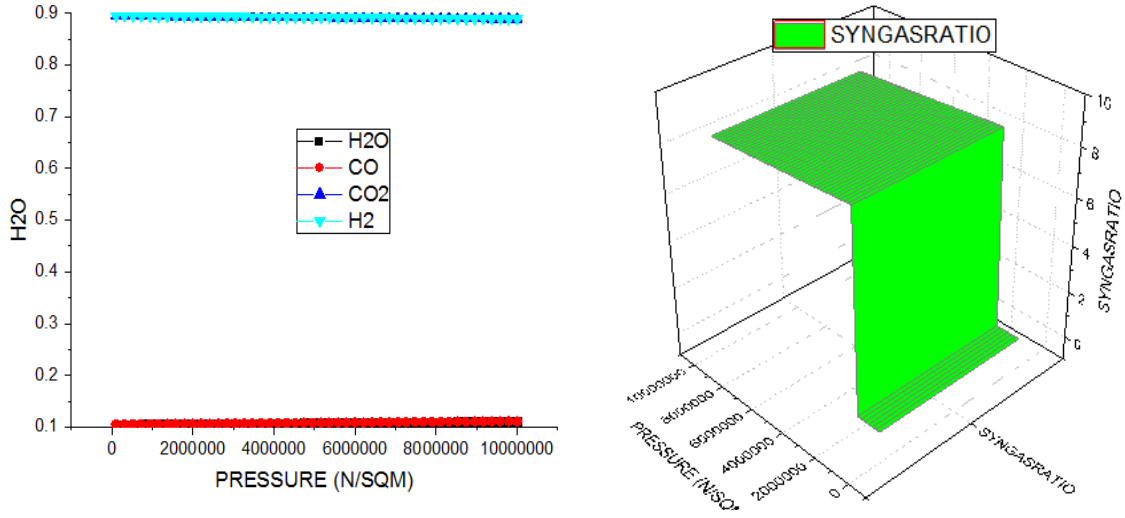

(A) (B)

Figure 4.34: (A) product composition of CO_2, CO, H_2 and H_2O and (B) Syngas ratio versus Pressure of WGS

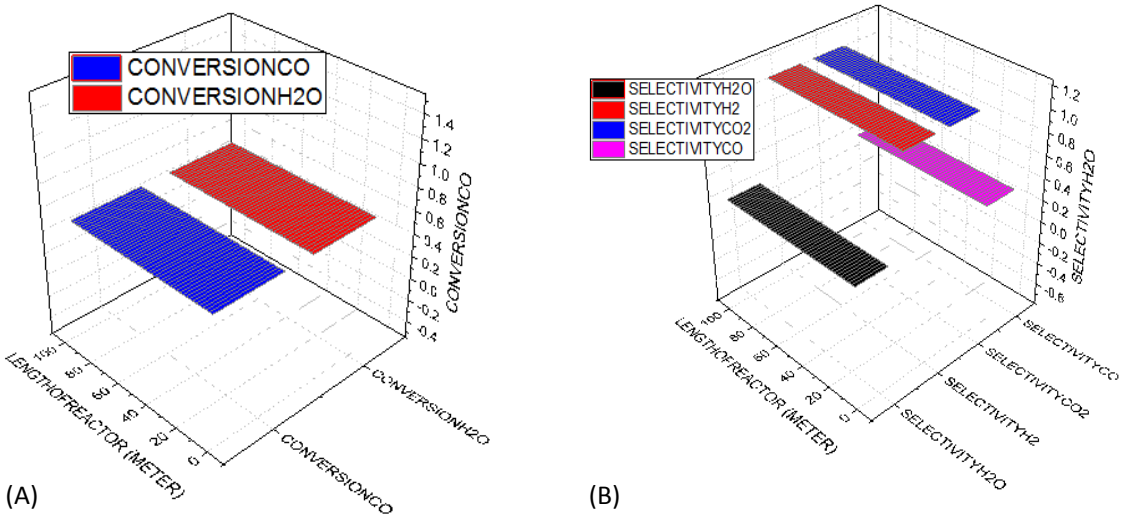

(A) (B)

Figure 4.35: (A) conversion of water and CO and (B) Selectivity of CO_2, CO, H_2 and H_2O versus length of WGS

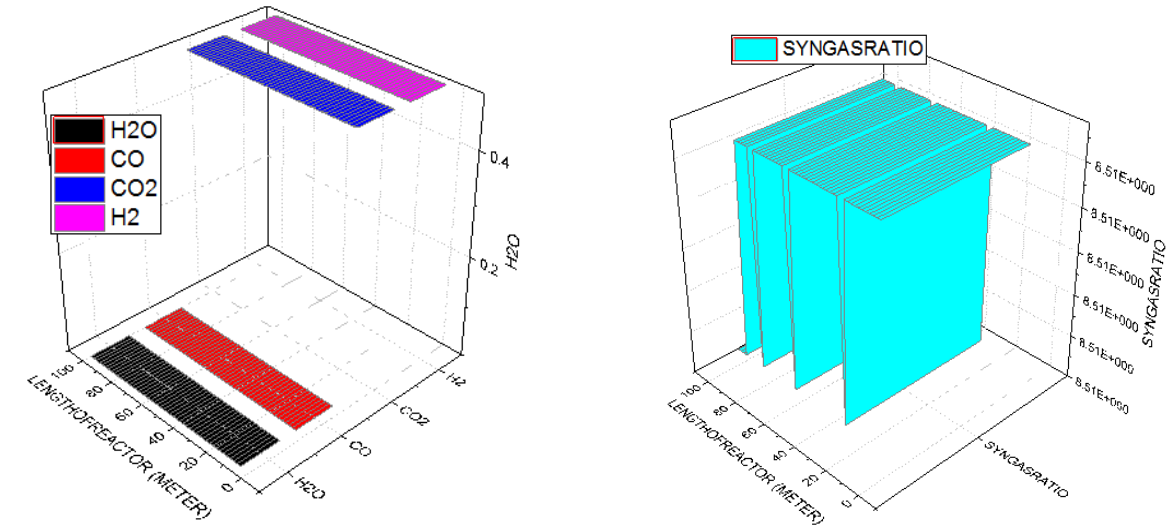

(A) (B)

Figure 4.36: (A) product composition of CO_2, CO, H_2 and H_2O and (B) Syngas ratio versus Pressure of WGS

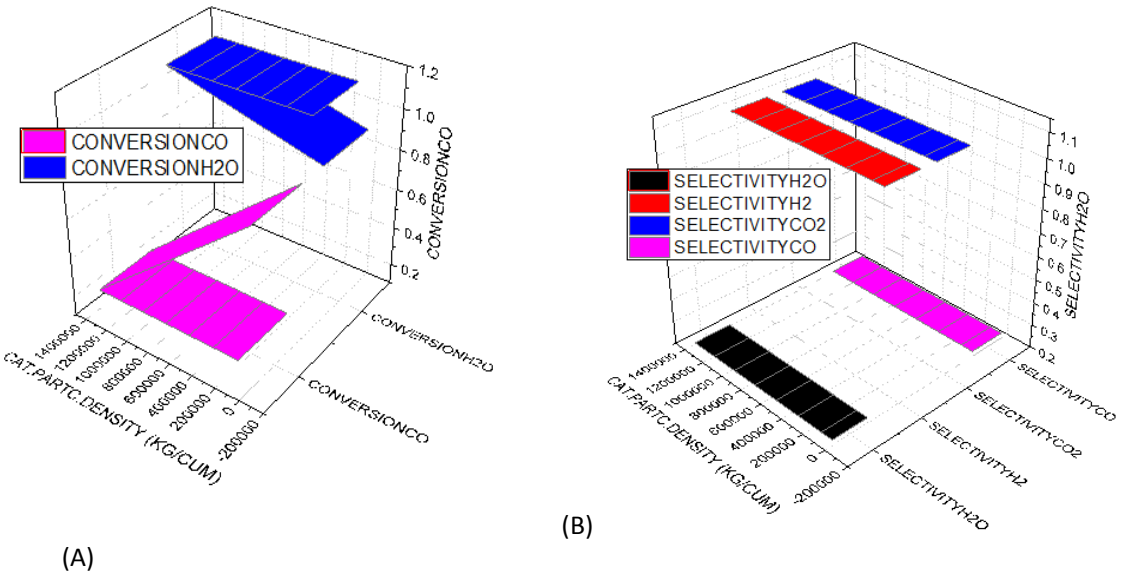

(A) (B)

Figure 4.37: (A) conversion of water and CO and (B) Selectivity of CO_2, CO, H_2 and H_2O versus Catalyst particle density of WGS

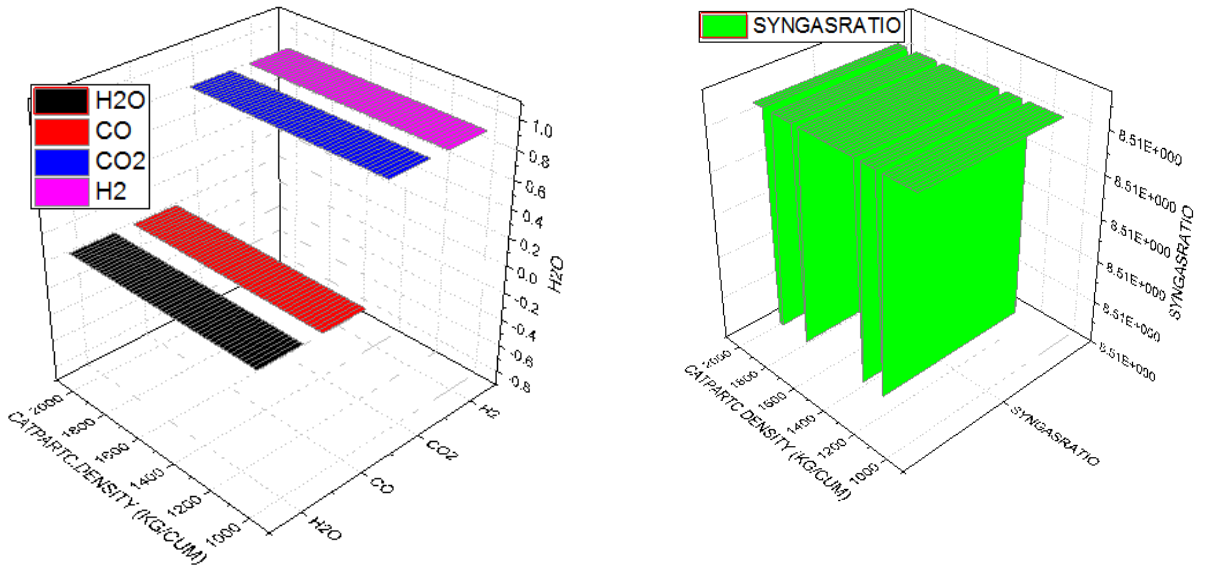

(A) (B)

Figure 4.38: (A) product composition of CO_2, CO, H_2 and H_2O and (B) Syngas ratio versus Catalyst particle density of WGS

4.3.3 Optimum Condition of the Parameters on Reforming and Water Gas Shift Reaction

Maximizing the syngas/hydrogen yield, selectivity and minimizing carbon dioxide emissions are the optimizations goals for the syngas production via glycerol dry reforming processes. Therefore, two types of strategies have been planned to achieve the goal.

The first, strategies was selectivity/yield of the hydrogen leaving the reactor in terms of the flow rate is defined in APPENDIX B1. This show that if the hydrogen product increases or the carbon dioxide decreases in the outlet flow rate of the reformer reactor, then the value of selectivity of hydrogen definitely increases.

The second strategy was the carbon dioxide selectivity/yield for the evaluation of the effect of carbon dioxide reduction as follows in APPENDIX B2. Notably, the total carbon dioxide reduction is relevant to the value of selectivity of carbon dioxide. Furthermore the comparison of the system before and after using optimization is shown in Appendix C.

5. Conclusion and Recommendation

5.1 Conclusion

The glycerol dry reforming was carried out with the aid of Aspen Plus^{TM} software in to two reactor models. The first was RGIBBS reactor model over wide range of parameters such as temperature, pressure and feed ratio i.e. molar flow rate of carbon dioxide to glycerol. This study was used RGIBBS reactors model for two combination processes; and they were reforming reactor process and Water gas shift reaction reactor process. The two reactor processes were carried out with sensitivity analyses and optimization of the parameters with the aid of Aspen Plus software. Sensitivity analyses of these parameters were done to know range of parameters that favour maximum yield and selectivity and eliminate carbon dioxide emission and other side products that will be affect the environment. For the reforming at the range of temperature 573-1273K, pressure range 1-30 bar and feed ratio1:5 feed ratio sensitivity analyses and optimization have been performed. Furthermore, for the water gas shift reaction at the range of temperature 473-873 K , pressure 1-20 bar and feed ratio 1-2.2 sensitivity analysis and optimization of the parameters have been conducted with the aid of Aspen plus software. The overall effects of the parameters on reforming processes and water gas shift reaction processes have been discussed in the result and discussion sections. From the parameters of reforming, temperature has positive effect on the processes than the other parameters like pressure and feed ratio. Based on this the yield of syngas was 92% over the range of temperature 573 -1273K whereas, over the range of pressure 1-30 bar and feed ratio 1-5; the yield of syngas were 50% and 51.24% respectively. Meanwhile, for the parameters of water gas shift reaction processes temperature has highly affected the process in terms of converted water i.e. 85% of conversion of water. In other side, pressure and feed ratio were recorded conversion of water 70% and 63.2% respectively. Apart from that, optimization was necessary to obtain satisfactory value of conversion, yield, selectivity and thoroughly syngas ratio. The optimum conditions of the two processes parameters also carried out with the using Aspen Plus software.

The second was RPLUG kinetic reactor model over the wide ranges of the parameters such as temperature, pressure, length of reactor and catalyst particle density. RPLUG kinetic reactor model was used for the two combination process such as reforming

process and water gas shift reaction. Furthermore, the kinetics based simulation was performed using Aspen plus RPLUG model blocks with rearranged power law and Langmuir –Hinshelwood –Hougen-Watson (LHHW). Both reaction models were carried out with power law and LHHW law to analyses sensitivity and optimization. For the power law model; the sensitivity analyses of the reforming reactor models have been carried out over the wide ranges of the parameters such as temperature (923-2800K), pressure (10-2000 bar), and length of the reactor (5-300 meter). Meanwhile, for the water gas shift reaction; sensitivity analysis has been carried out over the wide ranges of the parameters such as temperature (453-1000K), pressure (1.62-100 bar), and length of the reactor (5-200 meter). Additionally, for the reforming and water gas shift reaction processes; the Langmuir –Hinshelwood-Hougen –Watson kinetic law model also analyzed the sensitivity over the wide range of the parameters; such as temperature (1000-2800K) and (850- 1237K), pressure (10-200 bar) and(1-100 bar), length of the reactor (5-100 meter) and (1-100 meter) and catalyst particle density (1000-2000 KG/CUM) respectively. Effects of each parameters were analysed during the sensitivity and optimization with the aid of Aspen plus. Generally, higher pressures have a negative effect on syngas and hydrogen yield. The overall effect of parameters for kinetic reactor model was not much as the equilibrium reactor model. Meanwhile, for the reformer the maximum amounts of hydrogen and syngas were achieved at 1 bar pressure. Hydrogen yield increased with increased temperature. The optimization result of the reforming shows that over the reforming parameters were, the conversion of CO_2 increased from 73.1% to 84% after optimization with temperature and pressure 1273 K and 1 bar respectively. Meanwhile, syngas ratio was increased from 2.215 -0.63 to 2.233- 0.788 over the range of temperature (573-1273K) and pressure 1 bar. Furthermore, the yield of H_2 has been increased from 70% to 100% at a temperature and pressure 1273K and 1 bar respectively. This all about for the sample result data, for the detail see Appendix C.

5.2 Recommendation

Based on the scope of this research work, it is recommended that:

- The kinetic data for this study was obtained from literature; hence it could be interesting if it combine with experimental work and specific catalyst.

- For the simulation with aid of Aspen plus, it could be interesting if using different reactors to estimate the equilibrium level and compare with RGIBBS reactor.
- Based on this data further study will be necessary for the simulation to compare with the experimental data

References

Adhikari, S., Fernando, S., & Haryanto, A. (2007). Production of hydrogen by steam reforming of glycerine over alumina-supported metal catalysts. Catalysis, 129(3), 355-364.

Ahmad, A. (2017). Kinetic Based Simulation of Methane Steam Reforming and Water Gas Shift for Hydrogen Production Using Aspen Plus, (March).

Arif, N. N. M., Vo, D. V. N., Azizan, M. T., & Abidin, S. Z. (2016a). Carbon dioxide dry reforming of glycerol for hydrogen production using Ni/ZrO2 and Ni/CaO as catalysts. *Bulletin of Chemical Reaction Engineering & Catalysis*, *11*(2), 200–209.

Arif, N. N. M., Vo, D. V. N., Azizan, M. T., & Abidin, S. Z. (2016b). Carbon dioxide dry reforming of glycerol for hydrogen production using Ni/ZrO2 and Ni/CaO as catalysts. *Bulletin of Chemical Reaction Engineering & Catalysis*, *11*(2), 200–209.

Ayastuy, J. L., Gutiérrez-Ortiz, M. A., González-Marcos, J. A., Aranzabal, A., & González-Velasco, J. R. (2005). Optimization of inlet temperature for deactivating LTWGS reactor performance. *AIChE Journal*, *51*(7), 2016–2023.

Binti, N., & Yunus, M. (2015). carbon dioxide (CO2) dry reforming of glycerol for hydrogen production using Ni / La 2 O 3 AND Co / La 2 O 3.

Demsash, H. D., Kondamudi, K. V. K., Upadhyayula, S., & Mohan, R. (2018). Ruthenium doped nickel-alumina-ceria catalyst in glycerol steam reforming. *Fuel Processing Technology*, *169*.

Demsash, H. D., & Mohan, R. (2016). Steam reforming of glycerol to hydrogen over ceria promoted nickel–alumina catalysts. *International Journal of Hydrogen Energy*, *41*(48).

Demsash,H, H.D., Acharya C., and Mohan, R., (2014). Hydrogen Production from glycerol steam reforming *CHEMCON-2014, 67th Annual Session of Indian Institute of Chemical Engineers*, Chandigarh. INDIA.

Ebshish, A., Yaakob, Z., Narayanan, B., Bshish, A., & Wan Daud, W. R. (2012). Steam reforming of glycerol over Ni supported alumina xerogel for hydrogen production. *Energy Procedia*, *18*, 552–559.

Harriott, P. (2003). *CHEMICAL REACTOR DESIGN*.

Lin, K. H., Lin, W. H., Hsiao, C. H., Chang, H. F., & Chang, A. C. C. (2012). Hydrogen production in steam reforming of glycerol by conventional and membrane reactors. *International journal of hydrogen energy*, *37*(18), 13770-13776.

Adhikari, S., Fernando, S., Gwaltney, S. R., To, S. F., Bricka, R. M., Steele, P. H., & Haryanto, A. (2007). A thermodynamic analysis of hydrogen production by steam reforming of glycerol. International Journal of Hydrogen Energy, 32(14), 2875-2880.

Cheng, C. K., Foo, S. Y., & Adesina, A. A. (2012). Thermodynamic analysis of glycerol steam reforming in the presence of CO_2 or H_2 as carbon gasifying agent. International journal of hydrogen energy, 37(13), 10101-10110.

Demsash,H. D., and Mohan R., (2015) The Thermodynamic Analysis of Hydrogen Production from Glycerol Steam Reforming" Energy Engineering Research and Management: An Innovative Approach (book chapter), 16-25.

Wang, X., Li, M., Li, S., Wang, H., Wang, S., & Ma, X. (2010). Hydrogen production by glycerol steam reforming with/without calcium oxide sorbent: A comparative study of thermodynamic and experimental work. Fuel Processing Technology, 91(12), 1812-1818.

Silva, J. M., Soria, M. A., & Madeira, L. M. (2015). Thermodynamic analysis of Glycerol Steam Reforming for hydrogen production with in situ hydrogen and carbon dioxide separation. Journal of Power Sources, 273, 423-430.

Wang, H., Wang, X., Li, M., Li, S., Wang, S., & Ma, X. (2009). Thermodynamic analysis of hydrogen production from glycerol auto thermal reforming. International Journal of Hydrogen Energy, 34(14), 5683-5690.

Pompeo, F., Nichio, N.N., Ferretti, O.A., Re-sasco, D. (2005). Study of Ni Catalysts on Different Supports to Obtain Synthesis Gas. *International Journal of Hydrogen Energy*, 30: 1399-1405.

Mondal, P., Dang, G.S., Garg, M.O. (2011). Syngas Production through Gasification and Cleaning for Downstream Gasification – Re-cent Developments. *Fuel Processing Technology*, 92(8):1395-1410.

Fernandez, Y., Arenillas, A., Bermùdez, J.M., Menèndez, J.A. (2010). Comparative Study of Conventional and Microwave-assisted Pyrolysis, Steam and Dry Reforming of Glycerol for Syngas Production Using a Carbonaceous Catalyst. *Journal of Analytical and Applied Pyrolysis*, 88(2): 155-159.

Huang, Z., Xu, C., Liu, C., Xiao, H., Chen, J., Zhang, Y., Lei, Y. (2013). Glycerol Steam Re-forming over Ni/γ-Al2O3 Catalysts Modified by Metal Oxides. *Korean Journal of Chemical Engineering*, 30(3): 587-592.

Karinen, R.S., Krause, A.O.I. (2006). New Bio components from Glycerol. *Applied Catalysis A*., 306: 128-133.

Lin, Y. (2013). Catalytic Valorisation of Glycerol to Hydrogen and Syngas. *International Journal of Hydrogen Energy*, 38(6):2678-2700

Fan, X., Burton, R., Zhou, Y. (2010). Glycerol (By-product of Biodiesel Production) as a Source for Fuels and Chemicals - Mini Re-view. *The Open Fuels & Energy Science Journal*, 3: 17-22.

Wang, X., Li, M., Wang, M., Wang, H., Li, S., Wang, S., & Ma, X. (2009). Thermodynamic analysis of glycerol dry reforming for hydrogen and synthesis gas production. Fuel, 88(11), 2148-2153.

Siew, K. W., Lee, H. C., Gimbun, J., & Cheng, C. K. (2013). Hydrogen Production via Glycerol Dry Reforming over La-Ni/Al2O3 Catalyst. Bulletin of Chemical Reaction Engineering & Catalysis, 8(2), 160-166.

Mahmoud, A., & Ghani, A. (2014). UNIVERSITY OF REGINA FACULTY OF GRADUATE STUDIES AND RESEARCH..

Moon, K., Madhu, N., & Kale, G. R. (2013). Carbon Dioxide Utilization Using Combined Reforming, *7*(3).

Nikoo, M. K., & Amin, N. A. S. (2011). Thermodynamic analysis of carbon dioxide reforming of methane in view of solid carbon formation. *Fuel Processing Technology*, *92*(3), 678–691.

Preciado, J. E., Ortiz-martinez, J. J., Gonzalez-rivera, J. C., Sierra-ramirez, R., & Gordillo, G. (2012). Simulation of Synthesis Gas Production from Steam Oxygen Gasification of Colombian Coal Using Aspen Plus®, 4924–4940.

Siddharth Rao Gumuluru. (2012). Hydrogen Production by Supercritical Water Reforming of Bio-oil Components.

Silva, J. M., Soria, M. A., & Madeira, L. M. (2015). Thermodynamic analysis of Glycerol Steam Reforming for hydrogen production with in situ hydrogen and carbon dioxide separation. *Journal of Power Sources*, *273*, 423–430.

Silvey, L. G. (2011). Hydrogen and Syngas Production from Biodiesel Derived Crude Glycerol, 1–121.

Sisinni, M., Carlo, A. Di, Bocci, E., Micangeli, A., & Naso, V. (2013). Hydrogen-rich gas production by sorption enhanced steam reforming of woodgas containing TAR over a commercial Ni catalyst and calcined dolomite as CO2 sorbentx. *Energies*, *6*(7), 3167–3181.

Song, H. S. (2010). CH 4 Reforming for Synthesis Gas Production over Supported Ni Catalysts.

Wang, X., Li, M., Wang, M., Wang, H., Li, S., Wang, S., & Ma, X. (2009). Thermodynamic analysis of glycerol dry reforming for hydrogen and synthesis gas production. *Fuel*, *88*(11), 2148–2153.

Weng, K., Chyn, H., Gimbun, J., Yee, S., Khan, M. R., Hin, Y., & Kui, C. (2015). Syngas production from glycerol-dry (CO 2) reforming over La-promoted Ni / Al 2 O 3 catalyst, *74*(3), 441–447.

Appendix A: Total Heat of Vaporization of Glycerol Mixture

Sensible heat and latent heat of vaporization of glycerol mixture

For sensible heat of water

$$Qs = mC_p\Delta T \quad [A1]$$

$Qs = Sensible\ Heat\ of\ transfer = KJ/s$

$m = Mass\ flow\ rate = 1Kg/s$

$Cp = Specific\ heat\ water = 4.22KJ/Kg$

$\Delta T = Temperature\ change\ (373K - 298K$

$$Qs = 1Kg * \frac{4.22KJ}{Kg} * (373K - 298K) = \frac{316.5KJ}{s} = 316500J/s$$

For latent heat of vaporization of glycerol mixture

$$Ql = m\Lambda \quad [A2]$$

$\Lambda = Heat\ of\ vaporization$ = 88.174KJ/mol from Table 2.0

For the heat of vaporization need to convert the unit into KJ/kg, then divided by the reciprocal of molar mass and multiply by 1000g/kg.

$$\Lambda = \frac{88.174\text{KJ}}{\text{mol}} * \frac{\frac{1}{92\text{g}}*\text{mol}*1000\text{g}}{\text{mol kg}} = 958.413\text{KJ/kg} \quad [A3]$$

$$Ql = \frac{1kg}{s} * \frac{958.4KJ}{kg} = 958413\ J/s$$

Total heat of Vaporization $Q = Qs + Ql = 1274913J/s$ [A4]

Appendix B: Formulas to Check Optimum Condition

$$S_{H2} = \frac{molar\ flow\ H2\ out}{\sum(molar\ flow\ of\ i)out} \quad [B1]$$

$i\ represent\ , C_3H_8O_3, H_2O, CO_2, CO$

$$S_{CO2} = \frac{molar\ flow\ CO2\ out}{\sum(molar\ flow\ of\ j)out} \quad [B2]$$

$j\ represent\ , C_3H_8O_3, H_2O, H_2, CO$

Appendix C: Optimum Parameters of Glycerol Dry Reforming

TABLE C-1: Optimum Result on RGIBBS Reforming Reactor for Temperature (573-1273K)

Parameters optimized	Optimized component	Before optimum	After optimum	Objective function
1273K@1 bar	Conversion of CO_2	73.1%	84%	Maximize the X_{CO2}
(573-1273K)@ 1bar	Syngas ratio (H_2/CO)	2.215-0.63	2.233-0.788	Maximize the syngas ratio
1273K@ 1bar	Yield of H_2	70%	100%	Maximize Y_{H2}
573K@ 1bar	Yield of CO	100%	100%	Minimize Y_{CO}
1273K@14.89 bar	Selectivity H_2	4.85	4.87	Maximize S_{H2}
1273K)@14.89 bar	Selectivity CO_2	-	4.87	Minimize S_{CO2}

TABLE C-2: Optimum Result on RGIBBS Reforming Reactor for Pressure (1-30 BAR)

Parameters optimized	Optimized component	Before optimum	After optimum	Objective function
1 bar @1273K	Conversion of CO_2	Less than zero	84%	Maximize the X_{CO2}
(573-1273K)@ 1bar	Syngas ratio (H_2/CO)	0.81 -0.63	2.232-2.215	Maximize the syngas ratio
1 bar @ 573K	Yield of H_2	0.46%	0.46%	Maximize Y_{H2}
30 BAR @573K	Yield of CO	100%	100%	Minimize Y_{CO}

TABLE C-3: Optimum Result on RGIBBS WGS Reactor for Temperature (473-873K)

Parameters optimized	Optimized component	Before optimum	After optimum	Objective function
873K @ 1 bar	Conversion of H_2O	85%	85.5%	Maximize the X_{H2O}
(573-1273K)@ 1bar	Syngas ratio (H_2/CO)	0.81 -0.63	2.232-2.215	Maximize the syngas ratio
1 bar @ 573K	Yield of H_2	0.46%	0.46%	Maximize Y_{H2}
30 BAR @573K	Yield of CO	100%	100%	Minimize Y_{CO}

TABLE C-4: Optimum Result on RGIBBS WGS Reactor for Pressure (1-20 BAR)

Parameters optimized	Optimized component	Before optimum	After optimum	Objective function
20 bar @513K	Conversion of H_2O	70.96%	70%	Maximize the X_{H2O}
1bar @ 513K	Yield H_2O	100%	100%	Maximize the Y_{H2O}
(1-20bar)@ 637K	Syngas ratio (H_2O/CO	1.622-0.343	47-10.45	Minimize S_{CO2}
1-20bar@ 695K			96.64	Maximize X_{H2O}
1-20bar@513K			6.265-1.348	Minimize Y_{H2}

Appendix D: Aspen plus Process Flow diagram of DGR and WGS

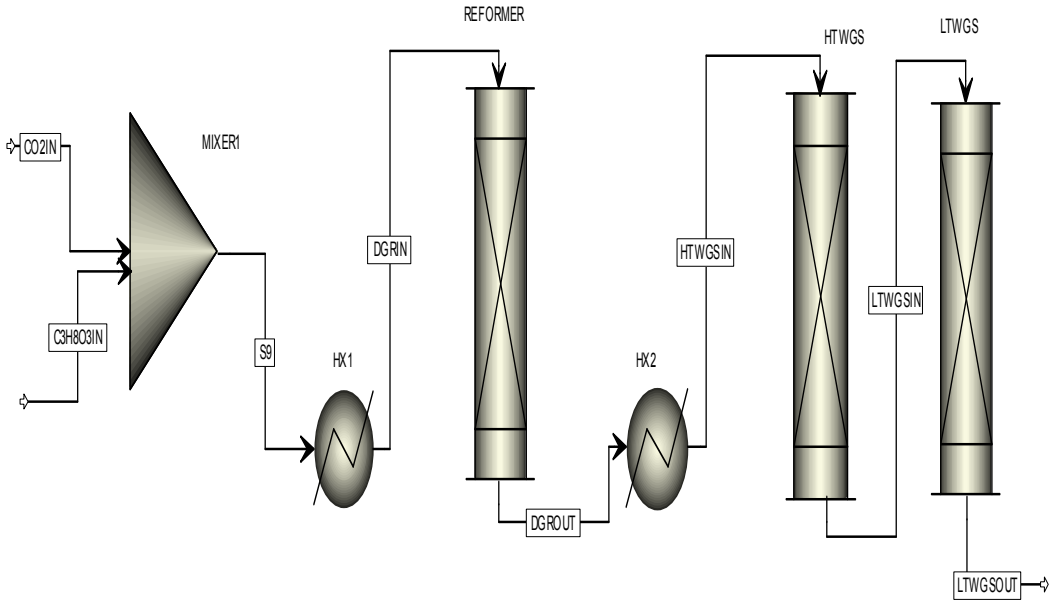

Figure D-1: Aspen plus Process flow diagram of DGR and WGS for Kinetic Reactor type

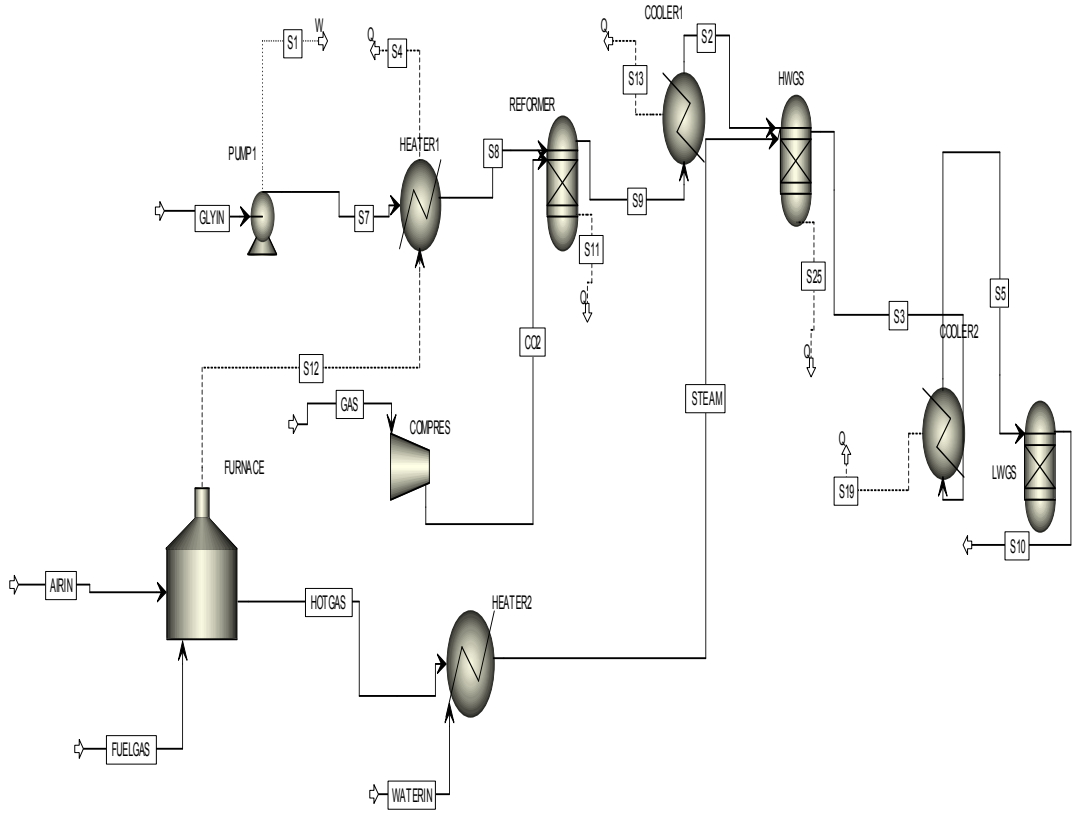

Figure D-2: Aspen plus Process flow diagram of DGR and WGS for RGIBBS reactor type

Appendix E: Material and Energy Balance Data from Aspen plus Run

Table E-1: Material Balance of RGIBBS from Aspen plus Run

	Units	AIRIN	CO2	FUELGAS	GAS	GLYIN	HOTGAS
From			COMPRES				FURNACE
To		FURNACE	REFORMER	FURNACE	COMPRES	PUMP1	HEATER2
Substream: MIXED							
Phase:		Vapor	Vapor	Vapor	Vapor	Liquid	Vapor
Component Mole Flow							
GLYCEROL	KMOL/SEC	0	0	0	0	1	0
CARBO-01	KMOL/SEC	0	1	0	1	0	0
CARBO-02	KMOL/SEC	0	0	0	0	0	0
WATER	KMOL/SEC	0	0	0	0	0	0
HYDRO-01	KMOL/SEC	0	0	0	0	0	0
ETHYL-01	KMOL/SEC	0	0	0	0	0	0
METHA-01	KMOL/SEC	0	0	1	0	0	1
ETHAN-01	KMOL/SEC	0	0	0	0	0	0
AIR	KMOL/SEC	0.79	0	0	0	0	0.79
AIR02	KMOL/SEC	0.21	0	0	0	0	0.21
Mole Flow	KMOL/SEC	1	1	1	1	1	2
Mass Flow	KG/SEC	28.8504	44.0098	16.04276	44.0098	92.09472	44.89316
Volume Flow	CUM/SEC	24.76342	4.410897	24.72173	24.22017	0.072337	9.603899
Pressure	N/SQM	100000	1000000	100000	100000	100000	
Vapor Fraction		1	1	1	1	0	1
Liquid Fraction		0	0	0	0	1	0
Solid Fraction		0	0	0	0	0	0
Molar Enthalpy	J/KMOL	-12424.05	-3.8E+08	-7.5E+07	-3.9E+08	-6.5E+08	36064500
Mass Enthalpy	J/KG	-430.6372	-8720300	-4646500	-8946700	-7112100	1606680
Enthalpy Flow	WATT	-12424.05	-3.8E+08	-7.5E+07	-3.9E+08	-6.5E+08	72129000
Molar Entropy	J/KMOL-K	4345.43	7802.704	-80547.8	2250.179	-587310	20932.3
Mass Entropy	J/KG-K	150.6194	177.2947	-5020.82	51.12904	-6377.28	932.5387
Molar	KMOL/CU	0.0403	0.226711	0.04045	0.04128	13.8241	0.208249

Density	M	821			8	2	
Mass Density	KG/CUM	1.165041	9.977518	0.648934	1.817072	1273.128	4.674472
Average Molecular Weight		28.8504	44.0098	16.04276	44.0098	92.09472	22.44658
Mole Flow							

Continued part

	Units	S10	S16	S2	S20	S22	S3
From		LWGS	COMPRES				FURNACE
To		COOLER3	REFORMER	FURNACE	COMPRES	PUMP1	HEATER2
Substream: MIXED							
Phase:		Vapor	Vapor	Vapor	Vapor	Liquid	Vapor
Component Mole Flow							
GLYCEROL	KMOL/SEC	7.63E-35	0	0	0	1	0
CARBO-01	KMOL/SEC	2.355153	1	0	1	0	0
CARBO-02	KMOL/SEC	4.55E-06	0	0	0	0	0
WATER	KMOL/SEC	1.709689	0	0	0	0	0
HYDRO-01	KMOL/SEC	0.000631	0	0	0	0	0
ETHYL-01	KMOL/SEC	1.04E-13	0	0	0	0	0
METHA-01	KMOL/SEC	2.644831	0	1	0	0	1
ETHAN-01	KMOL/SEC	5.45E-06	0	0	0	0	0
AIR	KMOL/SEC	0.79	0	0	0	0	0.79
AIR02	KMOL/SEC	0	0	0	0	0	0.21
Mole Flow	KMOL/SEC	7.500315	1	1	1	1	2
Mass Flow	KG/SEC	199.013	44.0098	16.04276	44.0098	92.09472	44.89316
Volume Flow	CUM/SEC	52.33445	4.410897	24.72173	24.22017	0.072337	9.603899
Pressure	N/SQM	423	1000000	100000	100000	100000	
Vapor Fraction		500000	1	1	1	0	1

Liquid Fraction		1	0	0	0	1	0
Solid Fraction		0	0	0	0	0	0
Molar Enthalpy	J/KMOL	0	-3.8E+08	-7.5E+07	-3.9E+08	-6.5E+08	36064500
Mass Enthalpy	J/KG	-2E+08	-8720300	-4646500	-8946700	-7112100	1606680
Enthalpy Flow	WATT	-7554300	-3.8E+08	-7.5E+07	-3.9E+08	-6.5E+08	72129000
Molar Entropy	J/KMOL-K	-1.5E+09	7802.704	-80547.8	2250.179	-587310	20932.3
Mass Entropy	J/KG-K	-27325	177.2947	-5020.82	51.12904	-6377.28	932.5387
Molar Density	KMOL/CUM	-1029.81	0.226711	0.04045	0.041288	13.82412	0.208249
Mass Density	KG/CUM	0.143315	9.977518	0.648934	1.817072	1273.128	4.674472
Average Molecular Weight		3.802714	44.0098	16.04276	44.0098	92.09472	22.44658
Mole Flow							

Continued part

	Units	S5	S7	S8	S9	STEAM	WATERIN
From		LWGS	COMPRES				FURNACE
To		COOLER3	REFORMER	FURNACE	COMPRES	PUMP1	HEATER2
Substream: MIXED							
Phase:		Vapor	Vapor	Vapor	Vapor	Liquid	Vapor
Component Mole Flow							
GLYCEROL	KMOL/SEC	7.63E-35	0	0	0	1	0
CARBO-01	KMOL/SEC	2.355153	1	0	1	0	0
CARBO-02	KMOL/SEC	4.55E-06	0	0	0	0	0
WATER	KMOL/SEC	1.709689	0	0	0	0	0
HYDRO-01	KMOL/SEC	0.000631	0	0	0	0	0
ETHYL-01	KMOL/SEC	1.04E-	0	0	0	0	0

		13					
METHA-01	KMOL/SEC	2.644831	0	1	0	0	1
ETHAN-01	KMOL/SEC	5.45E-06	0	0	0	0	0
AIR	KMOL/SEC	0.79	0	0	0	0	0.79
AIR02	KMOL/SEC	0	0	0	0	0	0.21
Mole Flow	KMOL/SEC	7.500315	1	1	1	1	2
Mass Flow	KG/SEC	199.013	44.0098	16.04276	44.0098	92.09472	44.89316
Volume Flow	CUM/SEC	52.33445	4.410897	24.72173	24.22017	0.072337	9.603899
Pressure	N/SQM	423	1000000	100000	100000	100000	
Vapor Fraction		500000	1	1	1	0	1
Liquid Fraction		1	0	0	0	1	0
Solid Fraction		0	0	0	0	0	0
Molar Enthalpy	J/KMOL	0	-3.8E+08	-7.5E+07	-3.9E+08	-6.5E+08	36064500
Mass Enthalpy	J/KG	-2E+08	-8720300	-4646500	-8946700	-7112100	1606680
Enthalpy Flow	WATT	-7554300	-3.8E+08	-7.5E+07	-3.9E+08	-6.5E+08	72129000
Molar Entropy	J/KMOL-K	-1.5E+09	7802.704	-80547.8	2250.179	-587310	20932.3
Mass Entropy	J/KG-K	-27325	177.2947	-5020.82	51.12904	-6377.28	932.5387
Molar Density	KMOL/CUM	-1029.81	0.226711	0.04045	0.041288	13.82412	0.208249
Mass Density	KG/CUM	0.143315	9.977518	0.648934	1.817072	1273.128	4.674472
Average Molecular Weight		3.802714	44.0098	16.04276	44.0098	92.09472	22.44658
Mole Flow							

Table E-2: Total Energy flow rate run from Aspen plus

	S1	S4	S11	S12	S13	S19	S25
QCALC Watt		-2.6E+08	161185833	-146684800	24508889	9524136.22	78097725
TBEGIN K		298.0012		297.981113	573	453	
TEND K		563		1723.68127	453	423	
POWER Watt	926.79881						

Table E-3: Summary of RPLUG Reformer with kinetics Model of power law

RPlug power law	
Name	**GDR**
Process stream property method	**SRK**
Process stream Henry's component list ID	
Process stream electrolyte chemistry ID	
Process stream use true species approach for electrolytes	**YES**
Process stream free-water phase properties method	**STEAMNBS**
Process stream water solubility method	**3**
Thermal fluid property method	**SRK**
Thermal fluid Henry's component list ID	
Thermal fluid electrolyte chemistry ID	
Thermal fluid use true species approach for electrolytes	**YES**
Thermal fluid free-water phase properties method	**STEAMNBS**
Thermal fluid water solubility method	**3**
Number of tubes	
Reactor dimensions length [meter]	**3**
Reactor dimensions diameter [meter]	**0.5**
Pressure at reactor inlet: process stream [N/sqm]	**0**
EO Model components	
Heat duty [Watt]	0
Minimum reactor temperature [K]	922.998215
Maximum reactor temperature [K]	923
Residence time [sec]	0.0385487
Thermal fluid inlet temperature	
Thermal fluid inlet vapor fraction	
Total feed stream CO2e flow [kg/sec]	44.0098
Total product stream CO2e flow [kg/sec]	44.0097288

Net stream CO2e production [kg/sec]	-7.12036E-05

Table E-4: Process Stream Profile of RPLUG Reformer with kinetics Model of Power law

Reactor length	Pressure	Temperature	Molar vapor fraction	Duty	Residence time	Liquid holdup
meter	N/sqm	K		Watt	sec	
0	1000000	923	1	0	0	0
0.3	1000000	922.9995	1	0	0.003865	0
0.6	1000000	922.9991	1	0	0.007731	0
0.9	1000000	922.9986	1	0	0.011596	0
1.2	1000000	922.9982	1	0	0.015461	0
1.5	1000000	922.9977	1	0	0.019327	0
1.8	1000000	922.9973	1	0	0.023192	0
2.1	1000000	922.9968	1	0	0.027057	0
2.4	1000000	922.9964	1	0	0.030922	0
2.7	1000000	922.9959	1	0	0.034788	0
3	1000000	922.9954	1	0	0.038653	0

Table E-5: Material and Energy Balance for RPLUG Reformer with Kinetics Model of Power law

	Units	CO2IN	GDRIN	GDROUT	GLYIN	MIXOUT
From			HEATER1	GDR		MIXER1
To		MIXER1	GDR		MIXER1	HEATER1
Substream: MIXED						
Phase:		Vapor	Vapor	Vapor	Vapor	Mixed
Component Mole Flow						
C3H8O3	KMOL/SEC	0	1	0.999998	1	1
CO2	KMOL/SEC	1	1	0.999998	0	1
H2O	KMOL/SEC	0	0	1.62E-06	0	0
CO	KMOL/SEC	0	0	6.47E-06	0	0
H2	KMOL/SEC	0	0	4.85E-06	0	0
Mole Flow	KMOL/SEC	1	2	2.00001	1	2
Mass Flow	KG/SEC	44.0098	136.1045	136.1045	92.09472	136.1045
Volume Flow	CUM/SEC	24.65396	15.24169	15.24173	21.93866	58.93724
Temperature	K	298	923	922.9982	298	510.496
Pressure	N/SQM	100000	1000000	1000000	100000	100000
Vapor Fraction		1	1	1	1	0.696388

Liquid Fraction		0	0	0	0	0.303612
Solid Fraction		0	0	0	0	0
Molar Enthalpy	J/KMOL	-3.9E+08	-4.2E+08	-4.2E+08	-5.8E+08	-4.9E+08
Mass Enthalpy	J/KG	-8942500	-6112800	-6112800	-6283100	-7143000
Enthalpy Flow	WATT	-3.9E+08	-8.3E+08	-8.3E+08	-5.8E+08	-9.7E+08
Molar Entropy	J/KMOL-K	2882.393	-111310	-111310	-440180	-201460
Mass Entropy	J/KG-K	65.49434	-1635.61	-1635.59	-4779.61	-2960.42
Molar Density	KMOL/CUM	0.040561	0.131219	0.131219	0.045582	0.033934
Mass Density	KG/CUM	1.785101	8.929755	8.929728	4.197829	2.309313
Average Molecular Weight		44.0098	68.05226	68.05193	92.09472	68.05226

Table E-6: Summary of RPLUG Reformer with kinetics Model of LHHW

RPlug	
Name	**REFORMER**
Process stream property method	**SRK**
Process stream Henry's component list ID	
Process stream electrolyte chemistry ID	
Process stream use true species approach for electrolytes	**YES**
Process stream free-water phase properties method	**STEAMNBS**
Process stream water solubility method	**3**
Thermal fluid property method	**SRK**
Thermal fluid Henry's component list ID	
Thermal fluid electrolyte chemistry ID	
Thermal fluid use true species approach for electrolytes	**YES**
Thermal fluid free-water phase properties method	**STEAMNBS**
Thermal fluid water solubility method	**3**
Number of tubes	
Reactor dimensions length [meter]	**2**
Reactor dimensions diameter [meter]	**0.5**
Pressure at reactor inlet: process stream [N/sqm]	**0**
EO Model components	
Heat duty [Watt]	0
Minimum reactor temperature [K]	1000
Maximum reactor temperature [K]	1000

Residence time [sec]	0.242941586
Thermal fluid inlet temperature	
Thermal fluid inlet vapor fraction	
Total feed stream CO2e flow [kg/sec]	44.0098
Total product stream CO2e flow [kg/sec]	44.0098
Net stream CO2e production [kg/sec]	0

Table E-7: Process Stream Profile of RPLUG Reformer with kinetics Model of LHHW

Reactor length	Pressure	Temperature	Molar vapor fraction	Duty	Residence time	Liquid holdup
Meter	N/sqm	K		Watt	sec	
0	10000000	1000	1	0	0	**0**
0.2	10000000	1000	1	0	0.0242941586	**0**
0.4	10000000	1000	1	0	0.0485883173	**0**
0.6	10000000	1000	1	0	0.0728824759	**0**
0.8	10000000	1000	1	0	0.0971766345	**0**
1	10000000	1000	1	0	0.121470793	**0**
1.2	10000000	1000	1	0	0.145764952	**0**
1.4	10000000	1000	1	0	0.17005911	**0**
1.6	10000000	1000	1	0	0.194353269	**0**
1.8	10000000	1000	1	0	0.218647428	**0**
2	**10000000**	**1000**	**1**	**0**	**0.242941586**	**0**

Table E-8: Summary of RPLUG WGS with kinetics Model of LHHW

WGS	
Name	**WGS**
Process stream property method	**SRK**
Process stream Henry's component list ID	
Process stream electrolyte chemistry ID	
Process stream use true species approach for electrolytes	**YES**
Process stream free-water phase properties method	**STEAMNBS**
Process stream water solubility method	**3**
Thermal fluid property method	**SRK**
Thermal fluid Henry's component list ID	
Thermal fluid electrolyte chemistry ID	
Thermal fluid use true species approach for electrolytes	**YES**
Thermal fluid free-water phase properties method	**STEAMNBS**
Thermal fluid water solubility method	**3**
Number of tubes	
Reactor dimensions length [meter]	**5**

Reactor dimensions diameter [meter]	**0.3**
Pressure at reactor inlet: process stream [N/sqm]	**0**
EO Model components	
Heat duty [Watt]	0
Minimum reactor temperature [K]	923
Maximum reactor temperature [K]	1311.68053
Residence time [sec]	0.001825001
Thermal fluid inlet temperature	
Thermal fluid inlet vapor fraction	
Total feed stream CO2e flow [kg/sec]	0
Total product stream CO2e flow [kg/sec]	41.107099
Net stream CO2e production [kg/sec]	41.107099

Table E-9: Material and Energy Balance for RPLUG Reformer with Kinetics Model of LHHW

	Units	**C3H8O3IN**	**CO2IN**	**S9**	**DGRIN**	**DGROUT**
From				MIXER1	HX1	REFORMER
To		MIXER1	MIXER1	HX1	REFORMER	
Substream: MIXED						
Phase:		Vapor	Vapor	Vapor	Vapor	Vapor
Component Mole Flow						
C3H8O3	KMOL/SEC	1	0	1	1	1
CO2	KMOL/SEC	0	1	1	1	1
CO	KMOL/SEC	0	0	0	0	2.0234E-11
H2	KMOL/SEC	0	0	0	0	1.5175E-11
H2O	KMOL/SEC	0	0	0	0	5.0584E-12
Mole Flow	KMOL/SEC	1	1	2	2	2
Mass Flow	KG/SEC	92.09472	44.0098	136.1045	136.1045	136.1045
Volume Flow	CUM/SEC	0.6361034	0.2503787	1.253719	1.616433	1.616433
Temperature	K	1000	100	842.9691	1000	1000
Pressure	N/SQM	10000000	10000000	10000000	10000000	10000000
Vapor Fraction		1	1	1	1	1
Liquid Fraction		0	0	0	0	0

Solid Fraction		0	0	0	0	0
Molar Enthalpy	J/KMOL	-460020000	-401700000	-430860000	-407620000	-407620000
Mass Enthalpy	J/KG	-4995000	-9127500	-6331300	-5989900	-5989900
Enthalpy Flow	WATT	-460020000	-401700000	-861720000	-815250000	-815250000
Molar Entropy	J/KMOL-K	-278080	-70700.76	-146670	-121400	-121400
Mass Entropy	J/KG-K	-3019.471	-1606.478	-2155.302	-1783.971	-1783.971
Molar Density	KMOL/CUM	1.572072	3.993949	1.595254	1.237292	1.237292
Mass Density	KG/CUM	144.7795	175.7729	108.5607	84.20054	84.20054
Average Molecular Weight		92.09472	44.0098	68.05226	68.05226	68.05226

Table E-10: Material and Energy Balance for RPLUG WGS with Kinetics Model of LHHW

	Units	**DGROUT**	**WGSIN**	**WGSOUT**
From			HX2	WGS
To		HX2	WGS	
Substream: MIXED				
Phase:		Vapor	Vapor	Vapor
Component Mole Flow				
CO	KMOL/SEC	1	1	0.0659557
H2O	KMOL/SEC	1	1	0.0659557
H2	KMOL/SEC	0	0	0.9340442
CO2	KMOL/SEC	0	0	0.9340442
Mole Flow	KMOL/SEC	2	2	2
Mass Flow	KG/SEC	46.02568	46.02568	46.02568
Volume Flow	CUM/SEC	141.3579	153.5047	218.1588
Temperature	K	850	923	1311.681
Pressure	N/SQM	100000	100000	100000
Vapor Fraction		1	1	1
Liquid Fraction		0	0	0
Solid Fraction		0	0	0
Molar Enthalpy	J/KMOL	-157810000	-155170000	-155170000
Mass Enthalpy	J/KG	-6857600	-6742800	-6742800

Enthalpy Flow	WATT	-315620000	-310340000	-310340000	
Molar Entropy	J/KMOL-K	62754.26	65733.56	67568.84	
Mass Entropy	J/KG-K	2726.924	2856.386	2936.137	
Molar Density	KMOL/CUM	0.0141484	0.0130289	0.00916763	
Mass Density	KG/CUM	0.3255967	0.2998324	0.2109733	
Average Molecular Weight		23.01284	23.01284	23.01284	

Appendix F: Steps of Sensitivity Analysis and Optimization for Aspen plus Reformer and Water Gas Shift Reaction

A. Steps of Sensitivity Analysis for Aspen plus RGIBBS Reformer

The steps of Sensitivity analysis in Aspen plus are as follows:

- Select on model analysis tools and then select sensitivity m from the submenu
- Click the new button
- Type glycerol, carbon dioxide, carbon monoxide, water, hydrogen, ethylene, ethane, and methane in the variable name field as inlet for glycerol and carbon dioxide, and as outlet for the remaining component and click OK to continue
- Under category, click the streams button to select the variable category
- In the reference frame, click the arrow to the right of the type box to display a list of flow sheet variable types that can be accessed for streams.
- Select the type mole flow, since the variable is a component mole flow.
- Select the outlet and inlet stream for specific components.
- Click the component list box to a list of valid components, select mole flow of glycerol, carbon dioxide, carbon monoxide, hydrogen, water, ethylene, ethane, and methane.
- Click the close button to close the variable definition dialog box and return to the define sheet.
- Click the blocks options under category
- Click the type list box to display the flow sheet variable types that can be accessed for blocks
- Select block variable for type
- In the block list box that appears, select block RGIBBS.
- Click the variable list box to display the list of variables
- Select Temperature, Pressure, and Feed ratio variable since it represents the result of interest.
- Defining manipulated variables on the input vary sheet, define the simulation variable to be manipulated for sensitivity analysis, indentify the variable

values to be used, and specify the labels for the variables to be used in the tabulated result.

- Click the type box to display a list of valid variable types.
- Select stream-variable for the type
- Select the stream types
- Select mole-flow for the variable
- Click the overall ranges option button
- Move to the lower box and enter the value for the bottom of the ranges
- On the upper box enter the value for the top of the range.
- Set the variables for the reactor block and the overall ranges, accordingly, the temperature, pressure and feed ratio was 573K- 1273K, 1-30 BAR, and 1-5 respectively
- Set the increment between the intermediate point and that this is 48
- Defining tabulated variables, on the tabulated sheet, specify the variables to be tabulated by the sensitivity analysis, and supply optional headings for the table column.
- In the column number, enter from the first to the 15^{th} rows indicating that this is the first tabulated variable.
- On the tabulated variable expression box from the first row enter up to 15^{th} row enter the selectivity of hydrogen and carbon monoxide, yield of hydrogen and carbon monoxide, syngas ratio conversion of glycerol and carbon dioxide and the mole flow of the outlet of glycerol, carbon dioxide, carbon monoxide, ethane, ethylene, water, methane, and hydrogen

B. Steps of Sensitivity Analysis for Aspen plus WGS

The steps of Sensitivity analysis in Aspen plus are as follows:

- Select on model analysis tools and then select sensitivity m from the submenu
- Click the new button
- Type carbon dioxide, carbon monoxide, water, and hydrogen, in the variable name field as inlet for water and carbon monoxide, and as outlet for the remaining component and click OK to continue
- Under category, click the streams button to select the variable category

- In the reference frame, click the arrow to the right of the type box to display a list of flow sheet variable types that can be accessed for streams.
- Select the type mole flow, since the variable is a component mole flow.
- Select the outlet and inlet stream for specific components.
- Click the component list box to a list of valid components, select mole flow of, carbon dioxide, carbon monoxide, hydrogen, and water..
- Click the close button to close the variable definition dialog box and return to the define sheet.
- Click the blocks options under category
- Click the type list box to display the flow sheet variable types that can be accessed for blocks
- Select block variable for type
- In the block list box that appears, select block WGS.
- Click the variable list box to display the list of variables
- Select Temperature, Pressure, and Feed ratio variable since it represents the result of interest.
- Defining manipulated variables on the input vary sheet, define the simulation variable to be manipulated for sensitivity analysis, indentify the variable values to be used, and specify the labels for the variables to be used in the tabulated result.
- Click the type box to display a list of valid variable types.
- Select stream-variable for the type
- Select the stream types
- Select mole-flow for the variable
- Click the overall ranges option button
- Move to the lower box and enter the value for the bottom of the ranges
- On the upper box enter the value for the top of the range.
- Set the variables for the reactor block and the overall ranges, accordingly, the temperature, pressure and feed ratio was 473K- 873K, 1-20 BAR, and 1-2.2 respectively
- Set the increment between the intermediate point and that this is 48

- Defining tabulated variables, on the tabulated sheet, specify the variables to be tabulated by the sensitivity analysis, and supply optional headings for the table column.
- In the column number, enter from the first to the 9^{th} rows indicating that this is the first tabulated variable.
- On the tabulated variable expression box from the first row enter up to 9^{th} row enter the selectivity of hydrogen and carbon monoxide, yield of hydrogen and carbon monoxide, syngas ratio, conversion carbon monoxide and water and the mole flow of the outlet of , carbon dioxide, carbon monoxide, water, and hydrogen

C. Steps of Sensitivity Analysis for Aspen plus RPLUG Reformer

The steps of Sensitivity analysis in Aspen plus are as follows:

- Select on model analysis tools and then select sensitivity m from the submenu
- Click the new button
- Type glycerol, carbon dioxide, carbon monoxide, water, and hydrogen, in the variable name field as inlet for glycerol and carbon dioxide, and as outlet for the remaining component and click OK to continue
- Under category, click the streams button to select the variable category
- In the reference frame, click the arrow to the right of the type box to display a list of flow sheet variable types that can be accessed for streams.
- Select the type mole flow, since the variable is a component mole flow.
- Select the outlet and inlet stream for specific components.
- Click the component list box to a list of valid components, select mole flow of glycerol, carbon dioxide, carbon monoxide, hydrogen, and water, Click the close button to close the variable definition dialog box and return to the define sheet.
- Click the blocks options under category
- Click the type list box to display the flow sheet variable types that can be accessed for blocks
- Select block variable for type

- In the block list box that appears, select block RPLUG REFORMER.
- Click the variable list box to display the list of variables
- Select Temperature, Pressure, catalyst particle density, length of reactor, diameter of reactor and Feed ratio variable since it represents the result of interest.
- Defining manipulated variables on the input vary sheet, define the simulation variable to be manipulated for sensitivity analysis, indentify the variable values to be used, and specify the labels for the variables to be used in the tabulated result.
- Click the type box to display a list of valid variable types.
- Select the reactor and stream-variable for the type
- Select the reactor and stream types
- Select mole-flow for the variable
- Click the overall ranges option button
- Move to the lower box and enter the value for the bottom of the ranges
- On the upper box enter the value for the top of the range.
- Set the variables for the reactor block and the overall ranges, accordingly, the temperature, pressure, catalyst particle density, length of the reactor, diameter of the reactor and feed ratio was 1000K- 2800K, 0.1-200 BAR, 1000-2000 KG/CUM, 5 – 300 meter, 0.5 -10 meter and 1-5 respectively
- Set the increment between the intermediate point and that this is 48
- Defining tabulated variables, on the tabulated sheet, specify the variables to be tabulated by the sensitivity analysis, and supply optional headings for the table column.
- In the column number, enter from the first to the 12^{th} rows indicating that this is the first tabulated variable.
- On the tabulated variable expression box from the first row enter up to 12^{th} row enter the selectivity of hydrogen, carbon dioxide, water and carbon monoxide, conversion of glycerol and carbon dioxide, syngas ratio and the mole flow of the outlet of glycerol, carbon dioxide, carbon monoxide, water, and hydrogen

D. Steps of Sensitivity Analysis for Aspen plus RPLUG of WGS

The steps of Sensitivity analysis in Aspen plus are as follows:

- Select on model analysis tools and then select sensitivity m from the submenu
- Click the new button
- Type carbon dioxide, carbon monoxide, water, and hydrogen, in the variable name field as inlet for water and carbon monoxide, and as outlet for the remaining component and click OK to continue
- Under category, click the streams button to select the variable category
- In the reference frame, click the arrow to the right of the type box to display a list of flow sheet variable types that can be accessed for streams.
- Select the type mole flow, since the variable is a component mole flow.
- Select the outlet and inlet stream for specific components.
- Click the component list box to a list of valid components, select mole flow of, carbon dioxide, carbon monoxide, hydrogen, and water..
- Click the close button to close the variable definition dialog box and return to the define sheet.
- Click the blocks options under category
- Click the type list box to display the flow sheet variable types that can be accessed for blocks
- Select block variable for type
- In the block list box that appears, select block RPLUG of HWGS and LWGS.
- Click the variable list box to display the list of variables
- Select Temperature, Pressure, and Feed ratio variable since it represents the result of interest.
- Defining manipulated variables on the input vary sheet, define the simulation variable to be manipulated for sensitivity analysis, indentify the variable values to be used, and specify the labels for the variables to be used in the tabulated result.
- Click the type box to display a list of valid variable types.
- Select stream-variable for the type
- Select the stream types

- Select mole-flow for the variable
- Click the overall ranges option button
- Move to the lower box and enter the value for the bottom of the ranges
- On the upper box enter the value for the top of the range.
- Set the variables for the reactor block of HWGS and LWGS and the overall ranges.

Accordingly, the temperature, pressure, catalyst particle density, length of the reactor, diameter of the reactor, and feed ratio was 850K- 1237K, 1-100 BAR, 1000-2000 KG/CUM, 5-100 meter, 0.3-5meter and 1-2.2 respectively for HWGS and 750K-1000K,1-2.5 BAR, 500-1500KG/CUM,1-80meter,0.1-2.5meter and 1-2.2 respectively for LWGS.

- Set the increment between the intermediate point and that this is 48
- Defining tabulated variables, on the tabulated sheet, specify the variables to be tabulated by the sensitivity analysis, and supply optional headings for the table column.
- In the column number, enter from the first to the 11^{th} rows indicating that this is the first tabulated variable.
- On the tabulated variable expression box from the first row enter up to 11^{th} row enter the selectivity of hydrogen and carbon monoxide, water, hydrogen syngas ratio, conversion carbon monoxide and water and the mole flow of the outlet of , carbon dioxide, carbon monoxide, water, and hydrogen

E. Steps for Using Optimization in Aspen plus

- ✓ Identify measured variables on define sheet
- ✓ Flow sheet variables used to calculate the objective function
- ✓ Specify objective function objective and constraints sheet
- ✓ Maximization or minimization of objective function
- ✓ Specify manipulated (varied) variable on vary sheet
- ✓ Varies the optimization block will change to maximize/minimize objective function
- ✓ Lower and upper bounds for the manipulated(varied) variables
- ✓ Specify constraints(optional in constraints folder

F. Optimization Procedure Dry Glycerol Reforming of using Aspen plus

Optimization is used to maximize or minimize the objective function and objective function is expressed in terms of flow sheet variables. Optimization can have zero or more constraints and constraints can be equalities or inequalities. In Aspen plus optimization is located under data/ model analysis tool/ optimization. Constraints specification is under/data/ model Optimization is a process of finding the optimum condition; such as temperature, pressure and feed ration therefore this have been determined by calculating the conversion(X) selectivity(S) and yield(Y).

$$X_{Gly} = \frac{Glycerol\ in - Glycerol\ out}{Glycerol\ in} * 100 \qquad [F\text{-}1]$$

$$S_{H2} = \frac{FH2\ \text{produced}}{C\ atom\ produced\ in\ gas\ phase} * \frac{1}{RR} 100 \qquad [F\text{-}2]$$

$$RR\ is\ reforming\ ratio, defined\ as\ the\ mole\ ratio\ of\ H2\ to\ CO2$$

$$S, co(\%) = \frac{F_{CO,\text{out}}}{C\ atom\ produced\ in\ gas\ phase} * 100$$

$$Selectivity, \boldsymbol{i}(\%) = \frac{FC\ atom\ in\ \text{species}}{C\ atom\ produced\ in\ gas\ phase} * 100 \qquad [F\text{-}3]$$

Where, i, species refer to CO, CH_4, CO_2 etc.

$$Yield, H2(\%) = \frac{FH2\ \text{produced}}{FGlycerol\ in\ the\ feedstock} * 100 \qquad [F\text{-}4]$$

Filename: Final draft of Msc thesis 2018.docx
Directory: C:\Ali\MSc Thesis 2018
Template: C:\Users\User\AppData\Roaming\Microsoft\Templates\Normal.dotm
Title: Simulation and Modeling of Syngas Production via Glycerol Dry Reforming Using Aspen plus
Subject:
Author: Ali Hassen
Keywords:
Comments:
Creation Date: 27/10/2018 10:13:00
Change Number: 317
Last Saved On: 05/12/2018 10:42:00
Last Saved By: User
Total Editing Time: 4,113 Minutes
Last Printed On: 05/12/2018 10:42:00
As of Last Complete Printing
Number of Pages: 125
Number of Words: 44,378 (approx.)
Number of Characters: 252,955 (approx.)